INVESTIGATIONS OF THE MOLECULAR STRUCTURE AND BONDING OF WATER AT THE LIQUID-LIQUID INTERFACE UTILIZING VIBRATIONAL SUM-FREQUENCY SPECTROSCOPY

by

CATHRYN LEAN MCFEARIN

A DISSERTATION

Presented to the Department of Chemistry
and the Graduate School of the University of Oregon
in partial fulfillment of the requirements
for the degree of
Doctor of Philosophy

March 2009

University of Oregon Graduate School

Confirmation of Approval and Acceptance of Dissertation prepared by:

Cathryn McFearin

Title:

"Investigations of the Molecular Structure and Bonding of Water at the Liquid-Liquid Interface Utilizing Vibrational Sum-Frequency Spectroscopy"

This dissertation has been accepted and approved in partial fulfillment of the requirements for the degree in the Department of Chemistry by:

Thomas Dyke, Chairperson, Chemistry
Geraldine Richmond, Advisor, Chemistry
David Tyler, Member, Chemistry
Paul Engelking, Member, Chemistry
Roger Haydock, Outside Member, Physics

and Richard Linton, Vice President for Research and Graduate Studies/Dean of the Graduate School for the University of Oregon.

March 20, 2009

Original approval signatures are on file with the Graduate School and the University of Oregon Libraries.

An Abstract of the Dissertation of

Cathryn LeAn McFearin for the degree of Doctor of Philosophy

in the Department of Chemistry to be taken March 2009

Title: INVESTIGATIONS OF THE MOLECULAR STRUCTURE AND BONDING OF WATER AT THE LIQUID-LIQUID INTERFACE UTILIZING VIBRATIONAL SUM-FREQUENCY SPECTROSCOPY

Approved: _____
Dr. Geraldine L. Richmond

The interface between water and an organic liquid is present in a variety of biological, environmental, and chemical processes throughout science and nature. Issues such as environmental remediation and ion transport are governed by the properties of these interfaces, thus the importance of understanding them at the molecular level is apparent. The research in this dissertation shows how the structure and bonding of the liquid-liquid interface changes as the interfacial environment is altered. Vibrational sum-frequency spectroscopy (VSFS), a surface specific, non-linear optical technique, is employed for these interfacial studies. The interfacial OH stretching modes are examined using VSFS under different conditions including organic liquids of varying polarity, as well as addition of acid, base, and salts to the aqueous phase. The effects of these different conditions on the water molecules' interactions both with each other and with

the non-aqueous liquid are studied in order to better characterize and understand this important system.

The effect of polarity of the non-aqueous phase is presented first through investigations of different mixed halocarbon liquid-water interfaces and the neat chloroform-water interface. These studies show that as the overall polarity of the organic phase increases, the water molecules exhibit less overall orientation and undergo some weak bonding interactions with the non-aqueous liquid.

Next, the influence of different salts on the water structure at the interface is studied. Examining this system shows that the dissolved ions, specifically the anions, are present within the interface and significantly alter the orientation and bonding of the interfacial water molecules. The charge, size, and polarizability of the anions all play a role in determining how the water orientation is changed within the interface.

Finally, the water-like ions H_3O^+ and OH^- are examined at the liquid-liquid interface by changing the pH of the aqueous phase through addition of HCl or NaOH. At the extremes of the pH scale, the acid and base have ordering or disordering effects, respectively, on the water structure within the interfacial region.

CURRICULUM VITAE

NAME OF AUTHOR: Cathryn LeAn McFearin

PLACE OF BIRTH: Dallas, Texas

DATE OF BIRTH: August 30, 1979

GRADUATE AND UNDERGRADUATE SCHOOLS ATTENDED:

University of Oregon, Eugene, Oregon
Pepperdine University, Malibu, California

DEGREES AWARDED:

Doctor of Philosophy in Chemistry, 2009, University of Oregon
Bachelor of Science in Chemistry, 2002, Pepperdine University

AREAS OF SPECIAL INTEREST:

Aqueous interfaces
Environmental chemistry
Physical chemistry

PROFESSIONAL EXPERIENCE:

Research Assistant, Department of Chemistry, University of Oregon, Eugene, Oregon, 2003 – 2009

Teaching Assistant, Department of Chemistry, University of Oregon, Eugene, Oregon, 2002 – 2003

Research Assistant, Pepperdine University, 2001 – 2002

Teaching Assistant, Pepperdine University, 2000 – 2002

GRANTS, AWARDS AND HONORS:

Henry V. Howe Scholarship, University of Oregon, 2007 - 2008

Chemistry Graduate of the Year, Pepperdine University 2002

PUBLICATIONS:

McFearin, C.L.; Richmond, G.L., The Role of Interfacial Molecular Structure in the Adsorption of Ions at the Liquid-Liquid Interface *Proc. Natl. Acad. Sci. USA* (in press)

McFearin, C.L; Beaman, D.K.; Moore, F.G.; Richmond, G.L., From Franklin to Today: Towards a Molecular Level Understanding of Bonding and Adsorption at the Oil-Water Interface. *J. Phys. Chem. C* **2009**, *113* (4), 1171-1188.

McFearin, C.L.; Richmond, G.L., Understanding How Organic Solvent Polarity Affects Water Structure and Bonding at Halocarbon-Water Interfaces. *J. Mol. Liq.* **2007** *136* (3), 221 – 226.

Hopkins, A.J.; McFearin, C.L.; Richmond, G.L., Investigations of the Solid-Liquid Interface with Vibrational Sum-Frequency Spectroscopy. *Curr. Opin. Solid S. M.* **2005** *9* (1-2), 19-27.

Walker, D. S.; Brown, M.; McFearin, C. L.; Richmond, G. L., Evidence for a Diffuse Interfacial Region at the Dichloroethane/Water Interface. *J. Phys. Chem. B* **2004,** *108* (7), 2111-2114.

ACKNOWLEDGMENTS

Although my name is on the byline of this dissertation, it would not have been possible save for the efforts of many people in different capacities. First, I would like to express my gratitude to Dr. Geri Richmond for believing in me and encouraging my scientific growth and progress. You are not only a great example with regard to your professional career success, but the balance you have with your family life and the interests in the welfare of others is very inspiring. To the Richmond lab members, past and present, you made the whole process so much more enjoyable and I learned a great deal from so many of you. Melissa, Teresa, and Megan, thanks for being great examples of hard work and for passing on your knowledge of the ways of laser spectroscopy. Dennis, I was continually inspired by your excitement about research. Thanks for always having an "open door" and a willingness to answer my long list of questions. Dan, you were the greatest officemate and laser partner ever. I will miss our coffee outings for discussions of research or whatever else. Steph, I definitely would not have stayed sane if it had not been for you. Thanks for being a great friend and confidante. Thanks to Davida, Pat, Adam, and Eric for making the lab a fun place to be. I wish you all the best.

My life has also been very blessed by my wonderful friends and family. To Jane, my undergraduate advisor, pchem teacher, and friend, thank you for your support and advice. I literally would not be here except for your teaching, guidance, and example. To Syd, Ariane, Jess, Jill L, and Jill S, my best friends, you guys were always there for me, helped me through the ups and downs of the last few years, and kept things fun for

me. To my parents, Anita and Dan, you instilled in me a love for learning and a drive to always do my very best at a very young age. I am the person I am today because of your unconditional love and support all my life.

Last, and most importantly, to Nate my husband and the love of my life. I cannot adequately describe how much you have done and how much you mean to me. Thank you for *everything*.

For Nate

TABLE OF CONTENTS

Chapter Page

LIST OF FIGURES

Figure Page

Figure Page

Figure Page

LIST OF TABLES

CHAPTER I

INTRODUCTION

Amazing as it may seem, water is the central topic of a vast array of research efforts ranging from the growing worldwide need for sanitary drinking water, to technological applications such as electrolysis for hydrogen fuel production, to the pure curiosity of its inherent liquid form. In a recent essay in *Nature*, Philip Ball claims, "No one really understands water. It's embarrassing to admit but the stuff that covers two thirds of our planet is still a mystery."[1] While many authors of papers worldwide might disagree somewhat with that statement, they must admit that the substance has a hold on people's interests for a variety of reasons and as such generates a plethora of research results every year, some of which are hotly debated.

These efforts can be traced back quite far in history. Charles Tanford writes in his book of the accounts given by Pliny the Elder from first century AD in the volumes of *Natural History*, regarding the seasonal temporal fluctuations of bodies of water, water displacement and density of materials, and a phenomenon regarding the use of oil to smooth the waves of the sea.[2] Many centuries later one of the United States' founding fathers, Benjamin Franklin, also took interest in this last point. When traveling from America to Europe, he noticed that the rough waves of the sea were calmed as the ship he

was traveling on sailed through them. It was explained to him that the cooks must have poured their cooking oil overboard resulting in the calmed waters. Franklin resolved to further investigate this and repeated the experiment several times both at sea and on ponds while traveling abroad. He described the phenomena and his interpretations regarding the "mutual repulsion" between the oil and water in letters that were eventually published in an early scientific journal, *Philosophical Transactions*.

Though technology has advanced quite far since both Pliny and Franklin, and the nature of the research has moved from outdoors to a laboratory setting, the interest in the characteristics of the boundary between water and oil still remains fervent. This is due in part to the applicability of the water-hydrophobic surface as a model for more complex systems such as the cell membrane or a large, solvated biomolecule. There is also a purely fundamental curiosity in understanding the unique properties that occur at the boundary between two media, especially when one phase is water. These ongoing interests are the inspiration for the research presented in this dissertation.

Despite the longevity of interest in the nature of the liquid-liquid interface, much is still not known about the physical and chemical characteristics of this surface that is buried between two liquid phases. Deeper knowledge of the structure of the interface requires appropriate experiments that are able to probe only those molecules that compose the molecularly thin region where the two phases meet and interact without contributions from the bulk molecules. However, this has proven to be quite difficult until relatively recently. Advances in laser technology have led to the use of powerful non-linear spectroscopic methods such as vibrational sum-frequency spectroscopy

(VSFS) for the investigation of interfaces.[3-5] The application of VSFS was soon extended to such buried interfaces as the organic liquid-water interface.[6, 7] The advantage of this technique over others lies in its inherent surface specificity, which allows for the determination of the bonding characteristics and orientations of the molecules that exist in the unique interfacial environment.

The studies presented here focus on the aqueous phase of the organic liquid-water interface. The hydrogen bonding interactions between water molecules, their overall orientation, and the bonding-type interactions between water and the organic phase are all examined under different conditions. Varying the properties of the organic phase, as well as addition of salts and acid/base allow for the examination of interfacial water in a variety of environments. The results offer information that can be applied to more complex systems such as proteins with polar moieties or the ionic or pH conditions present at the surface of a cell.

The investigations of the organic liquid-water interface used VSFS as the primary tool. Chapter II summarizes the background of this technique. This includes the equations for the Fresnel coefficients as well as how spectra are analyzed. The latter is composed of brief explanations of spectral fitting and computationally generated VSF spectra. In Chapter III, the laser instrumentation used to carry out the VSFS experiments is described along with an explanation of how the data was treated once it was acquired.

In order to discuss the essential features present in the acquired VSF spectra, a solid understanding of the spectral assignments is necessary. This is presented in Chapter IV by discussing the neat CCl_4-water interfacial VSF spectrum and the conclusions

derived both by VSFS experiment and computation taken from research efforts by previous members of the Richmond laboratory who also investigated the liquid-liquid interface.

In Chapter V, VI, and VII, the different liquid-liquid interfacial systems investigations are presented. The effect of the non-aqueous phase polarity on the water structure is the subject of Chapter V. This is done by systematically changing the organic polarity using mixtures of the non-polar liquid CCl_4 with other liquids that have varying degrees of polarity: chloroform, dichloromethane, and 1,2-dichloroethane. Examining the interfacial spectra of these mixtures adjacent to water shows that overall water orientation is significantly changed depending on the polarity of the organic phase. The neat chloroform-water interface is considered in more depth and detail as an example of a moderately non-polar organic liquid-water interface. The analysis shows that water molecules still contain a significant degree of orientation within the interface but there are stronger bonding interactions present between the two liquids than have been seen at some other interfaces.

Chapter VI presents VSFS experiments on the addition of salts to the aqueous phase of the CCl_4-water interface. The spectra show evidence for the presence of ions within the interfacial region that alter the orientation of the water molecules in the aqueous phase. Comparison of the liquid-liquid spectra with similar previously investigated air- $salt_{(aq)}$ spectra reveals that the unique organic phase-water interactions facilitate very different behavior of the ions at the interface.

The last interfacial system presented is found in Chapter VII. Here, the effect of pH at the organic liquid-water interface is discussed. The results indicate the presence of H_3O^+ and OH^- ions have very different structuring effects on water than those of simple salts further characterizing the different properties that govern adsorption and interaction of different charged species at interfaces.

In the experiments described here, progress is made toward understanding how the water structure at organic liquid interfaces changes under several different conditions. This advances the picture of this important interface and its potential applicability to many hydrophobic-water systems.

CHAPTER II

OVERVIEW OF VIBRATIONAL SUM-FREQUENCY SPECTROSCOPY

Vibrational sum-frequency spectroscopy (VSFS) is a unique optical technique because it has inherent surface specificity, which allows for investigation of those molecules within the narrow region of the boundary between two different phases. This chapter presents the background behind this extremely useful tool for studying surfaces and interfaces. The discussion includes the interaction between light and matter; the non-linear response of the molecules in the interface; the relationship between molecular properties and the response of the interface; and analysis of VSF spectra. The latter includes brief discussions of spectral fitting and use of computational VSFS determined by molecular dynamics (MD) simulations.

Sum-Frequency Generation

A textbook definition of spectroscopy is the "study of the interaction between light and matter that encompasses a wide range of physical and chemical behavior."[1] The properties of the radiation determine how it affects the matter and what type of information can be learned about the matter. If the electromagnetic radiation amplitude is

relatively small, the material response is directly proportional to the amplitude of the electric field vector of the radiation and the experiments fall in the linear spectroscopy regime. This response in the media is the polarization. The use of intense light, like that produced by lasers for example, yields an induced polarization in the material that is no longer directly proportional to the applied field but instead has a non-linear response. The total induced polarization $\vec{P}$ is shown as an expanded power series in the electric field, $\vec{E}$, in equation 2.1. The proportionality constant is the susceptibility of the material χ.

$$\vec{P} = \left(\vec{P}^{(0)} + \vec{P}^{(1)} + \vec{P}^{(2)} + \vec{P}^{(3)} + ...\right) \qquad (2.1)$$

$$\vec{P} = \varepsilon_0 \chi^{(1)} \vec{E} + \varepsilon_0 \chi^{(2)} \vec{E}\vec{E} + \varepsilon_0 \chi^{(3)} \vec{E}\vec{E}\vec{E} + ...$$

The first order polarization and the linear susceptibility, $\vec{P}^{(1)}$ and $\chi^{(1)}$, govern those processes such as reflection and refraction. The second order polarization $\vec{P}^{(2)}$ becomes significant under intense electric fields. The VSFS experiments in this dissertation lie within this spectroscopic regime and are concerned with the corresponding non-linear susceptibility $\chi^{(2)}$.[2-8] As shown in equation 2.1, $\vec{P}^{(2)}$ is induced in a material by two electric fields $\vec{E}_{\omega 1}$ and $\vec{E}_{\omega 2}$. These fields can be the same frequency ($\omega 1 = \omega 2$), which results in radiation produced at twice the frequency of $\omega 1$ (or $\omega 2$) called second harmonic generation. If the two electric fields are of different frequencies ($\omega 1 \neq \omega 2$), radiation can be produced at either the sum or difference of these two frequencies.

The non-linear susceptibility term $\chi^{(2)}_{ijk}$ is a third rank tensor and has a maximum of 27 different elements (χ_{xxx}, χ_{xxy}, χ_{xxz}...). However, the number of unique contributing

(non-zero) elements is less due to symmetry constraints. In a centrosymmetric environment, such as bulk media, the value of any two inverse elements must be identical, i.e. $\chi^{(2)}_{ijk} = \chi^{(2)}_{-i-j-k} = -\chi^{(2)}_{ijk}$. The only condition for this to always hold true is when $\chi^{(2)} = 0$ for all elements. The result is that any process related to $\chi^{(2)}$, second harmonic generation (SHG), sum-frequency generation (SFG), or difference frequency generation(DFG), is forbidden in any centrosymmetric medium, which is the case for most bulk media. The boundary between any two bulk phases is inherently non-centrosymmetric and, therefore, a non-zero value of $\chi^{(2)}$ can occur there. VSFS (and SHG) exploits this property in order to study interfacial systems. The probe depth of VSFS experiments is thus limited that region where molecules contain an anisotropic orientation. When considering a liquid interface, such as those studied in this dissertation, the surface contains C_∞ symmetry. Under this symmetry condition and by the same argument made above, the elements of $\chi^{(2)}$ that can contribute to SFG are $\chi^{(2)}_{xxz} = \chi^{(2)}_{yyz}$, $\chi^{(2)}_{xzx} = \chi^{(2)}_{yzy}$, $\chi^{(2)}_{zxx} = \chi^{(2)}_{zyy}$, and $\chi^{(2)}_{zzz}$. Within the interfacial plane, the x and y axes are interchangeable, which further reduces the number of unique elements to four.

In the VSFS experiments presented here, a laser beam with a fixed visible frequency is overlapped both spatially and temporally with a tunable infrared (IR) beam at the liquid-liquid interface. A resulting beam at the sum of these two frequencies, $\omega_{SF} = \omega_{vis} + \omega_{IR}$, is then generated. The intensity $I_{\omega_{SF}}$ of the VSFS light generated at the interface is given by

$$I_{\omega_{SF}} \propto \left|\vec{P}^{(2)}\right|^2 \propto \left|\chi^{(2)}_{eff}\right|^2 I_{\omega_{IR}} I_{\omega_{vis}} \qquad (2.2)$$

showing that it is proportional to the squared second order polarization and thus to the square of the effective non-linear susceptibility. $I_{\omega_{IR}}$ and $I_{\omega_{vis}}$ are the respective intensities of the incoming tunable IR beam and visible beam. $\chi^{(2)}$ is composed of a non-resonant term, $\chi^{(2)}_{NR}$, and a resonant susceptibility term, $\chi^{(2)}_{\upsilon}$. $\chi^{(2)}_{NR}$ is observed to be zero for the current experiments.

The effective non-linear susceptibility is related to the actual susceptibility by the Fresnel coefficients and unit polarization vectors.[9]

$$\chi^{(2)}_{eff} = \left[\hat{e}(\omega)\cdot L(\omega)\right]\cdot\chi^{(2)}:\left[L(\omega_{vis})\cdot\hat{e}(\omega_{vis})\right]\left[L(\omega_{IR})\cdot\hat{e}(\omega_{IR})\right] \tag{2.3}$$

The Fresnel factors determine the extent that a beam is reflected or transmitted at an interface. They are given by the following equations.

$$L_{xx}(\omega_i) = \frac{2n^a_{\omega_i}\cos\theta^b_{\omega_i}}{n^a_{\omega_i}\cos\theta^b_{\omega_i} + n^b_{\omega_i}\cos\theta^a_{\omega_i}} \tag{2.4a}$$

$$L_{yy}(\omega_i) = \frac{2n^a_{\omega_i}\cos\theta^a_{\omega_i}}{n^a_{\omega_i}\cos\theta^a_{\omega_i} + n^b_{\omega_i}\cos\theta^b_{\omega_i}} \tag{2.4b}$$

$$L_{zz}(\omega_i) = \frac{2n^b_{\omega_i}\cos\theta^a_{\omega_i}}{n^a_{\omega_i}\cos\theta^b_{\omega_i} + n^b_{\omega_i}\cos\theta^a_{\omega_i}} \tag{2.4c}$$

The angles of incidence (θ^a) and transmission (θ^b), and the bulk refractive indices of the two media (n^a and n^b) at wavelength ω_i are used in these equations. Snell's Law determines the incident and transmitted angles, $n^a_{\omega_i}\sin\theta^a_{\omega_i} = n^b_{\omega_i}\sin\theta^b_{\omega_i}$. Figure 2.1 shows the reflection geometry used in the liquid-liquid experiments. All spectra shown in this dissertation were taken in the ssp (s = SF s polarized, s = vis s polarized, p = IR p

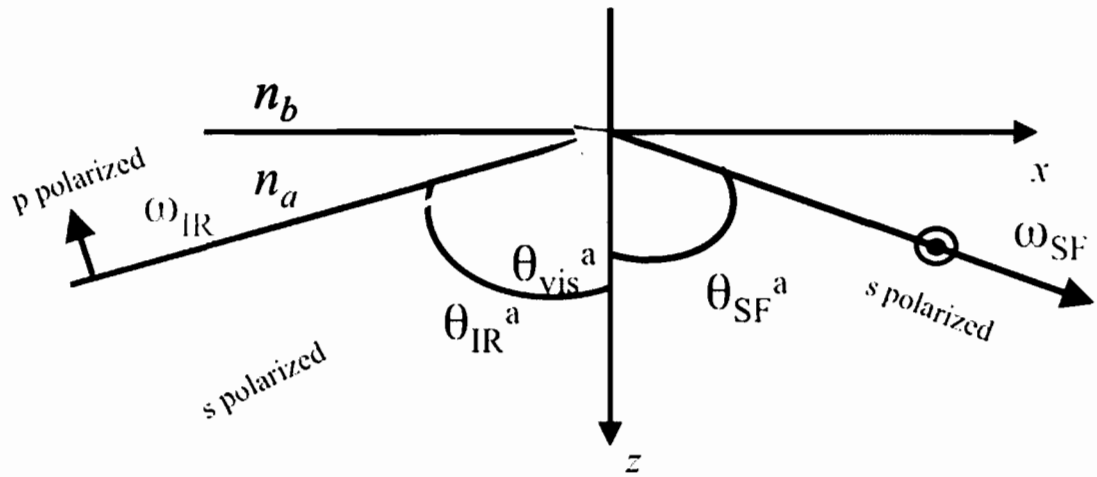

Figure 2.1 A Schematic of the experimental interface between two media with indices of refraction n_a and n_b. The incident angles (θ into medium a) for the visible and IR beams and reflected SF angle are shown.

polarized) polarization scheme, which probes the $\chi^{(2)}_{yyz}$ component of the tensor. This combination of input and output beams probes those vibrational modes that have a component of their transition dipole perpendicular to the interfacial plane. The equation for $\chi^{(2)}_{eff}$ then becomes

$$\chi^{(2)}_{effSSP} = L_{yy}(\omega_{SF})L_{yy}(\omega_{vis})L_{zz}(\omega_{IR})\sin\theta^a_{IR}\chi_{yyz} \tag{2.5}$$

The angle of the reflected sum-frequency beam is determined by the phase matching equation.

$$\sin\theta^a_{SF} = \frac{\omega_{vis}}{\omega_{SF}}\frac{n^a_{vis}}{n^a_{SF}}\sin\theta^a_{vis} + \frac{\omega_{IR}}{\omega_{SF}}\frac{n^a_{IR}}{n^a_{SF}}\sin\theta^a_{IR} \tag{2.6}$$

In order to achieve the maximum intensity possible from the buried liquid-liquid interface, a total internal reflection (TIR) beam geometry was employed.[10]

The non-linear susceptibility term $\chi_v^{(2)}$ is a macroscopic value related to the microscopic property, the molecular hyperpolarizability β, by the following equation.

$$\chi_v^{(2)} = \frac{N}{\varepsilon_0}\langle \beta_v \rangle \tag{2.7}$$

The angular brackets denote an ensemble average over all possible molecular orientations and N is the number density. Equation 2.7 shows that the VSF spectral response is directly proportional to the number of molecules contributing to SFG in addition to how oriented the molecules within the interface are. It should be noted that it is often difficult to distinguish between these two contributions when analyzing VSF spectral trends. The transition from the molecular frame (β) to the lab frame ($\chi^{(2)}$) requires a transformation via an Euler angle rotation for each element of the hyperpolarizability given by equation 2.8 where the lab frame coordinates x, y, z are represented by I, J, K and molecular frame coordinates are l, m, n.

$$\chi_{IJK,v} = \sum_{lmn} \mu_{IJK:lmn} \cdot \beta_{lmn,v} \tag{2.8}$$

Once this transformation has occurred and the orientational average is taken, an expression for the resonant macroscopic susceptibility can be obtained. This is given in equation 2.9.

$$\chi_{R,v}^{(2)} = \frac{NM_{IJ}A_K}{\varepsilon_0\left(\hbar\omega_v - \hbar\omega_{IR} - i\Gamma_v\right)} \tag{2.9}$$

In this expression, N is the number density, M_{IJ} is the Raman transition probability, A_K is the IR transition moment, and Γ_v is the inherent linewidth in the transition. As the IR is tuned over a range of frequencies and ω_{IR} approaches a resonance, ω_v, there is an increase in VSFS intensity producing a vibrational spectrum of interfacial molecules.

Interpreting VSF Spectra

Generally the non-linear susceptibility terms are complex quantities that have both phases and amplitude, which give rise to VSFS intensity that, as shown in equation 2.10, is the square of the sum of the terms.

$$I_{\omega_{SF}} \propto \left|P^{(2)}\right|^2 \propto \left|\sum_v A_{R_v} e^{i\phi_v}\right|^2 I_{vis} I_{IR} \tag{2.10}$$

Thus, the resulting spectrum can have either constructive or destructive interferences between contributions from different interfacial modes. This can result in distortions to the spectral appearance and renders interpretation of the spectra challenging. The equation, as written, is similar to 2.2 but written this way to show that the resonant second order susceptibility has an associated amplitude A_{R_v} that is defined by the response of the medium.

The VSF spectra can be fit to an expression for $\left|\chi^{(2)}\right|^2$ in order deconvolve the resonant modes from each other. The expression used by our laboratory was originally

developed by Bain and coworkers[6] and later implemented into the Igor Pro software by Dr. Fred Moore.[11] It is given by equation 2.11.

$$\chi^{(2)} = \chi^{(2)}_{NR} + \sum_{\upsilon} \int_{-\infty}^{+\infty} \frac{A_\upsilon e^{-\left[\frac{\omega_L - \omega_\upsilon}{\Gamma_\upsilon}\right]^2}}{\omega_{IR} - \omega_L - i\Gamma_L} d\omega_L \qquad (2.11)$$

The fit assigns a Lorentzian and a Gaussian width, a center frequency, an amplitude, and a phase to each resonant mode to account for the homogeneous broadening (Lorentzian lineshape) and inhomogeneous broadening (Gaussian lineshape) that results from the complex molecular environment found at the liquid-liquid interface. A non-resonant mode can also be assigned but, again, is not detected for liquid-liquid VSF spectra.

One of the first apparent challenges is how to determine the number of peaks to use when fitting a spectrum or series of spectra because a greater number of peaks corresponds, in general, to a better fit to the data but also is less justifiable in terms of assigning meaning to the vibrational mode. This is particularly true in the case of the spectra presented in this dissertation because of the broad nature of several spectral features representing a very diverse water hydrogen bonding environment. It is not entirely correct to think of these modes as originating from one particular water species but really to a continuum of different bonding geometries and strengths. If spectra are fit to three different resonant modes, for example, the result is 3 peaks x 5 parameters = 15 different variables. With so many parameters and several peaks present, ways to minimize arbitrary assignments are necessary. Isotopic dilution experiments have been performed, both for the CCl_4-water and the air-water interfaces, to aid in deconvolution of the OH interfacial spectrum.[12, 13] Using mixtures of H_2O and D_2O removes

intermolecular coupling between the two OH oscillators by forming HOD thereby greatly simplifying the complex spectrum of the OH region. Additionally by varying the ratio of HOD, H_2O, and D_2O there are several spectra that can be iteratively fit using a global fitting analysis that constrains many of the above parameters for each spectrum, thereby giving a more rigorous analytical fit to the data. This method was applied to the chloroform-*d*-water interface spectrum that is discussed in Chapter V.

Recently our research group has also begun to analyze VSF spectra with computational methods. The work by Dr. Dave Walker[14] focused on applying the methods originally developed by Morita and Hynes[15, 16] to generate computational spectra via molecular dynamics (MD) simulations. With the increased efficiency of computer processor speeds and the availability of modeling packages, these methods are more easily applied to increasingly complex interfacial systems. In this method, the molecular coordinates and forces acting on each atom are recorded at periodic intervals during the simulation. The coordinate information is used to project molecular hyperpolarizability tensor elements into the lab frame, providing the amplitude of the VSFS response. The force information is also used to determine the frequency of the stretching modes. Together, this information gives a calculated VSF spectrum that is directly comparable with experimental results, especially when Fresnel coefficients can be calculated. This provides a way to check the validity of the calculations as well. The calculated spectra can then be deconvolved into the detailed contributions from differently bonded water species with molecular resolution.

The combination of both experimental and computational approaches to spectral analysis has proven very powerful in furthering the understanding of the water species and environments at aqueous interfaces. Specific assignments and conclusions from these methods as applied to the neat CCl_4-water interface are the focus of Chapter IV.

CHAPTER III

EXPERIMENTAL CONSIDERATIONS

This chapter describes the apparatus and procedures used to acquire vibrational sum-frequency spectra of the liquid-liquid interface. First, a general description of experimental sum-frequency generation is provided. Next, the two different laser systems used in the non-linear optical experiments are described, including the generation of both visible and infrared pulses from picosecond and nanosecond lasers, the sample cell apparatus, and detection instrumentation. This is followed by a section that discusses the treatment of spectra once they are acquired, including normalization processes.

Sum-Frequency Generation

As described in Chapter II, Shen and coworkers pioneered the experimental exploitation of sum-frequency generation (SFG) almost two decades ago.[1, 2] Since then there have been many advances in laser and optical technology such as the ability to generate infrared pulses at longer wavelengths and ultrafast broadband SFG techniques.[3-6] These advances have brought many opportunities to investigate new interfacial systems using VSFS such as analysis of different functional groups or dynamical information

regarding adsorption processes.[7, 8] One outcome of these advances is that new instrumentation becomes more readily available. This is the reason that two different laser systems were used to carry out the VSFS experiments presented in this dissertation. Details of the first laser system used to obtain some of the spectra presented in Chapter V are described in the next section: The Nanosecond Laser System. This system was built by Dr. Larry Scatena, a former member of the Richmond laboratory and the present Shared Laser Facility Director at the University of Oregon. Details of this system have been published previously[9] so they will only be briefly summarized in the following section.

With the use of VSFS on the rise, some companies have begun to offer entire SFG systems for sale. These have some advantages over homebuilt systems. One advantage is that one company maintains all the system components, from pump laser to data acquisition software, which makes troubleshooting easier. Another advantage is that the entire apparatus is installed and ready to take data within a shorter period of time than it would take to build a system oneself. One company, Ekspla from Vilnius, Lithuania, has been selling such systems worldwide for several years to date. A commercially available system purchased from Ekspla was used for the majority of the experiments (part of Chapter V, all of Chapters VI and VII) described in this dissertation. It will be described in more detail in the third section, The Picosecond Laser System with particular note to modifications made to the commercial system. This laser system was installed by Dr. Irmantas Mikulskas of Ekspla and Lucian Hand of Altos Photonics Inc. and was maintained by Daniel Beaman and myself.

The Nanosecond Laser System

The system consists of a diode seeded Nd:YAG pump laser (Coherent Infinity-100) with 1064 nm output, 3.5 ns pulse width, and a 20 Hz repetition rate. The laser produces 500 mJ pulses. These are split with one portion being frequency doubled to make light at 532 nm that is sent to the interface for use in experiments. This is done using a beta-BaB_2O_4 (BBO) crystal that is temperature regulated to maintain constant energy output. The remainder of the 1064 nm beam is used for the infrared (IR) beam generation. It is again split into two portions, one of which is frequency doubled to generate 532 nm light using a potassium titanyl phosphate (KTP) crystal. This visible light is directed into the double pass optical parametric oscillator (DPOPO), which consists of two KTP crystals and high reflective cavity mirrors to allow two passes of the 532 nm pulses but partial output of the resulting signal (740 – 840 nm) and idler (1450 – 1850 nm) light. The crystals are counter-tuned to generate the range of wavelengths listed with minimal spatial beam walk-off. The idler beam's polarization is rotated and then sent collinearly into the potassium titanyl arsenate (KTA) crystals of the optical parametric amplifier (OPA) with the remaining portion of the 1064 nm light. Here the IR beam for use in the VSFS experiments is generated (2500 – 4000 nm) through difference frequency generation (DFG) in the angle tuned KTA crystals. The resulting resolution of the pulses is ~$2cm^{-1}$.

Both the 532 nm and IR beams are focused, collimated, and polarizations selected before being propagated to the interface. The pulse energies measured prior to the

interface are 2 mJ and ~1.2 mJ for the 532 nm visible and IR light (3200 cm^{-1}) respectively. A photomultiplier tube detects the generated signal. In order to detect only SFG light, a combination of blue glass, holographic notch, long and short wave pass filters are used. A polarizing beam cube is used to select for the SFG beam polarization. A small portion of the IR beam that is split off and collected concurrent with a VSFS scan is used to normalize some of the spectra presented in Chapter V, accounting for fluctuations in IR energies throughout the wavelength region studied.

The Picosecond Laser System

The system is a commercially available system purchased from Ekspla (Vilnius, Lithuania), the main components of which are shown in Figure 3.1. It is pumped by a Nd:YAG laser (model PL2143A), which has pulses ~30ps in width, a10Hz repetition rate, and up to ~600 μJ peak energy. This is accomplished first using a master oscillator comprised of a flash lamp pumped Nd:YAG rod within a cavity of both a convex and concave mirror. Active and passive mode locking through use of a Pockel's cell with a polarizer and a solid state modulator allow for high stability both in energy and time. By introducing dynamic and fixed energy losses so that the pulse energy remains at ~10 μJ within the master oscillator cavity for ~200 roundtrips, stable bandwidth-limited pulses are generated. An intra-cavity regenerative amplifier produces high pulse energies without damage to the solid state modulator. Pulses are directed into the regenerative

amplifier via another Pockel's cell and polarizer where they undergo a set number of oscillations to achieve peak power before they are dumped into the power amplifier.

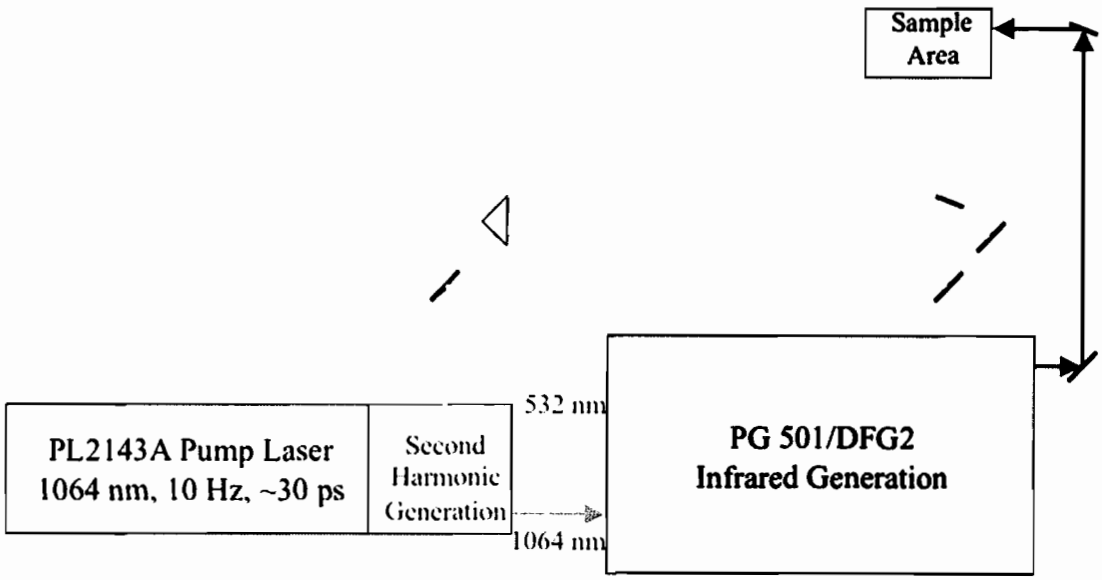

Figure 3.1 A schematic of the optical setup used for the VSFS experiments

After being spatially filtered by a lens and pinhole, the beam makes a double pass through a second Nd:YAG rod that is pumped by two flash lamps. From the power amplifier stage, the pulse is shaped by a series of lenses and a portion of the 1064 nm fundamental output is sent through a heated potassium dideuterium phosphate (K*DP) crystal where it is frequency doubled to generate 532 nm light. Prior to this, the beam is rotated by a half-wave plate (HWP) to achieve the maximum frequency conversion possible within the crystal. A dichroic mirror that, along with a beamsplitter, divides the 532 nm beam into two portions filters any 1064 nm that also propagates through along with the 532 nm light.

One portion of this 532 nm light is used as the visible portion (ω_{vis}) to generate the VSFS signal. After the pulses leave the box housing the pump laser optics, the beam polarization is selected using a combination of half-wave plates and a Glan prism polarizer. The beam is then sent through two lenses and a pinhole where it is spatially filtered and collimated. Next a small portion of the beam is split off and sent to a photodiode in order to monitor the energy output and stability. The beam is then propagated a few more feet and sent through a prism mounted on a micrometer stage. This prism allows for changes in the timing overlap of the visible and IR pulses at the interface. With pulses around 30 ps, the window of overlap is only around 9mm. After reflection through the prism, the visible beam is focused down to a few mm in diameter and then proceeds to the sample area optics.

The remaining 532 nm light, in addition to the 1064 nm light not frequency doubled, are used in a series of parametric processes (Ekspla model: PG501/DFG2-10P) to generate the tunable IR light. First, the 532 nm beam is divided into two lines using a beamsplitter. Both lines are telescoped to ~5 times smaller than the original diameter. The portion of 532 nm that passes through the beamsplitter (~15%) makes a double pass through a heated BBO crystal. A dichroic mirror separates the parametric and pumping 532 nm pulses. The parametric beam is telescoped and then sent to a diffraction grating where the spectral width is narrowed. A series of optics comprised of a filter, lenses, and pinhole generate a beam with the desired wavelength and breadth that is then directed to a second heated BBO crystal where it is overlapped with the remaining 85% of the 532

nm beam. After two passes through the crystal, a dichroic mirror and Glan prism polarizer separate the signal, and idler beams, respectively.

The 1064 nm fundamental is first relay imaged by two lenses and an evacuated tube to ensure a clean beam profile before being sent through a non-linear crystal. After being filtered, the 1064 nm beam is sent through a prism delay line so that it can be overlapped in both time and space with the idler beam (1.064 – 2.3 nm) from the OPA in a $AgGaS_2$ crystal where they mix through the DFG process. This generates IR radiation for use in the VSFS experiments that is tunable from ~1000 to 4300 cm^{-1}. The DFG crystal, like the other two BBO crystals, is angle tuned to generate a range of frequencies but the $AgGaS_2$ is tuned perpendicular to the plane of the optical table. With this vertical movement, the IR beam can move as the frequency is tuned. Therefore a compensator is employed that counter-tunes with the crystal to avoid beam movement. Residual 1064 nm and idler beams are then filtered. After leaving the box that houses the optics, a small portion of the IR beam is sent to a photodetector using a BaF_2 window and the remainder proceeds to the sample area optical set-up.

The sample area optical scheme is shown in Figure 3.2. After being focused (f = +700 mm), the 532 nm beam travels through a machined hole in a vertical breadboard where it is reflected three times by different dielectric mirrors (M1 – M3) in order to propagate the beam towards the sample cell. In the process, the beam polarization is rotated 90°. The IR beam polarization is also rotated by reflection off two periscoping gold mirrors mounted on a kinematic mount (P1). The beam is again sent through a periscope in order to achieve a trajectory towards the interface (P2). Before reaching the

sample cell, the IR beam is focused by a BaF_2 lens (f = +150 mm) mounted on a micrometer stage. A change in the position of this lens by a few mm so that the focal length is closer/further from the interface results in an increase/decrease in VSFS intensity but, for most experiments, the lens was kept ~200 mm from the liquid-liquid interface to avoid boiling the sample.

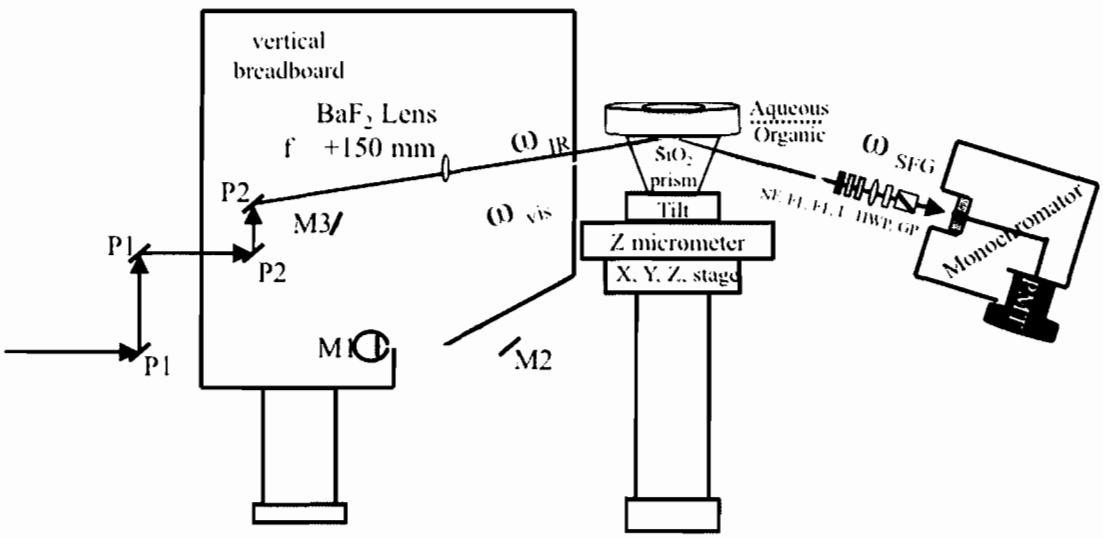

Figure 3.2 A schematic of the sample area P = periscope, M = mirror, NF = notch filter, EF = edge filter, L = lens, HWP = half-wave plate, GP = Glan prism, PMT = photomultiplier tube

In both the nanosecond and picosecond laser experimental set-ups, the 532 nm visible beams is overlapped at the liquid-liquid interface in a total internal reflection (TIR) geometry to maximize the VSFS signal intensity.[10] Because of limited space around the sample area, the IR beam is configured so that it will not be physically blocked by any optics resulting in a much shallower beam angle. For the halocarbon experiments, the visible and IR beams were overlapped at the liquid-liquid interface at angles of 66.3° and 71° from the plane perpendicular to the interface respectively. For both the salt and pH studies, the angles were chosen so that TIR was maintained for all

solutions. Beam angles to achieve this geometry were 69.5° and 75° with respect to the interface normal for the visible and IR beams respectively. Beam energies used are 80 μJ for the visible and ~200-250 μJ for the IR beams in the 2800 – 3800 cm^{-1} range.

In order to separate the reflected visible light from the generated SFG beam, two RazorEdge filters (Semrock) and one holographic notch filter (Kaiser Optical) are employed. The remaining VSFS light is focused by an anti-reflective coated BK7 lens (f = +100 mm) and the polarization selected by a Glan prism polarizer and half-wave plate, all part of the Ekspla system. The beam is then sent through a monochromator (model MS2001) and detected by a photomultiplier tube (Hamamatsu R7899).

Sample Cell and Materials

A similar liquid-liquid sample cell was used in the experiments conducted on both laser systems. It consists of an IR grade fused silica prism clamped to a Kel-F cylinder and sealed by a Viton o-ring. The prism is cut at an angle 66° from the vertical plane to limit the amount of reflected visible radiation when working with typical TIR beam angles. Some advantages of using an IR grade fused silica prism are that the index of refraction in the visible wavelength region is very similar to that of CCl_4, which is used as the organic liquid for most of the experiments presented in this dissertation. It is also a relatively robust material. However, a disadvantage is the limited transparency of light in the IR wavelength region. This is discussed further below. A watchglass was placed over the opening of the Kel-F cell in order to keep out debris. The base of the cell is attached

to a one inch optical post that goes into a post holder screwed into a tilt stage. This allows the beams to propagate in a straight line without being deviated by slight rotations in the prism or skewed angle of the cell. A digital level was used to assure that the cell was not askew.

The spectra of the liquid-liquid interface are especially susceptible to the effects of contaminants. Therefore these experiments used high purity liquids, salts, acid, and base. Specific grades and purification techniques will be presented at the beginning of each of the chapters discussing the work. The H_2O used for the aqueous phase in all experiments came from a Barnstead Nanopure II system (~17.9 - 18 MΩ cm). All measurements presented here were taken at room temperature. The sample cell and all glassware used in the experiments were soaked in concentrated sulfuric acid containing NoChromix and then rinsed thoroughly with the Nanopure filtered water before use.

Spectra Collection and Manipulation

All spectra shown in this dissertation were taken in the ssp (s = SF, s = vis, p = IR) polarization scheme. This probes the yyz element of $\chi^{(2)}$ and those molecules who have a component of their transition dipole in the plane perpendicular to the interface. The following steps were taken during and after VSFS spectral acquisition to ensure the most accurate data possible. First, as shown in Chapter II, because the VSFS intensity is dependent on the incoming beam energies, both the IR and visible beams were measured before each spectrum was taken and adjusted as needed to keep the energies constant.

The photodiodes in the picosecond laser system also aided in assuring there was no drift in pumping energies. They only report relative count numbers though, so measurement with an external joule meter was necessary.

Second, multiple spectra were taken of each interface and averaged together on a given day to obtain greater signal to noise for the spectra. Spectra were also taken over several days in order to assure reproducibility and average out any slight changes in beam overlap or focusing that might affect the spectral intensity. When the nanosecond laser system was employed, a VSF spectrum was normalized by dividing the raw spectrum by the IR spectrum taken concurrently with it. This accounts for fluctuations in the IR energy with wavelength. For all other experiments, spectra were normalized to account for variations in IR energy resulting from the non-linear optical generation processes, the decreased transparency below ~2900 cm^{-1}, and for the small absorption of IR energy at ~3600 cm^{-1} by the fused silica prism. Taking spectra of the non-resonant SFG response of an uncoated gold mirror in place of the aqueous phase but still in contact with the respective organic liquid and dividing them into the raw spectra accomplished this.

It is important to note that normalizing by dividing the spectra by the IR profile alone, which is taken concurrently with each spectrum, can generally compensate for many of the features that affect the overall VSF spectrum such as the IR profile and absorption of water vapor that occurs in the spectral region around ~3600 cm^{-1}. However, the small absorption by the prism is not accounted for by this normalization procedure and, if not taken into account, results in different ratios for the different spectral modes. This does not significantly affect the overall conclusions drawn from the

spectra but accounting for any contributing factors that alter the shape of the spectrum outside the actual vibrational signatures should always be a goal if possible. Figure 3.3 shows the IR profiles from both laser systems in the 2800 – 3800 cm^{-1} region along with the gold-CCl_4 VSF spectrum in order to show how different ways of normalization could affect the resulting spectra.

Local field corrections were taken into consideration only for the comparison of the neat CCl_4-water and $CDCl_3$-water spectra (Chapter V) taken in the ssp polarization scheme by calculating the Fresnel factors and unit vectors using a two state model adapted from a paper by Shen and coworkers.[11] Figure 3.4 shows the resulting corrections for CCl_4-water with the air-water for coefficients comparison. The effect on the CCl_4-water interface spectrum is also shown in Figure 3.4. This was done using values for the real refractive indices of the fused silica in both the visible and IR.[12] In addition, the calculations assumed real and constant indices of refraction for both the CCl_4 and chloroform liquids (1.4607 and 1.4419 respectively) based on their transparency through the spectral regions used in the current experiments.[13, 14] The real and imaginary values of the indices of refraction for water in both the visible and IR energy regions were used.[15] Previous analysis of isotopic dilution spectra at the air/water interface have shown that the use of Fresnel factors incorporating D_2O and HOD indices of refraction did not significantly change the conclusions so they were not used with regards to the isotopic dilution experiments.[16] The beam angles used in the calculations were those cited in the previous section. When the normalized spectra are then divided

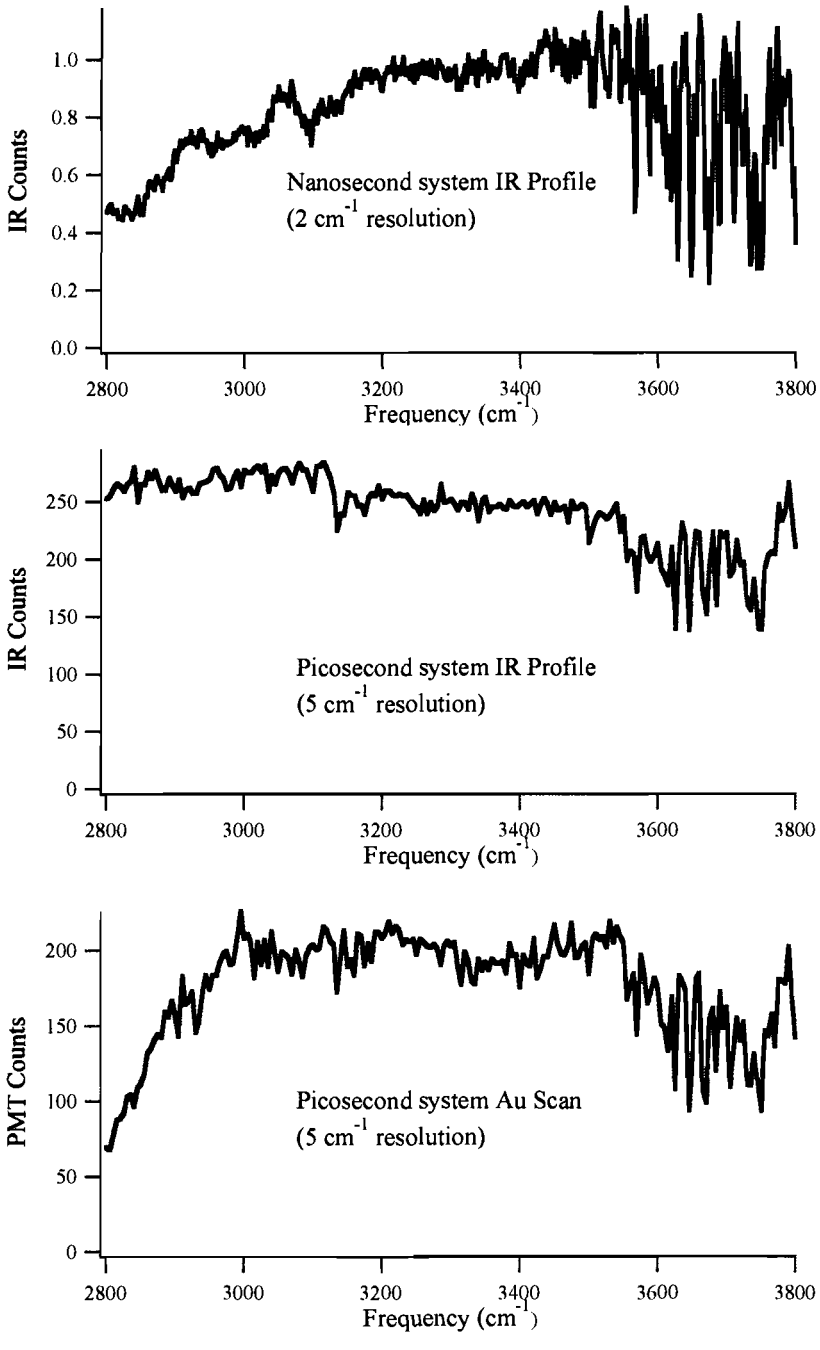

Figure 3.3 IR profiles from the nanosecond and picosecond laser systems with the Au/CCl_4 spectrum for comparison.

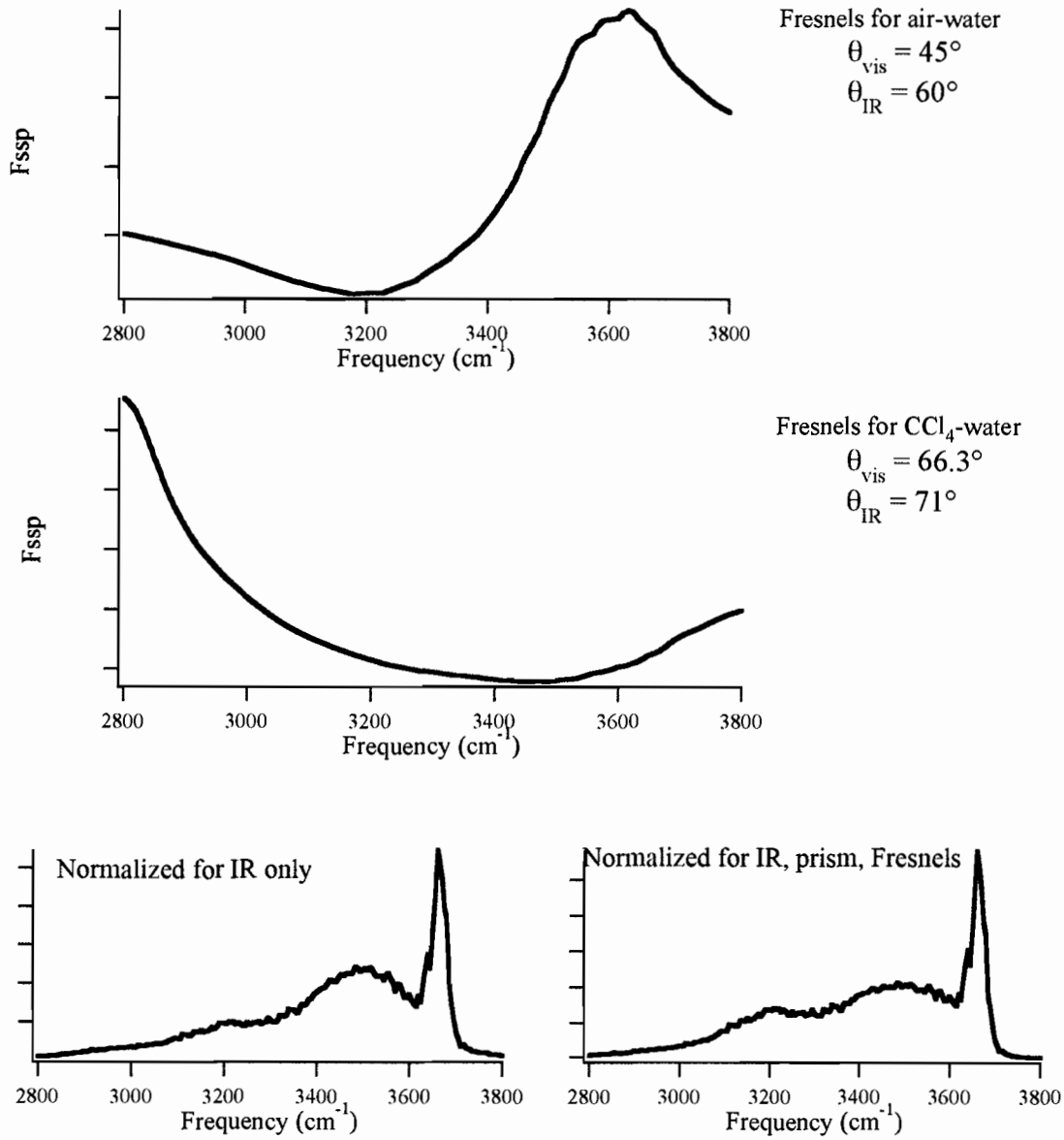

Figure 3.4 Fresnel coefficients calculated for ssp spectra for the air-water (top) and CCl_4-water (middle) interfaces using the formalism outlined by Shen and coworkers in Reference 11. Beam angles used for the calculations are listed. The bottom two plots show the difference that accounting for prism absorption and Fresnels makes on the CCl_4-water spectrum appearance.

by these corrections, the resulting spectra are $\left|\chi^{(2)}\right|^2$ not $\left|\chi_{eff}^{(2)}\right|^2$ which allows for a more direct comparison between VSF spectra.

These Fresnel factors were not calculated for other interfaces studied in this dissertation. This is due to the lack of availability of the real and imaginary values of the indices of refraction, in both the visible and IR, for the different organic liquid mixtures (Chapter V), aqueous salt solutions (Chapter VI), and aqueous pH solutions (Chapter VII). While it is more rigorous to compare spectra of $\left|\chi^{(2)}\right|^2$ than $\left|\chi_{eff}^{(2)}\right|^2$, it is not possible at this time without the available data to do the calculations. With advances in ellipsometry, perhaps this type of information will be more widely available or at least measureable in the future. In addition, the model used to calculate the Fresnel factors makes a difference in the overall effect on the spectrum. Because the properties at the interface are different than in the bulk, using a two state model, i.e. bulk values of the indices of refraction may also introduce some errors. Nonetheless, analysis of $\left|\chi_{eff}^{(2)}\right|^2$, especially when comparing spectra taken in similar experimental conditions (beam angles etc) can provide valuable information regarding the interfacial environment.

CHAPTER IV

THE NEAT ORGANIC LIQUID-WATER INTERFACE

In order to understand and interpret the VSF spectra presented in the following chapters, an overview of the general features for the neat CCl_4-water spectrum is necessary. The broad nature of the modes exhibited by much of the spectral region resulting from the condensed phase interface, and the complicated lineshapes resulting from VSF spectral interferences, make analysis and assignment of spectral features challenging. The interpretation of the CCl_4-water spectrum described in this chapter is a result of a combination of efforts, consisting of isotopic dilution in conjunction with spectral fitting[1, 2] as well as MD analyses,[3, 4] that provides a detailed picture of the interface and a reference point for the experiments in the chapters that follow.

Introduction

The neat organic liquid-water interface is an attractive system to study for several reasons. This interface, comprised of two immiscible liquids, is a good example of water adjacent to a hydrophobic surface. Further, the interactions between water and hydrophobic media find application in many research areas such as materials science,

environmental science, and biochemistry. In recent years a number of new experimental techniques have emerged that provide increased understanding of the liquid-liquid interfaces. Such techniques include vibrational sum-frequency spectroscopy (VSFS),[2, 5-7] second harmonic generation (SHG),[8-11] x-ray[12-17] and neutron reflectivity,[18-20] and other methods.[21, 22] Computational methods have also been shown to provide invaluable information regarding the interfacial structure.[3, 4, 23-30]

A clear advantage of using VSFS to investigate the organic liquid-water interface is that it provides experimental molecular-level insight into the orientation, structure, and bonding of the interface. In the experiments presented herein, the aqueous phase is the focus. The spectra are comprised of water OH stretch modes that are highly sensitive, in both frequency and spectral width, to their local bonding environment. However, this high sensitivity also has its challenges. Once a VSF spectrum is obtained, analysis and assignment are made more difficult due to the homogeneous and inhomogeneous broadening of the peaks in addition to interference effects arising from the nature of the VSFS response.

One method of mitigating the complexity of the vibrational spectrum of water is the use of isotopic dilution where spectra of mixtures of H_2O, HOD, and D_2O are acquired. Looking at primarily HOD at the interface largely removes the inter- and intra-molecular coupling of water, thereby reducing the number of hydrogen bonded species that contribute to a spectrum. These simplified spectra can then be fit and assignments made with more confidence.

Another method used to understand the complex water vibrational modes is to generate theoretical spectra whose molecular coordinates and properties are determined by molecular dynamics (MD) simulations following the technique of Morita and Hynes.[31] This method has an inherent check in that if the calculated spectra agree reasonably well with experiment, the computational models are validated. From these spectra, further insight is gained regarding hydrogen bonding species, interfacial depth, and orientation. MD can also provide valuable information regarding the nature of the non-aqueous phase at the organic liquid-water interface, which is more difficult to probe spectroscopically and has not been investigated thus far by VSFS.

The following summarizes the general, current understanding of the environment at the CCl_4-water interface. The conclusions drawn from experiment and computation are described together rather than separately, as they are complimentary methods and the picture is better understood this way. The experimental VSFS, isotopic dilution, and fitting results were taken from the work of Dr. Larry Scatena[2] and the computational VSFS results come from the studies by Dr. Dave Walker.[3, 4] The investigations into the non-aqueous phase were done primarily by Dr. Dennis Hore.[28, 29] The spectrum shown below was acquired using the picosecond laser system and normalization procedures described in Chapter III. The analysis of the neat CCl_4-water interfacial spectrum discussed here will be referred to in Chapters V, VI, and VII in order to compare the changes in the spectrum due to alteration of the interface.

The CCl_4-Water Interface

The experimental VSF spectrum of the neat CCl_4-water interface is shown in Figure 4.1. The distinct spectral features convey a great deal about the structure and interactions at the boundary between the two phases. A cartoon of the interfacial picture formed from the following results is shown in Figure 4.2. To begin, water molecules at the CCl_4-water interface are highly oriented. This is shown in part by the presence of the sharp, intense spectral feature near 3665 cm^{-1}. It corresponds to one of the energetically uncoupled OH stretch modes of water molecules that "straddle" the interface. The OH oscillator from these water molecules, referred to as the "free OH," interacts directly with the CCl_4 phase. This interaction results in the vibrational mode at the high energy side of the spectrum, at a stretching frequency more similar to those of gas phase water, due to the lack of other water molecules for the oscillators to bond with. Because these water molecules are in direct contact with the organic phase, they physically reside in the topmost interfacial layer closest to the dividing surface.

Additionally, because the free OH is in contact with the non-aqueous phase, its frequency is a good indicator of the degree of interaction between the two liquid phases comprising the interface. As depicted in Figure 4.2(a), the straddling water molecules' free OH modes undergo a certain degree of weak bonding or dipole-type interactions with the non-aqueous phase molecules. This has been noted not just for the case of organic liquid-water interfaces but also the air-water and solid phase-water interfaces studied with VSFS by this group. The greater the frequency value, the less interaction

exists between the two phases, which is a certain measure of hydrophobicity of the non-aqueous phase. This will be discussed further in Chapter V with regards to free OH values for different liquid-liquid interfaces.

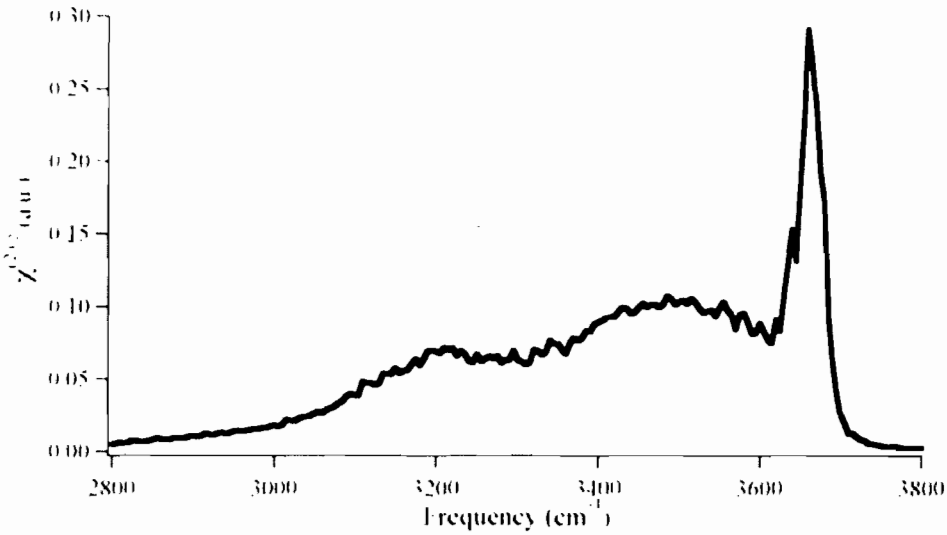

Figure 4.1 VSF spectrum of the CCl_4-water interface

Due to the geometry of water molecules, the companion OH oscillators on the straddling water molecules that are not pointing into the organic phase are necessarily oriented towards the aqueous phase where they can hydrogen bond to other water molecules. These OH oscillators can act as hydrogen bond donors to other water molecules slightly deeper within the interfacial region and are thus referred to as the "donor OH" modes. Again, these straddling water molecules that have weak hydrogen bonding character are found within the top region of the interface. These interactions are depicted in Figure 4.2(b). The broad spectral region seen in Figure 4.1 of the CCl_4-water spectrum around 3500 cm^{-1} is attributed mostly to these weakly hydrogen bound oscillators.

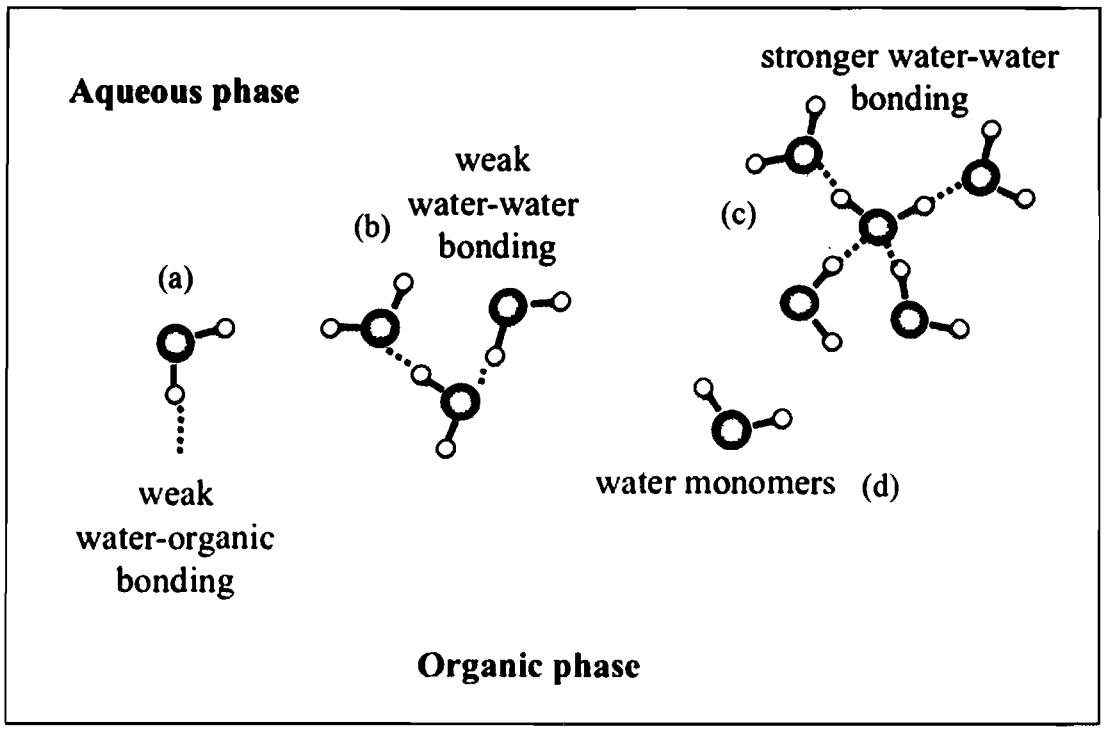

Figure 4.2 Cartoon of the neat CCl_4-water interface showing the general different types of bonding environments present

The assignment of this spectral region was initially based on isotopic dilution experiments in conjunction with spectral fitting methods.[2] Computational VSF spectra generated from MD simulations performed by our research group also support the assignment that the types of water molecules that comprise this spectral region are mainly weakly bonded species with one OH oscillator donating a hydrogen bond.[3] Because the computational spectra can be further deconvoluted to give even more detail regarding how each water molecule in the simulation is bonded, results show that the broad peak centered around 3500 cm^{-1} is also due to water molecules that both accept hydrogen bonds through one or both of the lone pairs on the oxygen atoms as well as donate hydrogen bonds through the hydrogen atoms. This is also shown in Figure 4.2(b). With

the configuration of the straddling water molecules, the transition dipole moments of these OH oscillators are mostly in the plane perpendicular to the interface. This allows them to contribute significantly to the spectra taken in the current ssp polarization scheme.

Additional computational studies analyzed the VSF spectral intensity as a function of interfacial depth in order to better understand the physical picture of water at the interface. Although arguments, such as those given above for the straddling water molecules, can be made from the experimental spectra with regards to where in the interface a particular water species resides, these types of additional computational studies provide confirmation of those conclusions with added molecular detail. The results for the simulations and calculated VSF spectrum of the CCl_4-water interface confirm that the spectral region around 3500 cm^{-1}, from the weakly bound straddling water molecules, arises from water molecules near the top of the interface.[4] All of these different water moieties, including the single donor OH and the OH donor/acceptor, have overlapping spectral signatures, thus generating the broad peak seen around 3500 cm^{-1}. This exemplifies the complexity of these liquid systems, which must be kept in mind when interpreting the data and attributing peaks not to distinct species but to a collection of modes.

In addition to the straddling, more weakly bound water molecules, the interfacial region also houses water molecules with greater hydrogen bonding character. These water molecules form a network with stronger hydrogen bonds to a greater number of neighboring water molecules. They are pictured in Figure 4.2(c). Their spectral

contributions are assigned to the lower frequency region of the spectrum centered at 3200 cm^{-1}. Initial experimental observations led to the conclusion that water molecules contributing to this spectral region mainly reside deeper in the interfacial region in comparison to the free OH and donor OH, which have weaker bonding character.[2, 6] This is supported by the recent interfacial depth-sensitive MD simulations.[4] The structure of molecules in the spectral region around 3200 cm^{-1} is referred to as a "tetrahedral" bonding structure due to similarities with vibrational signatures seen in bulk IR studies of water-ice that exhibit broad modes also in the same frequency region. Although simulation results have confirmed that these types of fully coordinated water species contribute in part to this portion of the spectrum, there is also intensity in this region, as well as throughout most of the OH stretch region, arising from collections of more and less coordinated or bonded water molecules as well.[3]

From the VSFS experiments and spectral fits of the CCl_4-water VSF spectrum, there is also evidence of a very small concentration of "water monomers" in the interfacial region that exhibit a high degree of orientation. These species are defined as those water molecules that typically reside on the non-aqueous side of the dividing surface and have no hydrogen bonding interactions with other water molecules. Figure 4.2(d) shows them pictorially. The peak frequencies are from both the symmetric and anti-symmetric stretches since they are not energetically uncoupled. They show up at the high energy side of the spectrum where they can spectrally interfere with the other modes. Their existence has been confirmed by the MD simulations and shows that a

weak interaction exists between water and CCl_4 in the interfacial region, which allows for a small amount of mixing to occur between the two liquids.

The focus of this dissertation research, and other past VSFS studies of organic liquid-water interfaces, has been on the structure of the aqueous phase. This is due largely to experimental limitations, both in the necessary sample geometries and in accessing the vibrational frequencies of the organic phase molecular functional groups. This is another area that MD simulations can provide useful information. In one study, it has been shown that the structure of CCl_4 at the interface is affected by the overall water orientation.[28] In this study, the CCl_4 phase was observed to have a layered structure consisting of corner and face orientations directed towards the bulk water phase. It is thought that this structuring occurs in response to the out-of-plane field created by the highly oriented water molecules at the interface. In the pioneering MD work of the CCl_4-water interface, done by Chang and Dang in 1996, results also showed both the water and CCl_4 molecules have significant structural ordering at the interface that was very different than in the bulk.[25] As a result of the orientation of interfacial water molecules, the CCl_4 molecules have a larger induced dipole. The authors of both studies hypothesized that these interactions might have implications for charge accumulation at the interface. This will be discussed further in Chapters VI and VII.

Conclusions

With advances in both experimental[2, 11, 16] and computational techniques,[3, 4, 24, 28, 29, 31] an overall picture of the CCl_4-water interface is emerging that incorporates the interplay between both liquids and the complex bonding environment of the water phase. Those water molecules that straddle the interface undergo very weak interactions with the non-aqueous phase resulting in a free OH spectral peak at ~3665 cm^{-1}. They also have weak bonding interactions with other water molecules through several bonding geometries resulting in a broad spectral region centered at 3500 cm^{-1}. Water molecules with stronger bonds to a higher number of other waters are responsible for the VSF intensity found in the lowest frequency spectral region, below 3400 cm^{-1}. The properties of the non-aqueous solution are also integrally related to the structure of the water orientation. This picture is a solid foundation to build on for the experiments found in Chapters V – VII.

CHAPTER V

HALOCARBON-WATER INTERFACES: EFFECTS OF THE NON-AQUEOUS PHASE POLARITY ON INTERFACIAL WATER BONDING AND ORIENTATION

This chapter presents vibrational sum-frequency spectroscopy (VSFS) studies of the bonding and structure of water molecules at different halocarbon-water interfaces. The OH stretching modes of interfacial water molecules are used to characterize and compare the interactions between water and the different halocarbons in the organic phase. First, mixtures of non-polar CCl_4 with more polar solvents $CHCl_3$, dichloromethane (DCM), and 1,2-dichloroethane (DCE) are used to vary the polarity of the organic phase. Next, the neat chloroform-water interface is examined in more detail using spectral fits incorporating isotopic dilution. The spectroscopic results show differing degrees of interaction between water and the various halocarbon molecules in the interfacial region as manifested in spectral shifts and intensity changes in the OH stretching modes.

Introduction

The organic liquid-water interface is a relatively simple system that can serve as a model for many more complex hydrophobic-aqueous interactions such as a large, solvated biomolecule. Many times these interactions are not between water and a completely hydrophobic or non-polar medium but with one that possesses domains that are more polar in nature. The studies presented here use VSFS to obtain a more detailed picture of the effect of the variation of the polarity of the organic liquid on the structure and bonding of the interfacial water molecules. This chapter builds on the previous work done in our research group that has examined water adjacent to non-polar liquids such as CCl_4 and *n*-alkanes.[1, 2] In a more recent study by Walker et al, there was also work on the effect of the addition of polar organic solvents to the non-polar CCl_4 organic phase.[3]

The work presented here in first section of the chapter takes the next step by using mixtures of three organic liquids ($CHCl_3$, dichloromethane (DCM), and 1,2-dichloroethane (DCE)) that have different dipole moments with non-polar CCl_4. This way the polarity of the organic phase is altered systematically to look at the effects on the interfacial water structure. The dipole moment values for $CHCl_3$ and DCM are 1.04 D and 1.60 D respectively. DCE has a dipole moment of 2.1 D for the gauche conformation, which has been shown in simulation results have shown that a higher population at the interface than in bulk DCE.[4] Comparison of the vibrational spectra of interfacial water in these mixture studies with that obtained for CCl_4-water, allows deeper understanding about how the polarity of the organic phase affects the interfacial water

structure and the interactions between water and halocarbon molecules that are present at the interface.

The studies presented in the second portion of this chapter delve into one interface, chloroform-water, in order to achieve a more detailed analysis. This is motivated both by results of the mixture studies and by computational results that have provided a great deal of information regarding the liquid-liquid interface.[4-7] Our laboratory has simulated the CCl_4-water, DCE-water interfaces as well as the neat DCM-water and chloroform-water interfaces in order to generate computational VSF spectra to compare to experiment.[8-11] In addition, several MD studies by Hore et al have focused on elucidating the interfacial behaviors of both the water molecules and the organic molecules (not accessible in the past VSFS studies) of several halocarbon interfaces through calculations of the order parameters of these molecules as a function of the distance from the interface and comparing the different interfacial behaviors.[12-14]

The picture emerging from these experimental and computational studies is that there are clear differences in the water orientation, bonding, and population distribution depending on the interactions between the two liquids. These interactions are largely governed by the degree of polarity of the non-aqueous phase resulting in more or less mixing of the two liquids. When comparing the different halocarbon interfaces, as has been done in many of the aforementioned computational studies, the chloroform-water interface is revealed as a unique "intermediate" interface. The simulation results show it is not as molecularly sharp and the water molecules are not as highly oriented as they are at the CCl_4-water interface. Howeve,r the chloroform-water interface is also not as

diffuse or rough as the interfaces between DCE (which resulted in very low experimental VSFS intensity) or DCM and water making it an ideal interfacial system to examine experimentally. The studies presented in the second portion of this chapter use VSFS to fill the gap in experimental exploration of the aqueous phase of the neat chloroform-water interface. This is accomplished by analyzing the OH stretch spectral response of interfacial water molecules through a combination of isotopic dilution and spectral fitting. The results are then discussed in light of past experimental studies as well as recent MD simulations that explored the structure of both the water and chloroform molecules thereby achieving a more complete picture of the interfacial environment.

Experimental Considerations

The nanosecond laser system described in Chapter III is used to carry out the VSFS mixture studies of CCl_4+DCM and CCl_4+DCE presented here. The CCl_4+chloroform mixtures and the neat chloroform-water interfacial studies used the picosecond laser system described in Chapter III. Since two different laser systems were used to acquire data for these experiments, the spectra for the mixture studies were scaled to give comparable intensity values. In experiments on both systems, the visible and IR beams were overlapped at the liquid-liquid interfaces at angles of 23.7° and 19°, respectively, from the horizontal plane used to maximize the VSFS signal by achieving a total internal reflection (TIR) beam geometry.[15]

The spectra for the mixture studies were not corrected for Fresnel coefficients due to unknown indices of refraction for the mixed organic phases. However because the neat halocarbon liquids have similar dielectric properties, and thus similar indices of refraction (for wavelengths known), it is assumed that this will not have a significant effect on the spectra that would change the overall interpretation discussed below. These corrections have been made for the spectra of the neat CCl_4-water and chloroform ($CDCl_3$)-water interfaces.

The halocarbon liquids used in the experiments were: twice distilled CCl_4 (Aldrich 99.9% HPLC grade), twice distilled DCE (Mallinckrodt, AR), and twice distilled DCM (Aldrich, 99.9% A.C.S. HPLC). The $CHCl_3$, used only in the mixture studies, was also purchased from Aldrich (>99.9% Chromosolv Plus for HPLC with 0.5% ethanol stabilizer) and was extracted twice with water to remove the ethanol. The ethanol was shown to be surface active and, if used as is, the spectra exhibited a peak around 3020 cm^{-1}. The experiments on the neat chloroform-water interface used chloroform-d (Aldrich 99.8% d atom). Deuterated chloroform was chosen in place of $CHCl_3$ because it does not have the same strong CH absorption in the spectral region used for the experiments. Because the $CDCl_3$ can breakdown upon prolonged light exposure, bottles were wrapped in foil and refrigerated while not in use. The liquid was allowed to come to room temperature in the dark before use in the VSFS measurements. The H_2O used for the aqueous phase came from a Barnstead Nanopure II system (~17.9 MΩ cm). The D_2O used in the isotopic dilution measurements was purchased from Cambridge Isotope Laboratories (99.9% d atom). All measurements presented here were taken at room

temperature. The sample cell and all glassware used in the experiments were soaked in concentrated sulfuric acid containing NoChromix and then rinsed thoroughly with the Nanopure filtered water before use.

Results and Discussion: Mixed Halocarbon-Water Interfaces

Figure 5.1 shows the VSF spectra for mixtures of $CHCl_3$, DCM, and DCE with CCl_4, all at comparable mole fractions (mf) of the added polar halocarbon. One of the first trends evident from these spectra is a shift of the free OH mode towards lower frequency. This trend is shown in all three sets of spectra as the concentrations of the more polar liquids increase. As shown in Chapter IV, the free OH peak frequency for the neat CCl_4-water interface is ~3665 cm^{-1}. Figure 5.1 shows that at the highest concentration, 0.40 mf, of added $CHCl_3$ the mode has a peak position of ~3650 cm^{-1}. At this same concentration of DCM, the free OH mode now has a frequency of ~3642 cm^{-1}, and for 0.40 mf DCE it is ~3636 cm^{-1}. At concentrations of the more polar halocarbons above 0.40 mf the free OH positions of the $CHCl_3$ and DCM mixtures do not differ significantly from the values given above. The very low signal intensity of the free OH response for the DCE mixture prohibits the determination of any subsequent frequency shift beyond 0.40 mf. Clearly as the polarity of the organic phase increases the frequency of free OH shifts to lower and lower energies. These spectral shifts occurring with the addition of the more polar halocarbon molecules indicate an increased interaction between water and the adjacent halocarbon molecules. The extent of these shifts

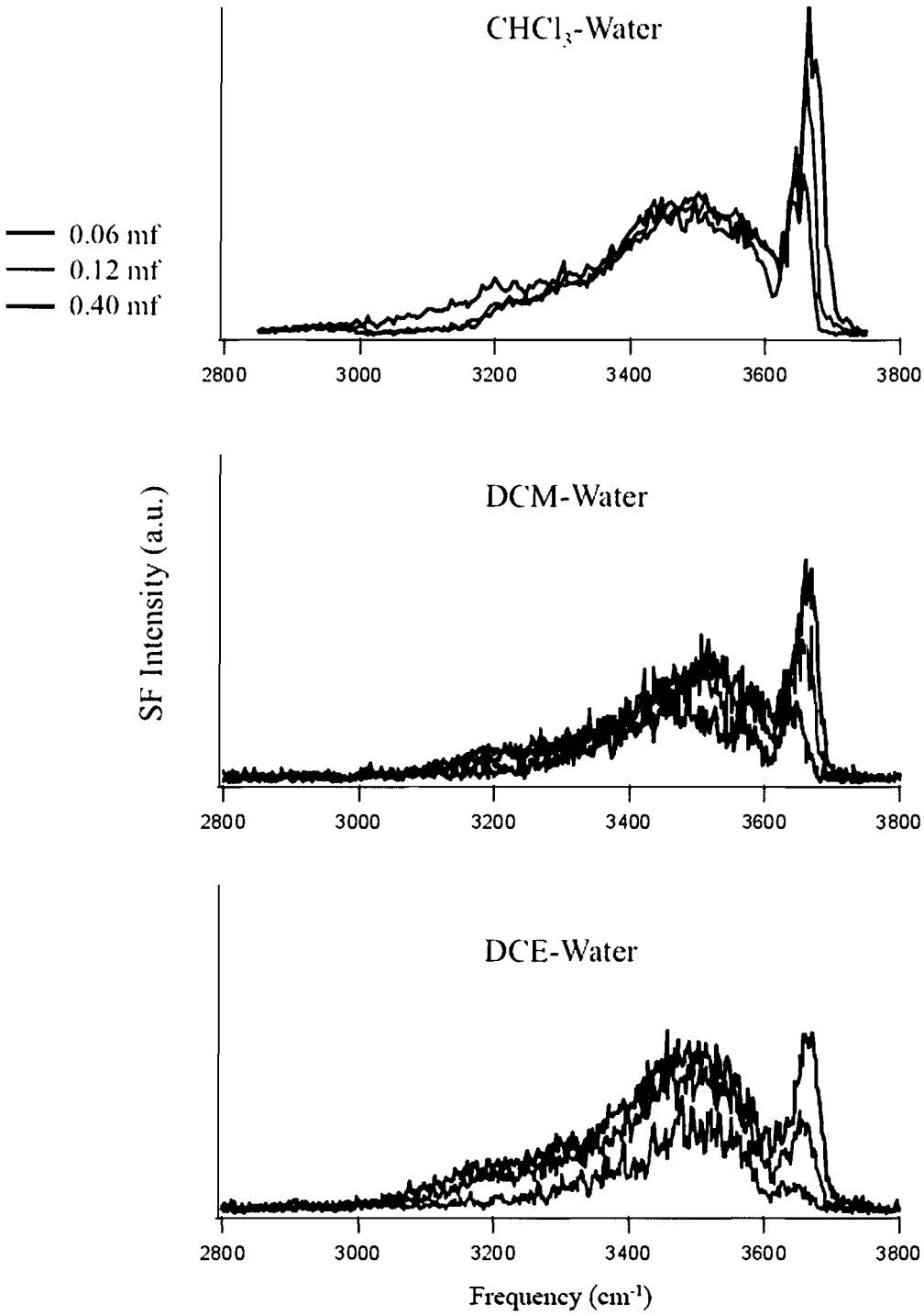

Figure 5.1 VSF spectra of CCl_4 mixed with different concentrations of more polar halocarbons chloroform (top) dichloromethane (middle) and 1,2-dichloroethane (bottom) at the interface with water

correlates with the dipole moments of the added halocarbon. $CHCl_3$ has the smallest dipole moment and its mixtures show the smallest frequency shift of the free OH mode. DCM has a larger dipole moment than $CHCl_3$ and shows a larger red shift for the same mode at the same concentration. Finally DCE, which has the largest dipole moment of the three halocarbons, shows the largest shift of the free OH peak to lower energy. The fact that spectral features, particularly the free OH peak, are clearly apparent in the initial additions of $CHCl_3$, DCM and DCE demonstrates there is still significant interfacial water bonding and orientation present.

Because the free OH mode originates from those water molecules that have direct contact with the non-aqueous phase, its frequency can be used as a measure of the extent of interaction that takes place at the interface. To compare the frequencies of the halocarbon-water interfaces with those of other liquid interfaces, Table 5.1 shows the free OH frequencies from VSFS results obtained in other studies by the Richmond group[1, 2, 16] as well as those taken from the spectra in Figure 5.1. For these systems, the frequencies of the free OH from liquid-liquid interfaces are found at significantly lower frequencies compared to that of the air-water interface. Comparing the CCl_4 and alkane interfaces, their respective free OH frequencies show that water molecules at the interface with CCl_4 interact to a greater degree than with the alkanes. The free OH peaks of the halocarbon mixtures in the present study exhibit the largest frequency shifts compared to the air-water interface. The value obtained for the neat chloroform-water interface shown here is from fitting the data and will be discussed in the next section. It should be noted that the frequencies of the halocarbon mixture peaks shown in Table 5.1 are not values

determined by spectral fits of the data. Interferences that occur between the free OH and companion donor OH modes can alter the apparent peak frequency somewhat. Nonetheless, the data indicates that for these interfaces the water molecules at the outermost layer of the interface are participating in increased weak bonding type interactions with the more polar halocarbon molecules in the non-aqueous phase.

Non-Aqueous Phase	Free OH Frequency (cm^{-1})
Air	3706
Alkanes	3674
CCl_4	3669
Chloroform + CCl_4	3650
DCM + CCl_4	3642
DCE + CCl_4	3636
Chloroform	3645

Table 5.1 Frequencies for the free OH mode for different hydrophobic phases adjacent to water. Values for air, alkanes, and CCl_4 were taken from References 16, 1, 2 respectively.

With the addition of the different polar liquids, there is also an accompanying decrease in spectral intensity for all three sets of mixtures presented. As shown in Figure 5.1, the free OH, the donor OH, and the tetrahedral region in all three sets of spectra show loss of intensity as the concentrations of $CHCl_3$, DCM, and DCE increase. Like the dipole dependent trend seen in the frequency shift of the free OH, there is also a qualitative correlation between the amount of VSFS signal intensity loss seen in the spectra of the mixtures and the polarity of the added liquid, i.e. when comparing spectra of similar mixture concentrations the greater the dipole moment of the added liquid, the greater the loss of intensity. The spectra shown of mixtures of CCl_4 with the least polar halocarbon, $CHCl_3$, show the least loss in spectral intensity. At the highest concentration

of $CHCl_3$, the three peaks in the spectrum can still be clearly distinguished. In contrast, at a similar concentration of DCE, the liquid that has the highest dipole moment, there is very little intensity in the tetrahedrally bonded and free OH spectral regions and a large decrease at intermediate frequencies. DCM has a polarity that is between those of $CHCl_3$ and DCE. The spectrum with the highest concentration of DCM shows loss of signal intensity that is greater than that of the $CHCl_3$ mixture but less than that of the DCE mixture for the same concentration. There are still contributions from the free OH and companion donor OH modes but no significant intensity in the tetrahedral region for the DCM and CCl_4 mixture. The spectra for concentrations of the more polar halocarbon mixtures above 0.40 mf reveal that the VSFS intensity continues to decrease for all three mixtures but does not disappear completely. The VSF spectrum of the neat DCE-water interface has been shown to have very weak signal that is very broad and largely featureless.[3]

In order to understand what is happening at the molecular level to cause this decrease in spectral intensity, one must return to the fundamentals of VSFS. As explained in the previous chapters, the combination of beam polarizations used in these experiments probes those vibrational modes that are perpendicular to the interface thus giving an indication of the orientation of the molecules at the interface. VSFS signal is dependent not only on the number of oscillators at the interface, N, but also on how they are oriented, $<\beta>$. The overall loss in intensity can then be concluded to be a result of the increased interfacial halocarbon-water interactions that occur with increased halocarbon polarity. This increased weak bonding interaction leads to a decrease in

oriented OH oscillators, particularly the free OH and donor OH modes that dominate the CCl_4-water spectrum. Such a loss in oriented water molecules indicates that this stronger water-halocarbon interaction leads to more randomly oriented interfacial water molecules, and likely a more diverse set of hydrogen bonding interactions amongst water molecules in the aqueous phase. Another result of the greater interaction between the more polar halocarbon molecules and a wider array of water-water interactions is a reduction in the number of interfacial water molecules that have energetically uncoupled OH oscillators (i.e. those that have a free and donor OH mode). Consequently the number of uncoupled and oriented water molecules that straddled the interface and were responsible for the large portion of spectral intensity for the water-non-polar organic interface are reduced as the interfacial water molecules adopt a broader distribution of angles and bonding interactions with the adjacent molecules. The trends observed in the intensity and spectral shifts for the three added halocarbons of increasing polarity are consistent with these conclusions.

The conclusions discussed above are supported by MD simulations done in our laboratory that calculate VSF spectra of the CCl_4-water, (CCl_4+DCE)-water, and DCE-water interface. The results of these studies show that there are stronger interactions between water and DCE molecules than are present between water and CCl_4.[8] A shift of the free OH to lower frequency is also seen for the computational spectra when more DCE is present in the mixed organic phase just as is described above. In addition to these MD results, several other simulations from different groups also corroborate the picture formed by the present VSFS studies. Benjamin's simulations show that stronger DCE-

water interactions versus CCl_4-water are responsible for longer lifetimes of hydrogen bonds at the respective interfaces.[17] MD simulations by Dang show that the binding energy for the DCM-water dimer is stronger than that of the CCl_4-water interaction.[5]

Simulation results have also shown that there are an increased number of oriented but very weakly hydrogen bonded and non-bonded water molecules present in the organic phase at the more polar halocarbon-water interfaces compared to the CCl_4-water interface.[8, 11] These oriented and weakly bonded species contribute to the VSF spectrum to reduce the intensity of the free OH and donor OH peaks through destructive interference, resulting in an overall loss in VSFS intensity for these interfaces. The penetration of more water molecules into the organic phase supports the picture formed above of increased interaction of the aqueous phase with the more polar halocarbon organic phase.

Another set of MD simulations done in this laboratory also supports the above arguments about the degree of orientation of water molecules at the interface with different halocarbons. In these studies, the tilt and twist angles of interfacial water molecules are calculated for the CCl_4-water, $CHCl_3$-water, and DCM-water interfaces.[14] Order parameters based on these angles showed the same trend that is described in this section. Water molecules are most highly ordered at the interface with CCl_4, less ordered at the interface with $CHCl_3$, and showed the least ordering at the interface with DCM. Because of the nature of VSFS, if the water molecules are becoming less ordered as the organic phase becomes more polar the resulting intensity should decrease as is observed in the present studies.

Understanding how water behaves as a hydrophobic surface takes on increasingly polar character is necessary to further the use of this interface as an important model for more complex systems. These VSFS studies have done this by systematically varying the polarity of the non-aqueous halocarbon phase in order to observe the effect on the interfacial region and within it, the water structure. The increased polarity of the organic phase upon addition of the more polar halocarbon to CCl_4 results in a stronger interaction between water and the interfacial organic halocarbons and a reduction in the number and orientation of the uncoupled OH oscillators that are found to dominate the spectrum for water adjacent to a non-polar liquid such as CCl_4.

Results and Discussion: The Neat Chloroform-Water Interface

The VSF spectrum of water in the OH stretch region for the chloroform-water interface is shown in Figure 5.2. The chloroform-water interface is unique in that it possesses structural and mixing qualities that are intermediate between those of the CCl_4-water and DCE (or DCM)-water interfaces that have been previously studied and characterized by VSFS. Thus the CCl_4-water spectrum is shown in Figure 5.2 for comparison. Although deuterated chloroform was used in the experiments presented here, it will be referred to as the chloroform-water interface for simplicity.

Both spectra shown in Figure 5.2 share many similarities but the more interesting information lies in the differences between the two. Different peak locations as well as varying peak intensities reveal a great deal about the bonding interactions and structure of

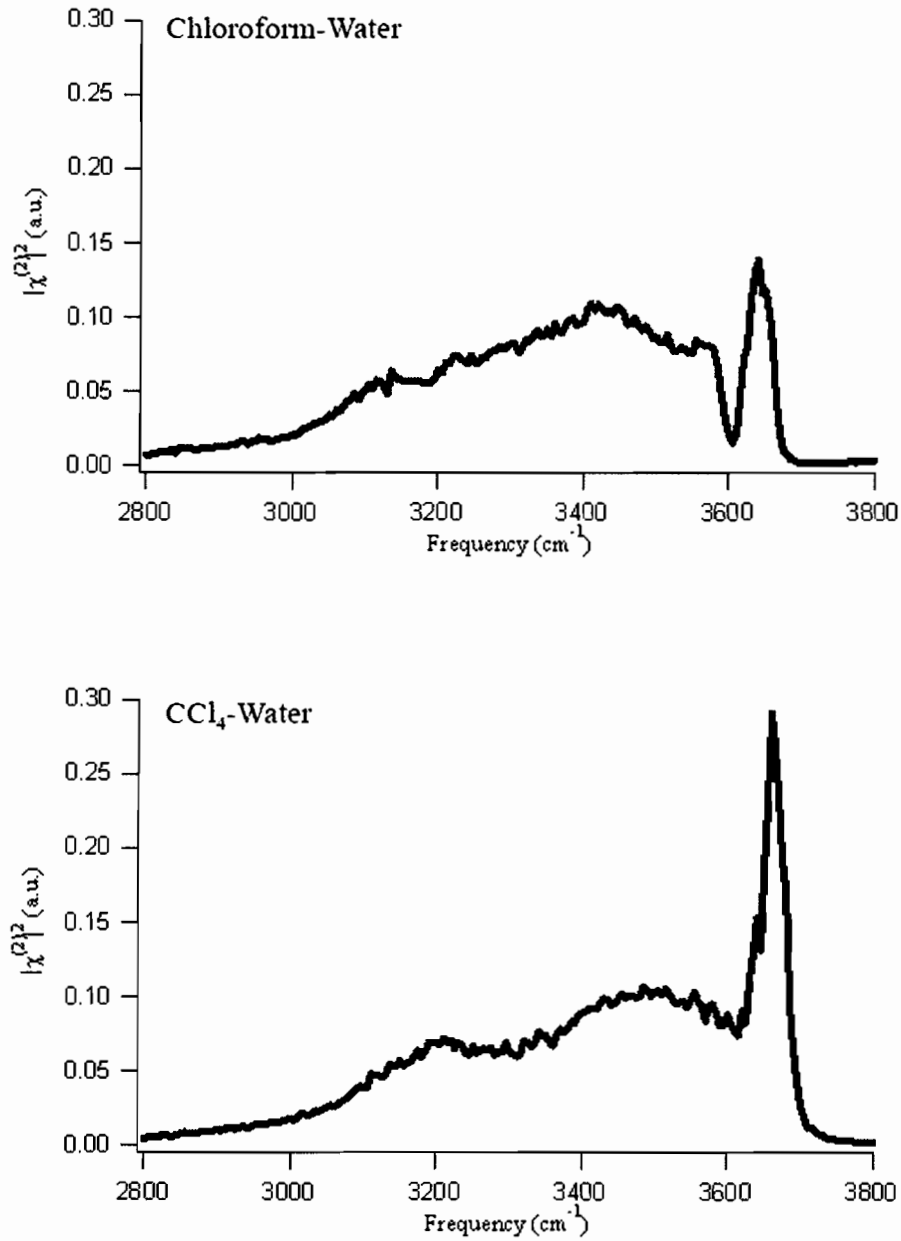

Figure 5.2 VSF spectra of the chloroform-water (top) and CCl_4-water (bottom) interfaces.

the water molecules at these interfaces. However, interference effects that are characteristic of VSFS can affect both the intensity and apparent peak frequency. These effects are taken into account by spectral fitting, beginning with the isotopic dilution

spectra. The spectrum that is primarily HOD (0.46 mf HOD, 0.42 mf D_2O) is fit first because much of the intramolecular coupling is removed by the difference in atomic masses of the hydrogen and deuterium of HOD making it the simplest spectrum to fit. Spectra attempted at higher concentrations of D_2O gave too little signal intensity to be fit accurately. The spectrum of chloroform-D_2O showed no intensity indicating there was not a non-resonant contribution to the VSFS response. For the isotopic mixture containing 0.46 mf HOD, shown in Figure 5.3, the aqueous phase is only ~10% H_2O. Consequently the majority of spectral intensity should come from the OH of HOD molecules either interacting with chloroform or other water molecules. This allows the spectrum to be fit primarily to only two peaks, a free and donor OH peak, with a very small contribution from the tetrahedrally coordinated water peak. The spectrum and resulting fit line are shown in the top portion of Figure 5.3. The Lorentzian widths[16] and phase relationships[18] of the peaks were held to values determined in previous VSFS experiments. The peaks that comprise the fit are shown in the bottom portion of Figure 5.3. These results determine the peak frequencies that are then used to simultaneously fit the other H_2O/D_2O mixture spectra and the chloroform-water spectrum using the global fitting routine that tightly constrains the parameters to be the same or within a similar range for each spectrum.

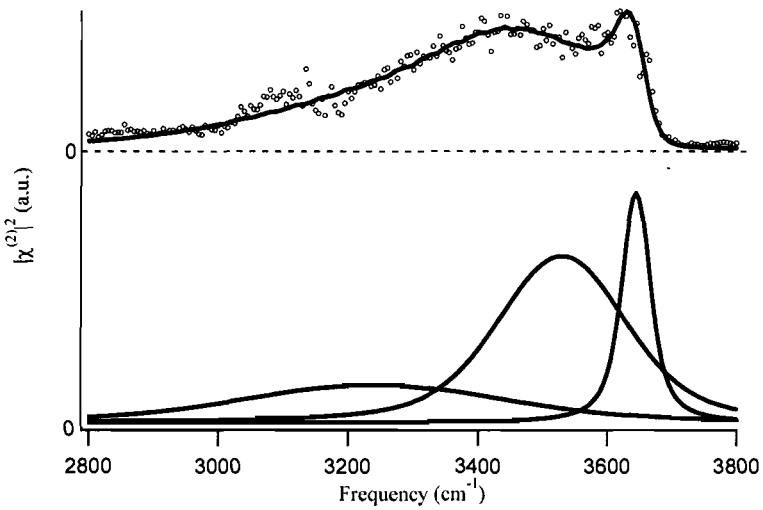

Figure 5.3 VSF spectrum of the chloroform-0.46mf HOD + 0.42mf D_2O + 0.12mf H_2O interface with best fit line (top) and the peaks that comprise the fit (bottom)

The spectra of the chloroform-water, chloroform-0.49 mf HOD, and chloroform-0.46 mf HOD interfaces with their respective fits are shown in Figure 5.4. They are offset vertically for clarity. As the concentration of H_2O increases, the intensities of the free and donor OH peaks increase. There is also increased contribution to the spectrum from the tetrahedral peak. This is accounted for in the fits by increases in peak amplitudes but also in significant broadening (increase in the Gaussian widths) of the peaks, particularly the donor OH peak known to occur because of the increased number of various water - water interactions that take place with increased H_2O concentration.[10, 16] Additionally a sharp dip appears at ~3600 cm^{-1} that was not seen in the highest HOD concentration spectrum. Initial attempts at fitting the spectra in used only the three peaks discussed above. However changes to the peak parameters, both physically reasonable and not, resulted in fits that did not reproduce the sharp dip at ~3600 cm^{-1}. The only way to account for this spectral feature was to add a fourth peak to the fitting routine. This

peak is attributed to water species, most likely found on the organic side of the interface, where they can only weakly interact with other water molecules if at all. This new peak will be discussed in more detail later in this section.

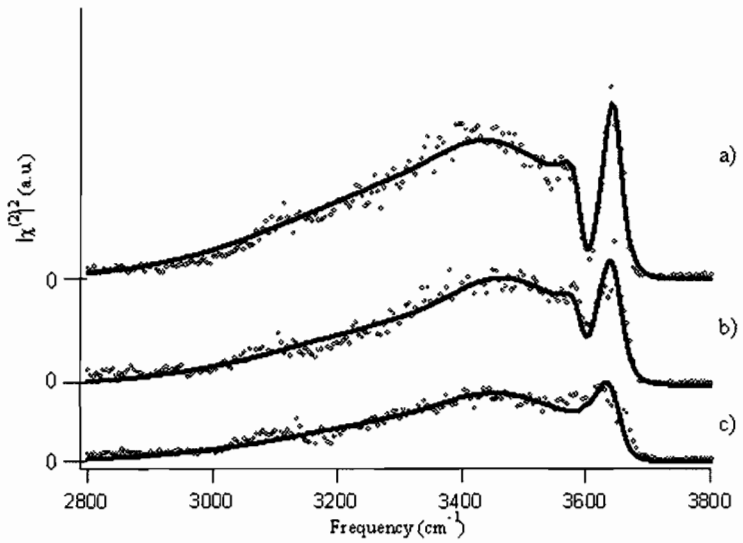

Figure 5.4 VSF spectra of the interface of chloroform with a) H_2O b) 0.20 mf D_2O + 0.49 mf HOD c) 0.42 mf D_2O + 0.46 mf HOD Dots are the data points and the solid line denotes the best fit to the data.

The spectrum of the chloroform-water interface with the fit line and its composite peaks are shown in Figure 5.5. A summary of the fitting parameters is found in table A.1 in the Appendix. The broad peak found at the lowest frequency is the tetrahedrally coordinated water peak centered at 3240 cm^{-1}. This frequency is very close to the value determined for the same peak at the CCl_4-water interface in a previous analysis.[2] Upon visual inspection, the intensity for the tetrahedral peaks for both the chloroform-water and CCl_4-water spectra are very similar. This indicates that those water molecules that are participating in a more highly coordinated hydrogen bonding geometry are in similar aqueous environments for both halocarbon interfaces. These molecules are also known

to mainly reside deeper within the aqueous side of the interfacial region[9] so it would make sense that they would not be as affected by the different organic phase characteristics and thus exhibit similar peak parameters to the CCl_4-water interface.

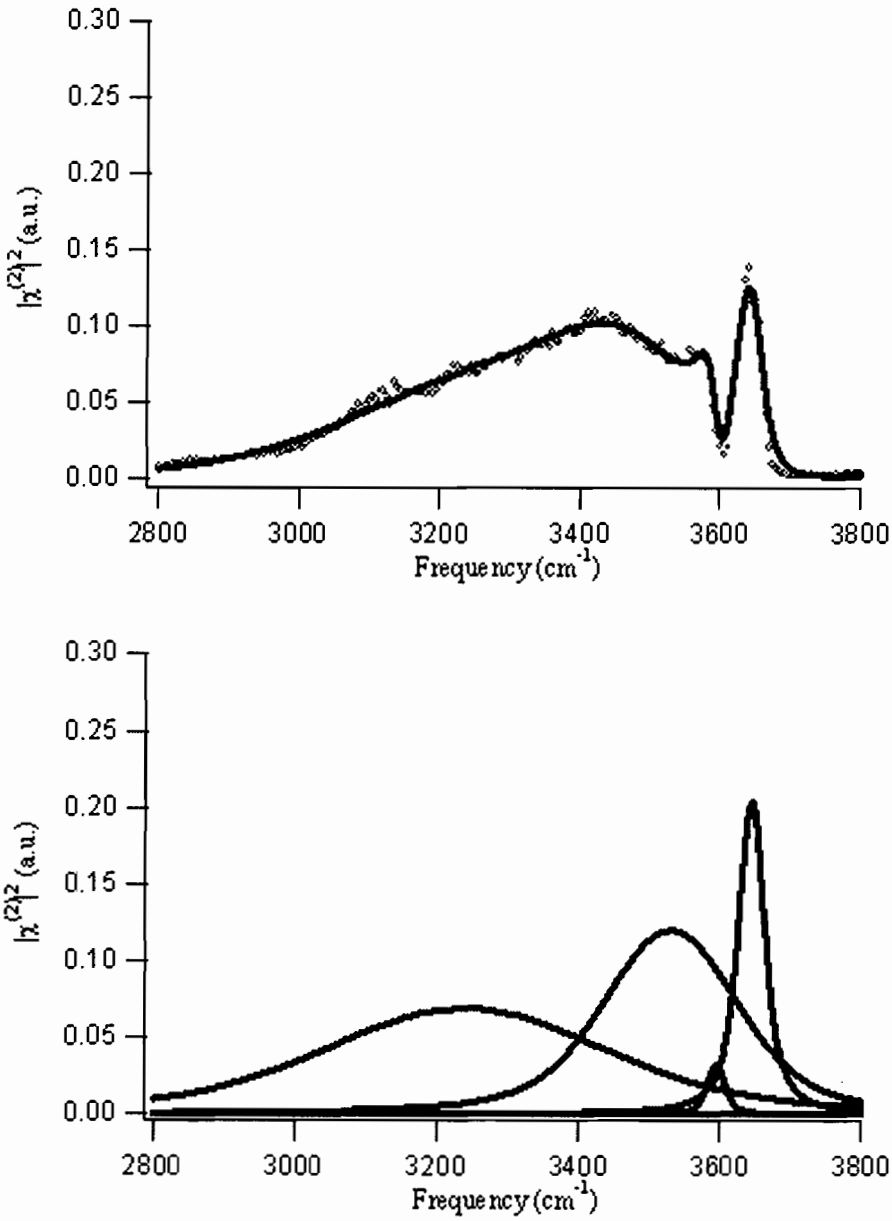

Figure 5.5 VSF spectrum of a) the chloroform-water interface and b) the composite peaks resulting from the spectral fit.

In contrast, the peaks corresponding to the straddling water molecules are quite different when the results in Figure 5.5 are compared to those for the CCl_4-water interfacial spectrum. This is not surprising due to the presence of more polar liquid in the organic phase, which should most affect those water molecules directly in contact it. First, the center peak frequency for the free OH mode is found to be 3645 cm^{-1}, very close to the value of 3649 cm^{-1} for the uncoupled OH oscillator seen for IR spectra of HOD in $CDCl_3$.[19] This is a shift to lower frequency of ~25 cm^{-1} when compared to the free OH frequency of the CCl_4-water interface.[2] This large shift to lower frequency when compared to other frequency values obtained in VSFS experiments (Table 5.1) indicates that there are weak bonding type interactions that are taking place between the water molecules that are in direct contact with the chloroform molecules. This is explained by the permanent dipole of chloroform molecules (1.04 D) that was not present in the other liquids previously studied (CCl_4 or *n*-alkanes) and obviously not in the vapor phase.[1, 2, 16] Additionally if the intensity of the free OH peak for the chloroform-water interface is compared to that of CCl_4-water, a decrease is seen. This is most likely due to a change in orientation adopted by those straddling interfacial water molecules resulting from the increased interactions of the two liquids. As a result, there are fewer water molecules that are straddling the interface thus lowering the VSFS intensity.

Because the free OH peak changes position and intensity indicating changes in bonding properties and orientation of the straddling water molecules, it follows that the corresponding donor OH oscillators are also affected. The donor OH mode frequency of those straddling water molecules at the interface with chloroform is at 3530 cm^{-1}. This is

a shift of ~90 cm^{-1} from the donor OH mode previously determined by isotopic dilution experiments at the interface with CCl_4.[2] This large frequency shift indicates that the weak hydrogen bonding environment is very different for the chloroform-water interface in comparison to the CCl_4-water interface resulting, again, from the increased interactions between the water and more polar chloroform molecules. The shift to higher frequency of this peak suggests that donor OH oscillators are not participating in as strongly interacting hydrogen bonds as in the CCl_4-water interface and/or there is an increase in water molecules that undergo a more broken or weaker hydrogen bonding geometry. These straddling water molecules are now less ordered so that the donor OH oscillators can no longer participate in hydrogen bonding to the same extent as at the CCl_4-water interface where there so little interaction between the two phases.

These experimental findings are supported by MD studies of the liquid-liquid interfacial systems. Simulations of VSF spectral depth profiles show evidence of a slightly broader interface for chloroform-water compared to CCl_4-water due to increased mixing of the two liquids.[11] This study also showed that the calculated free OH frequency for the chloroform-water interface shifted to lower energy and the donor peak shifted to higher energy when their values are compared to the calculated frequencies for the CCl_4-water interface further corroborating these experimental results.

In another MD study, closer examination of the structure of the chloroform-water interface was done by calculating the order parameters for both the chloroform and the water molecules by MD.[12] The results show that although there is a significant population of the water molecules in the interfacial region that are still straddling the

interface, there are also many water molecules that adopt an in plane configuration. This orientation serves to maximize the hydrogen bonding with the chloroform molecules that are oriented with the CH bond (which is the positive portion of the molecule's permanent dipole) pointed toward the water phase. Because there is no positive portion of the CCl_4 molecules due to the zero dipole moment, most likely there are not as many water molecules that adopt this configuration at the CCl_4-water interface resulting in higher intensity for the free and donor OH peaks in the VSF spectrum. This MD result also helps explain the higher frequency of the donor OH peak for chloroform-water. With more water molecules adopting an in plane configuration to hydrogen bond with the chloroform molecules through the oxygen, the water-water interactions through the donor OH oscillator are weakened or broken altogether thereby increasing the peak frequency.

The last peak remaining in Figure 5.5 to be discussed is the small and relatively narrow peak found between the free and donor OH peaks. It is assigned to very weakly interacting water molecules, most likely found on the organic side of the interface. Several IR studies of small volumes of water dissolved in chloroform or $CDCl_3$ show that the symmetric OH vibrational stretch signature is between 3604 cm^{-1} and 3607 cm^{-1} giving support for this spectral assignment.[20-23] In addition, the MD-VSF studies have also shown intensity in this region due to water molecules solely in contact with the organic molecules.[11] Fitting efforts for the CCl_4-water interface spectrum also showed evidence for these organic solvated water molecules but their resulting VSFS interference is to a lesser degree than that seen for the chloroform-water interface.[2] This is most likely due to a higher number of these types of water molecules existing and thus

contributing to the VSFS intensity in this spectral region. The slightly more polar nature of chloroform allows for an increase of these types of water molecules that mix into the organic phase.

Conclusions

This chapter focuses on the effects of the polarity of the organic liquid phase on the structure and orientation of the interfacial water molecules. Mixtures of non-polar CCl_4 with three polar solvents, $CHCl_3$, DCM, and DCE, were used to systematically vary the polarity of the organic phase at the interface with water providing insight into how the interactions between the two phases change as the dielectric properties of the non-aqueous phase become more and more like that of water. The resulting VSFS spectra of these mixtures showed dipole dependent trends for 1) the frequency shifting of the free OH mode, which indicates higher degrees of interaction between the two liquids, and 2) decrease in VSFS intensity resulting from changes in number of orientation of water molecules as they are increasingly affected by the presence of the organic liquid.

The chloroform-water interface was analyzed in more detail in order to investigate the structure of water at a more polar organic liquid-water interface. Mixtures of H_2O, HOD, and D_2O were used to deconvolve the different OH modes that contribute to the interfacial spectrum by fitting the spectra using tightly constrained values for the peak parameters. The results showed that the mode corresponding to the tetrahedrally coordinated water region around 3200 cm^{-1} is almost identical in frequency and intensity

to results for the CCl_4-water interface. This indicates that those water molecules participating in the most coordinated hydrogen bonding geometries do not "feel" the difference in polarity between chloroform and CCl_4; both interfacial environments have very similar orientations and hydrogen bonding interactions for this type of water species. In contrast the peaks attributed to the donor and free OH modes in the spectrum show frequency shifts to higher and lower energies respectively, as well as decreases in intensities for both peaks when compared to the results for CCl_4-water indicating that there is significantly more interaction between those water molecules that are directly in contact with the chloroform due to the moderately polar nature of the chloroform liquid. As shown in the mixture studies, this higher polarity also leads to increased mixing between the two phases resulting in less oriented straddling water molecules as well as the appearance of a peak around 3600 cm^{-1} attributed to water molecules that are most likely on the organic side of the interface and therefore not in contact with many other water molecules. Several recent MD simulations as well as experimental IR studies support the interpretation of these conclusions.

CHAPTER VI

IONS AT THE ORGANIC LIQUID-WATER INTERFACE: EFFECTS OF CHARGE ON THE STRUCTURE AND BONDING OF WATER

Interest in the nature of water at hydrophobic surfaces and in the emerging picture of ions at aqueous surfaces provides a unique setting for the studies presented in this chapter. Vibrational sum-frequency spectroscopy (VSFS) has been used to investigate the effects of small, inorganic ions on the structure and bonding of water at the CCl_4-water interface. By examining the different OH stretching spectral regions, which are comprised of collections of modes of water molecules in varied hydrogen bonding environments and depths within the interface, a molecular picture of the aqueous environment is formed where ions clearly reside in the interfacial region and affect the water hydrogen bonding in a manner specific to the ion under study. Additionally, comparison of the different spectral trends at the organic-water interface in the presence of ions versus similar studies at the air-water interface provide further insights into the unique interactions that occur when water is adjacent to a hydrophobic surface resulting in quite different ion-water interfacial behavior.

Introduction

Progress in the development of experimental and computational methods appropriate for investigating surfaces have resulted in a great wealth of studies regarding ions at interfaces in recent years.[1-3] From these studies, a picture emerges that ions are present within the interfacial region and, for some ions, have a significant impact on the structure and bonding of the water molecules within the region.

Studies utilizing simulation methods have provided invaluable information regarding the organic liquid-water environment with ions present. For example, pioneering work on the mechanisms of ion transfer at the 1,2-dichloroethane(DCE)-water interface was done by Benjamin using molecular dynamics (MD) simulations[4] in addition to more recent work on solvation during ion transfer at the nitrobenzene-water interface.[5] Recent MD studies by Wick and Dang have examined the distribution of several different ions at the CCl_4 and DCE-water interfaces, with comparison to the air-water interfaces.[6-8] These studies have provided a great deal of molecular level analysis of the behavior of ions at liquid-liquid interfaces.

Experimental investigations of ions at liquid-liquid interfaces have not been as prevalent due to the difficulty of accessing only the thin boundary between the phases without overwhelming contributions from the bulk. However, there are some key studies that have been reported recently. Schlossman and co-workers have done work utilizing both x-ray reflectivity and MD on tetrabutylammonium salts at the nitrobenzene-water interface that showed common mean field theories such as Gouy-Chapman theory give

predictions that are not in agreement with experimental measurements.[9, 10] This was attributed to lack of consideration of molecular-scale structure of the liquid solution by the theory excluding such parameters as ion size and ion-solvent interactions. Experiments utilizing second harmonic generation (SHG) by Walker and coworkers examined solvation properties at the cyclohexane-water interface that showed interfacial polarities have very different characteristics than the bulk.[11] These studies exemplify the growing understanding that the interfacial environment is unique in comparison to the bulk, and the interactions that take place there between solvent and solute produce results that are in contrast to the picture formed many years ago that charged species are repelled from the interfacial region.

Because the interactions that take place between ions and water play such a large role in determining how these charged species will behave at the interface, which will ultimately govern their role in other processes like ion transport at membranes, a firm understanding of the structure and bonding of the aqueous side of the organic-water interface is of great importance. This chapter focuses on how interfacial water molecules at the CCl_4-water interface are affected by the presence of different ions. The use of surface specific vibrational sum-frequency spectroscopy (VSFS) allows studies of only the interfacial region in order to better understand the behavior of ions within this unique environment.

Experimental Considerations

The experiments presented here used the picosecond laser system described in Chapter III. Beam energies used in the current experiments are 80 μJ and ~200-250 μJ for the visible and IR beams respectively. Beam angles were chosen to maintain a TIR geometry of the visible beam for all concentrations of all the salts used in the aqueous solution: 69.5° and 75° from the interface normal for the visible and IR beams respectively. Multiple spectra of each interface were taken and averaged to achieve an acceptable signal to noise level. Spectra of the same salt concentrations were taken on multiple days to assure reproducibility. A neat CCl_4-water spectrum was taken at the beginning and end of each day that salt solution data was collected in order to estimate fluctuations in intensity from day to day, as well as assure no contamination effects.

Because the use of bulk molar concentrations of salts in the present experiments can alter the pH of the solution, there is also a question any potential effects of pH on the structure of the water molecules. Therefore the pHs of equivalent concentration solutions were measured and, for some of the salts, there were a slight increases or decreases in pH observed. However, as shown in Chapter VII, studies focused specifically on the effects of acid and base on the water at an organic-liquid interface do not give results similar to what is shown in the present experiments. This shows that the anions discussed are indeed responsible for the effects seen in the OH stretching region of the VSF spectra.

Due to the higher ionic strength of the solutions of Na_2SO_4 in comparison to the other salts studied, the effect of ionic strength on the spectra was explored by holding it

constant using excess NaCl. As was seen in similar studies at air-water,[12] the effect of ionic strength was not apparent due to the anion present in highest concentration (either Cl^- or SO_4^{2-}) dominating the spectral appearance. Said another way, the spectra of NaCl in higher concentration looked similar to the CCl_4-$NaCl_{(aq)}$ spectra and the spectra with Na_2SO_4 in higher concentration looked like the CCl_4-$Na_2SO_{4(aq)}$. Ionic strength appears to not affect the structure of the interfacial water molecules. This further emphasizes that the differences in the resulting spectra are due to the specific anion being studied.

The VSF spectral results were shown to be extremely sensitive to chemical impurities so great care was taken to eliminate any effects from these. CCl_4 (≥99.9%+, Chromosolv HPLC grade) was purchased from Sigma-Aldrich and then distilled twice before use in any experiments. All salts used were also purchased from Sigma-Aldrich (99.0% Sigma Ultra grade). Although a high grade purity, using the salts as purchased resulted in inconsistent spectral results as well as peaks in the VSF spectra at ~2850-3000 cm^{-1} indicating the presence of organic, surface active impurities. The salts were therefore baked in an oven at 220° for ~12 hours prior to use. The resulting spectra were very consistent and free of any peaks in the CH stretching region. Water used in these experiments came from a Nanopure II filtering system (Barnstead) with an ~17.9 MΩ cm resistivity. Fresh salt solutions were prepared every day of data collection. All glassware used in addition to the sample cell components were cleaned in NoChromix dissolved in concentrated sulfuric acid, and then rinsed copiously with the Nanopure filtered water. Due to lower aqueous solubility at room temperature, the Na_2SO_4 solutions were sonicated prior to use.

Results for the CCl_4-Salt Solution Interface

Figure 6.1 presents spectra of 1.2M NaX (X=Cl^-, Br^-, NO_3^-, SO_4^{2-}) solutions at the interface with CCl_4. In each panel, the spectrum in color(grey) is of the CCl_4-salt solution interface while the neat CCl_4-water spectrum is shown in black for comparison. First, it is obvious that the presence of the ions has a clear effect on the interfacial structure such that the resulting spectra are different than the neat spectrum. More specifically, the spectra of the different solutions, all with the same cation, show markedly different behavior in comparison both to each other and to the neat CCl_4-water spectrum.

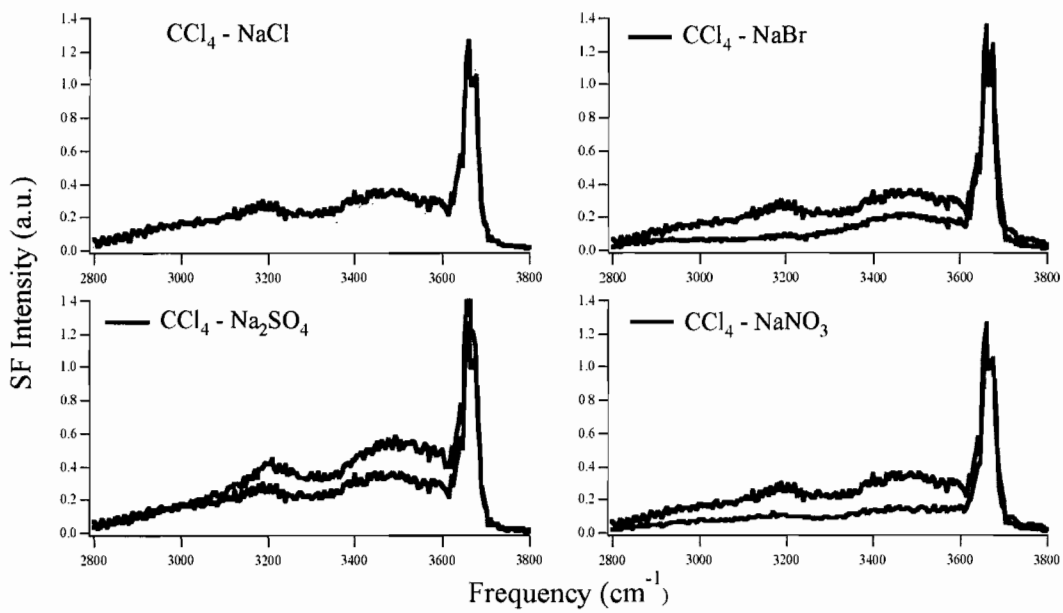

Figure 6.1 VSF spectra of the CCl_4 – NaX interface where X = (Cl^-, Br^-, NO_3^-, SO_4^{2-}) The salts are at bulk concentrations of 1.2 M.

For the Na^+ solutions of monovalent ions (Cl^-, Br^-, NO_3^-) the trend is a decrease in intensity below ~3600 cm^{-1} with little to no change in the intensity of the free OH peak.

However, the degree of intensity decrease differs for each anion solution. Beginning with the spectrum of the CCl_4-$NaCl_{(aq)}$ interface, shown in the green trace, there is the most change in comparison to the neat spectrum seen in the decrease of the more strongly bonded or tetrahedral peak around 3200 cm^{-1}. There is also a slight decrease in the more weakly bonded, or donor OH, peak around 3500 cm^{-1} but to a lesser extent. The spectrum of the CCl_4-$NaBr_{(aq)}$ shown in blue exhibits a similar overall shape to the NaCl spectrum. The decrease in the tetrahedral peak is to a similar intensity but the decrease in the donor OH peak is greater for NaBr in comparison to that of NaCl. In comparison the spectrum of the CCl_4-$NaNO_{3(aq)}$, shown in red, exhibits the greatest change in comparison to the neat CCl_4-water spectrum. Again the tetrahedral peak intensity is similar for $NaNO_3$ in comparison to the NaCl and NaBr spectra. However the donor OH region has very little intensity, with no defined peak structure detectable.

In contrast to the trend for the spectra of the NaCl, NaBr, and $NaNO_3$ solutions, which show decreases in both the more strongly and weakly bonded OH portions of the VSF spectra, the spectrum of the CCl_4-$Na_2SO_{4(aq)}$ interface shows an increase in intensity for both regions. Displayed in the purple trace in Figure 6.1, one can see that in comparison to the neat CCl_4-water spectrum there is significant enhancement in the intensity for both the tetrahedral peak around 3200 cm^{-1} and in the higher energy donor OH peak between ~3400-3600 cm^{-1}.

For all the spectra shown in Figure 6.1, the common cation was Na^+. To examine the role of the counter ion on the structure of the water, solutions with the same anions were made substituting K^+ for Na^+ as the counterion. The results are shown in Figure

6.2. When the spectra of the same concentration and the same anion are compared, the same trends are observed. Spectra of Cl^- and Br^-, both with Na^+ and K^+, show decreases in the intensity below 3600 cm^{-1} with the extent of decrease greater for Br^- compared to Cl^-. Again in contrast are the spectra of the Na_2SO_4 solutions, which display an increase in intensity for solutions with both cations.

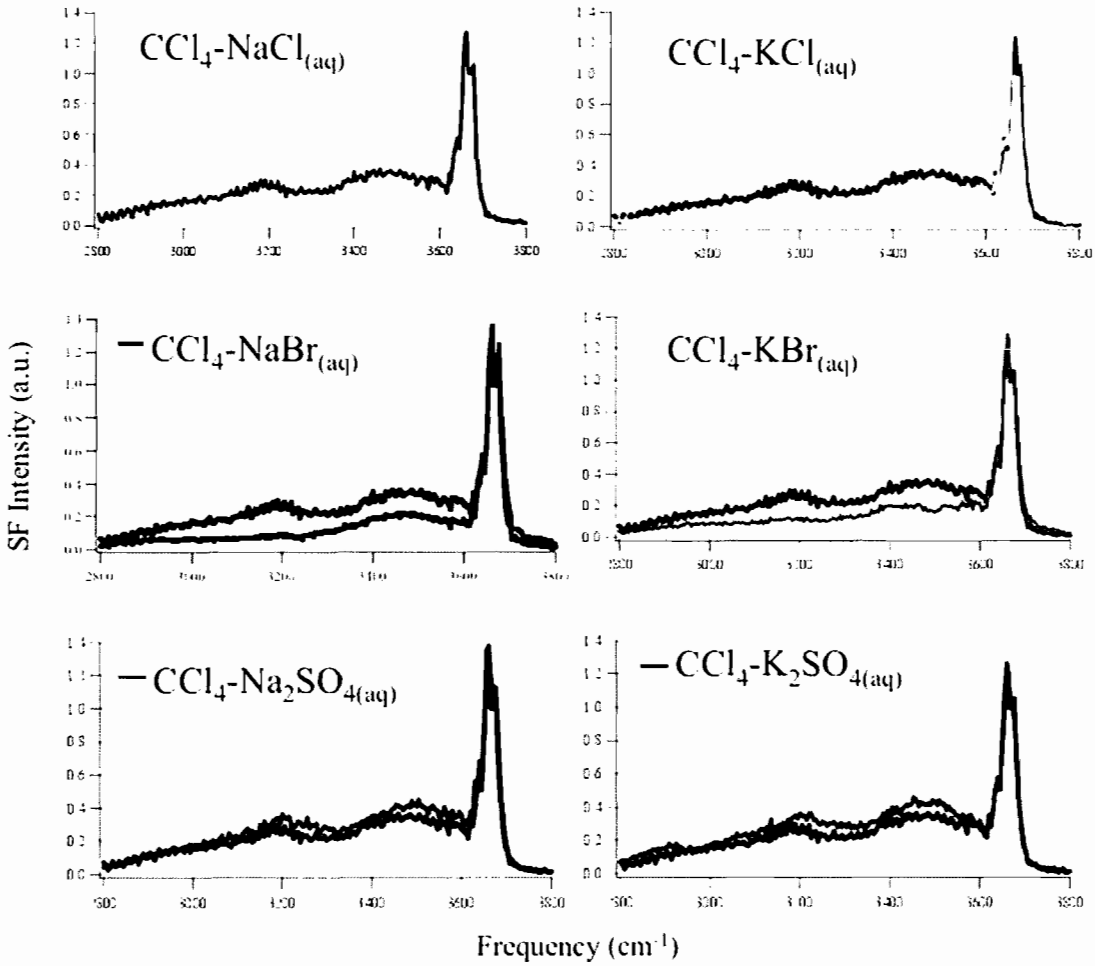

Figure 6.2 Comparison of the VSF spectra for the CCl_4-$salt_{(aq)}$ interfaces with Na^+ and K^+ as the cations

The trends outlined above were also shown to be concentration dependent. Figure 6.3 shows how the intensities of the different spectral regions are affected by the presence

of several concentrations of the different anions. The value for the neat CCl_4-water spectrum is given by the horizontal, dashed, black line for comparison. Intensity values are taken from the Na^+ solution data but for the same concentration of salts with K^+ as the cation, the results were identical within experimental error.

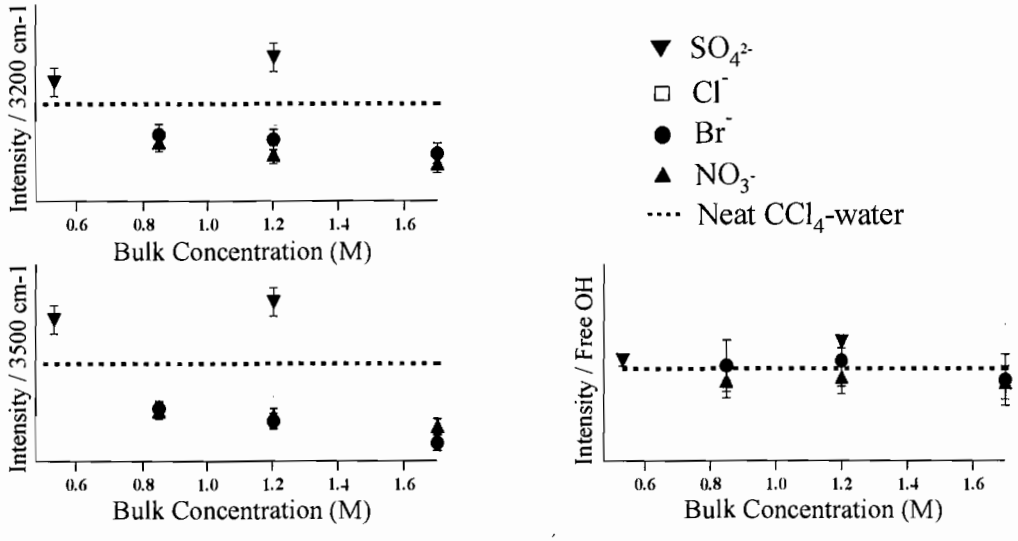

Figure 6.3 Plots of VSFS Intensity versus bulk salt concentration for the three main spectral regions at 3200 cm^{-1}, 3500 cm^{-1}, and the free OH at 3665 cm^{-1}. The black dotted line shows values for the neat CCl_4-water interface for comparison.

Beginning with the monovalent ions, it is evident from both the plots of the peaks at 3200 and 3500 cm^{-1} that, upon addition of these salts, there are decreases in the peak intensities. For the top plot showing the intensities of the 3200 cm^{-1} tetrahedral peak, they show very similar values. In fact for the lowest bulk concentration the spectra of the different solutions have almost identical intensities for this peak. As the bulk concentrations are increased, the spectral peak decreases at a similar rate for the different solutions as well. In contrast, the bottom left plot that shows intensities for the donor OH peak at 3500 cm^{-1} presents more distinctly different effects by the different salt solutions.

The NaCl data points decrease relatively slowly as the bulk concentration increases whereas the decrease for the NaBr spectra values is significantly steeper and even more so for the $NaNO_3$ spectra values, i.e. with increased concentration of NaBr and $NaNO_3$ there is a more drastic decrease in intensity for this spectral region in comparison to NaCl. For the Na_2SO_4 spectra, the concentration range is smaller and only composed of two data points due to limits of solubility. However, the trend is still apparent that upon addition of Na_2SO_4 the spectra show an increase in intensity for both spectral regions. The bottom right panel of Figure 6.3 shows the bulk concentration dependence of the free OH intensity. In contrast to the clear bulk concentration dependent trends seen for the two plots on the left side of the figure, these data points show no clear trend for the ions studied, with deviations away from the neat CCl_4-water values all being mainly within the experimental errors. The free OH thus exhibits no significant change with the addition of these added salts.

Discussion of the Anions at the CCl_4-Water Interface

The addition of ions to the aqueous phase causes distinct changes to the VSF spectra in comparison to the neat spectrum. Although the ions themselves are not being probed spectroscopically, the changes to the OH stretching region can nevertheless convey a great deal about what is happening within the interface. Very generally, the first conclusion is that ions *are* present within the interfacial region and significantly perturb it to give the resulting spectra. This is an important determination, albeit simple, in light of the evolving picture of ion behavior at interfaces. Additionally, from the comparison of spectra using both K^+ and Na^+ salts of the same anions, shown in Figure 6.2, it can be concluded that the anions are primarily responsible for the spectral changes. This is consistent with previous studies that have indicated the smaller, less polarizable cations are most often present closer to the bulk region of the aqueous phase and would therefore have less effect within the interfacial region.[1-3] The focus will therefore be on how the four anions Cl^-, Br^-, NO_3^-, and SO_4^{2-} affect the structure of the water molecules to change the overall picture of the liquid-liquid interface.

The discussion will begin with the monovalent ions. The presence of these ions in the interfacial region clearly alters the way interfacial water molecules behave as manifested in these spectral changes. In particular, for the monovalent ions, the result is a decrease in the VSFS intensity. As described in Chapter II, there can be two apparent contributing factors for these intensity changes which are (1) a change in the number of contributing water bonded species in their corresponding spectral region, and (2) a

change in orientation of various water bonded species relative to the surface normal. The first effect comes from the fact that VSFS intensity is proportional to the number density, *N*. The latter arises from the dependence of the VSFS response on molecular orientation through the molecular hyperpolarizability values, β, and consequently through $\chi_v^{(2)}$. When the water molecules are in a more random configuration, their direction dipoles will cancel to a certain degree leading to a lower value for the orientationally averaged β value and therefore a decrease in $\chi_v^{(2)}$.

For further insight into the molecular reasons behind the spectral trends, comparisons can be made to the air-water interface for which similar experiments have been conducted. The NaCl and NaBr spectra were taken by Dr. Elizabeth Raymond[13] and the Na_2SO_4 spectra were taken by Dr. Teresa Tarbuck.[12] This comparison is shown in Figure 6.4. It displays the VSF spectra of the CCl_4-salt$_{(aq)}$ interfaces with air-salt$_{(aq)}$ spectra of similar bulk concentration taken from previous studies done in our research group.[12, 13] The results for the monovalent ions at the organic liquid-liquid interface is distinctly different than what we and other laboratories observe for these ions at the air-water interface using VSFS.[13-15] The air-salt spectra show that the presence of the monovalent ions results in a increase of VSFS intensity in the 3200 cm^{-1} region, and an almost negligible change in the weaker bonded 3500 – 3600 cm^{-1} region.[13] This is in sharp contrast to the measurable decrease in intensity found for these anions at the CCl_4-water interface throughout the spectral regions. The small increases observed at the air-water interface upon addition of these salts has been attributed mostly to the ions widening the interfacial region further into the aqueous bulk water resulting in increased

VSF spectral intensity. This has been observed both by experimental[13, 15, 16] as well as computational methods.[2, 17]

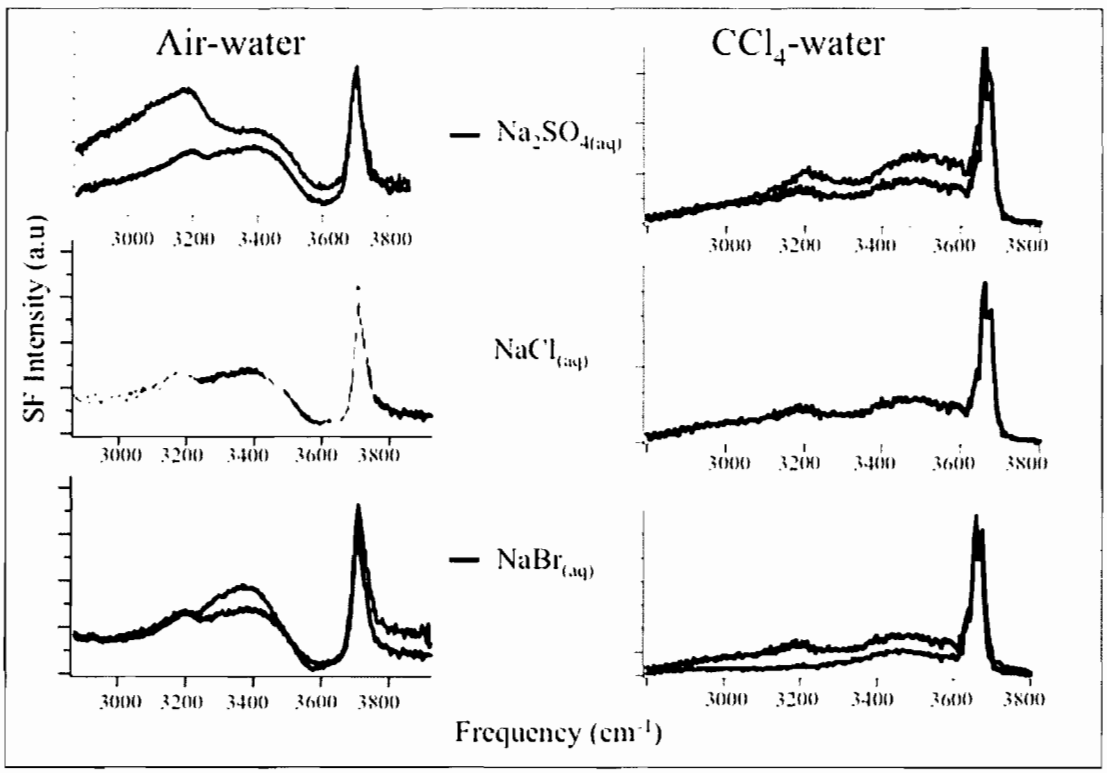

Figure 6.4 Comparison of the VSF spectra of different ions at the air-water and CCl_4-water interfaces

The unique nature of the organic-water interface must be responsible for this difference in ion behavior for these two interfaces. The interaction present between the two liquids facilitates the adsorption of anions into the organic-water interface differently relative to the air-water interface. What is known from evidence from experimental and computational efforts by both our laboratory and others indicates that the neat CCl_4-water interface consists of water molecules with a relatively high degree of orientational ordering.[18-21] This is true in particular for the topmost region of the interface where the water molecules adopt specific orientations due to their contact with the organic phase, in

this case the non-polar liquid CCl_4. Calculations suggest that the combination of the orientational ordering of the water *and* the organic together lead to an electric field across the interfacial region.[18, 19] This resulting field would then have an influence on charged species in the aqueous phase.

With this picture in mind, the effect that the presence of the different anions has on different physical regions of the interface is particularly interesting. If the accumulation of ions within the interface were simply an electrostatic effect, then all the monovalent ions should have the same spectral results. This is actually what is observed, in part, as shown in the top, left plot of Figure 6.3. When the bulk monovalent anion concentration is increased, the intensity around 3200 cm^{-1} decreases in a nearly identical manner for all the ions. The interfacial field is screened by the presence of these ions resulting in fewer of these more strongly bonded water molecules that reside somewhat deeper in the interface being oriented by the field. This manifests as a reduction in VSF spectral response. This is the region most commonly found to exhibit effects due to a reduction in interfacial field.[22]

The water molecules that reside more in the topmost interfacial region and undergo weaker bonding interactions show greater sensitivity to the characteristics of the different ions, and to a much higher degree than observed for the air-water interface. In this region, at a given concentration, the monovalent ions can be ranked according to their ability to decrease the VSFS intensity in the 3500 cm^{-1} region as shown in the bottom left plot of Figure 6.3: $Cl^- < Br^- < NO_3^-$. This trend follows the size of the ions, with Cl^- being the smallest and NO_3^- the largest. Cl^- is also the least polarizable with

NO_3^- and Br^- calculated to have similar polarizabilites.[2, 23] These VSF spectral trends are attributed to the differences in the degrees of penetration of the ions into the topmost interfacial region. MD studies by Wick and Dang of halide ions at the CCl_4-water interface also show that larger and more polarizable ions have a higher presence at this interface.[8] The higher polarizability of the larger ions results in their higher concentration at the interface. The overall consequences of the ions' presence are a narrower interfacial region, disruption of ordering, and a displacement of water molecules in the topmost water layers, which reduce the number of contributing water molecules, N, and lower the average β thereby reducing the VSFS intensity.

Interfacial SO_4^{2-} also alters the water bonding character at the CCl_4-water interface but in an opposite trend than what is observed for the monovalent ions throughout the spectral region. This different behavior is attributed to the higher charge of the SO_4^{2-} ion, which makes it more energetically favorable for it to be found deeper within the interfacial region. This has also been observed computationally at the air-water interface.[24] Experimental VSF spectral trends given in Figure 6.4 for air-water are similar to CCl_4-water for the case of the Na_2SO_4 solutions. These spectral trends indicate that the presence of SO_4^{2-} within the interfacial region causes a higher degree of water orientation relative to the interface normal and no reduction in the depth of oriented water molecules that is observed for the monovalent anions. This behavior would result in an increase in VSFS intensity throughout the spectral region as observed.

Conclusions

This chapter presents a surface spectroscopic study of simple inorganic salt solutions (NaCl, NaBr, $NaNO_3$ and Na_2SO_4) adjacent to liquid CCl_4 in order to experimentally probe the behavior of simple inorganic ions at the organic liquid-aqueous solution interface and the their effect on interfacial molecular structure. These studies show that the anions from the salt solutions are indeed present within the interfacial region. Their presence is found to significantly alter the molecular bonding and orientation of water at the interface.

The experimental results reported in this chapter are very different than what has been seen in previous VSFS studies of salt solutions at the surface of air. Explanation of the different spectral trends in response to the presence of the same bulk concentrations of the same ions is found in the unique nature of the weak interactions between the organic phase and water that influences the adsorption and interactions of ions within the liquid-liquid interface. These interactions result in an average net orientation of the water molecules whose dipoles are oriented such that an electric field is created across this very narrow region of the interface. This field promotes the existence of ions within the region of the interface. For the monovalent anions studied, Cl^-, Br^-, and NO_3^-, the accumulation of the ions into the interfacial region screen the field causing a reduction of the orientating force on interfacial water molecules and a narrower interfacial region. For SO_4^{2-}, the trend is opposite that of the monovalent ions. Due to the higher charge, SO_4^{2-} tends to remain more highly solvated and thus to reside further away from the interface

where its presence actually causes additional orientation of interfacial water molecules that results in an increase in VSFS intensity that is contrast to the other ions studied.

The results of these spectroscopic studies further the understanding of water at hydrophobic surfaces and ions at aqueous surfaces. In particular, they illuminate the importance of the non-aqueous phase in the behavior of ions at interfaces and the role that polarizability, charge, and polarity of this non-aqueous phase will all play in the adsorption and interaction of ions within the interfacial region. Understanding the importance of how the ions respond not only to the surrounding solvating water molecules but also to the forces present from the non-aqueous moieties has important implications in many processes including ion transport across a membrane, groundwater contaminated by organic solvents, and even chemical synthesis at organic liquid-water interfaces.

CHAPTER VII

EFFECTS OF PH AT THE ORGANIC LIQUID-WATER INTERFACE

This chapter presents experiments employing vibrational sum-frequency spectroscopy (VSFS) to examine the effect of hydrogen and hydroxide ions on the water structure at the organic liquid-water interface. Solutions of HCl and NaOH were used to elucidate how water molecules adjacent to the non-polar liquid CCl_4 respond to changes in pH. The interfacial water structure changed significantly at the extremes of the pH scale, below pH 2 and above pH 10. These effects are similar to those seen in analogous experiments at the air-water interface showing that the water-like ions have very different interfacial behavior than was observed for charges species such as simple salts or small concentrations of surfactants.

Introduction

Interest in acidic and basic aqueous solutions stems from their importance in many processes, such as how proton solvation affects transport in biological systems. This has prompted numerous studies to better understand the structure and bonding of these solutions, most of which have been done primarily in the bulk.[1-6] Recently, interest in how the acid and base products of water, H^+ and OH^-, are adsorbed at interfaces has begun to receive a great deal of attention. Experimental investigations using non-linear surface selective spectroscopies, VSFS[7-14] and second harmonic generation (SHG)[15], in addition to many computational efforts[16-24] have greatly aided in furthering the understanding of these aqueous surfaces. A general agreement amongst most of these studies is that H^+ (or the solvated form H_3O^+) is found to be present amongst the top layers of the interface whereas the behavior of OH^- is not as clear. It does not appear to accumulate at the interface and may actually be repelled from the surface. One exception to these conclusions is for the theoretical system comprised of a rigid solid phase adjacent to the aqueous solution. Studies of these interfaces by simulation show some accumulation of OH^- and also for solvated H^+.[19, 23, 24]

The focus thus far, both experimentally and computationally, has been almost exclusively on the air-water interface, along with some attention paid to the solid-water interfaces. Only a few MD simulations have broached the subject of the nature of these ions at liquid-liquid interfaces.[23, 25] As shown in the studies discussed in Chapter VI regarding simple ions at the CCl_4-water interface, the unique structure of the surface

defined by the interactions of liquid organic molecules with water can result in very different ion adsorption behavior. In addition, the liquid-liquid environment is more similar in nature to that of a solvated cell making it a more realistic model for interfacial study that can be applied to more biological systems.

The goal of the experiments presented in this chapter is to understand how acidic and basic solutions affect the water structure at the organic liquid-water interface. With a detailed picture of the neat interface already established, the influence of H^+ and OH^- will be examined by VSFS studies of the OH stretching region of the CCl_4-water interface. The spectral results of the interface of CCl_4 adjacent to solutions of HCl and NaOH are compared to those obtained for simple inorganic ions to show that H^+ and OH^- are responsible for the trends observed here. The discussion also incorporates a comparison between the liquid-liquid and air-water results in addition to pertinent simulations studies.

Experimental Considerations

The experiments presented here used the picosecond laser system described in Chapter III. Beam energies used in the current experiments are 80 μJ and ~200-250 μJ for the visible and IR beams respectively. Beam angles were chosen to maintain a TIR geometry of the visible beam for all concentrations of HCl and NaOH used in the aqueous solutions: 69.5° and 75° from the interface normal for the visible and IR beams respectively. Multiple spectra of each interface were taken and averaged to achieve an acceptable signal to noise level. Spectra of the same pH concentrations were taken on

multiple days to assure reproducibility. A neat CCl_4-water spectrum was taken at the beginning and end of each day that pH data was collected in order to estimate fluctuations in intensity from day to day, as well as assure no contamination effects.

The VSF spectral results were shown to be extremely sensitive to chemical impurities so great care was taken to eliminate any effects from these. CCl_4 (≥99.9%+, Chromosolv HPLC grade) was purchased from Sigma-Aldrich and then distilled twice before use in any experiments. The HCl and NaOH were also both purchased from Sigma-Aldrich. The HCl was A.C.S. reagent grade, 37%, and was used from the bottle for making the acidic solutions. NaOH pellets, 99.998% metals basis purity, were used for the basic experiments. Although a high grade purity, using the NaOH as purchased resulted in inconsistent spectral results as well as giving VSF spectra resembling those taken of small concentrations of surfactants, indicating the presence of organic, surface active impurities in the NaOH. The NaOH pellets were therefore baked in an oven at 220° for ~12 hours prior to use. The spectra using the baked NaOH were very consistent and showed no signs of organic contamination. Water used to make the solutions for these experiments came from a Nanopure II filtering system (Barnstead) with a ~17.9 MΩ cm resistivity. Fresh solutions of acid or base were prepared every day of data collection. The pH was tested before use to assure the correct pH of each of the solutions. All glassware used in addition to the sample cell components were cleaned in NoChromix dissolved in concentrated sulfuric acid, and then rinsed copiously with the Nanopure filtered water.

Results for HCl and NaOH at the CCl_4-Water Interface

Figure 7.1 shows the spectra taken at low pH by adding HCl to the aqueous phase. The black traces in each plot show the neat CCl_4-water spectrum for comparison. At the lowest concentration, pH 1, there is increased spectral intensity within most of the OH stretching region. This occurs for both the more strongly and more weakly bonded water regions around 3200 cm^{-1} and 3500 cm^{-1}, respectively. With further addition of HCl, the spectra of solutions with pH 0.5 and 0.1 adjacent to CCl_4 follow this same trend with additional increases in VSFS intensity throughout the OH stretching spectral region. The free OH oscillator modes in the spectra of Figure 7.1 show only a slight increase in intensity for the lowest pH (highest HCl concentration). VSF spectra that were acquired of solutions having pH = 2 – 5 are not shown here but they did not show any significant changes in comparison to the neat CCl_4-water spectrum.

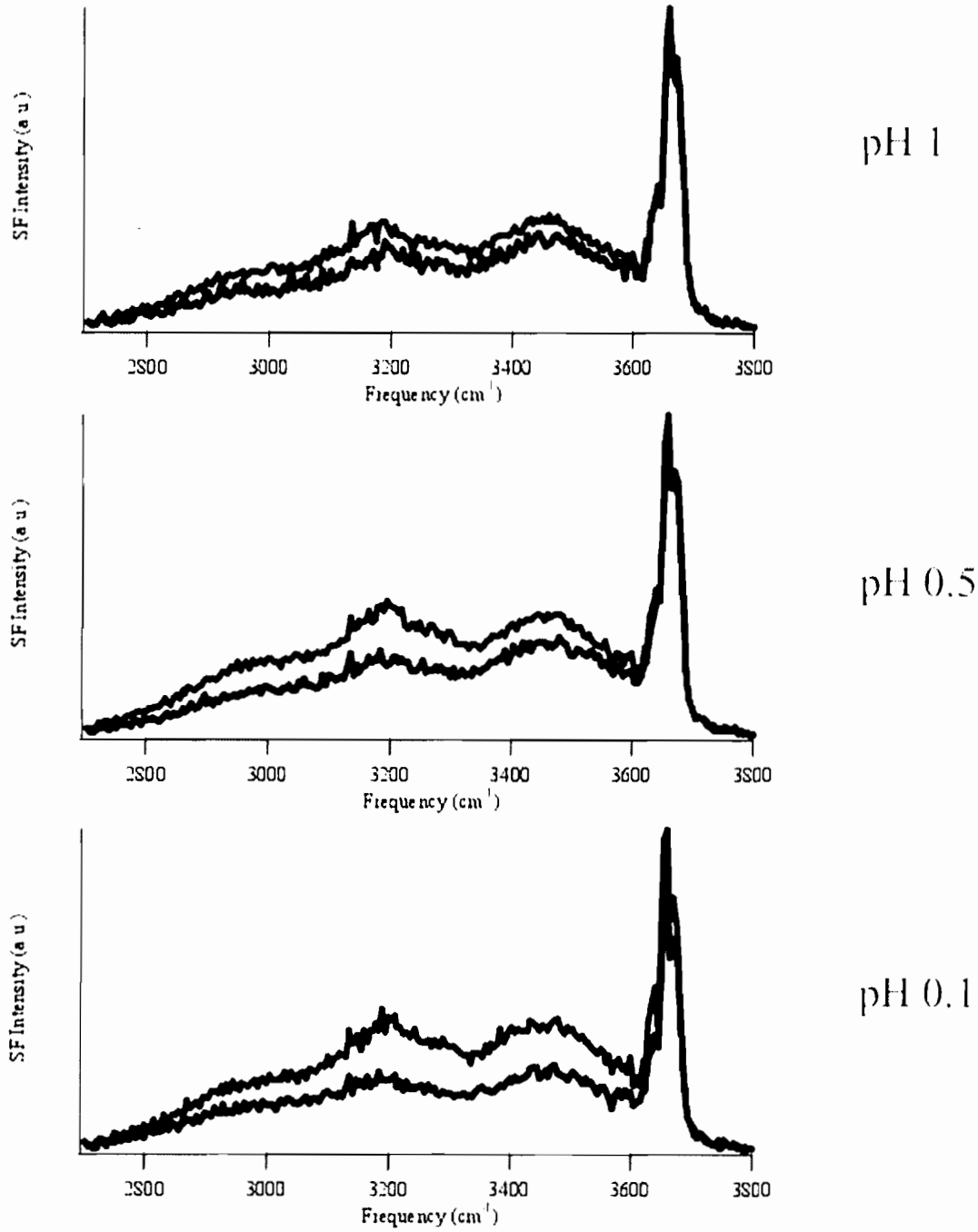

Figure 7.1 VSF spectra of low pH solutions made with additions of HCl at the interface with CCl_4. The red traces are the pH data and the black traces are the neat CCl_4-water interface spectra.

In order to assure that the spectral changes are indeed due to effects from H^+ and not Cl^- present from addition of the acid, Figure 7.2 presents the spectra of CCl_4 at the interface with the pH 1 solution and spectra of solutions of NaCl and KCl, at ~1 M in concentration. In all three of these plots, the black trace is the neat CCl_4-water spectrum for comparison. It is evident from Figure 7.2 that addition of Cl^- salts causes a decrease in intensity in the spectral region below the free OH. In contrast, for this same spectral region, there is an increase in VSFS intensity observed when HCl is added to the aqueous phase.

This opposite behavior provides evidence that the trends seen in Figure 7.1 are due to effects of H^+ on the water structure from the dissociation of the acid and not the Cl^-. In addition, the similarities in spectra for the solutions of NaCl and KCl spectra, in addition to the other salts shown in previous studies presented in Chapter VI, indicate that these cations do not affect the interface significantly. The experiments for NaOH, presented below, assume that all changes to the water structure come from the presence of OH^- and not Na^+.

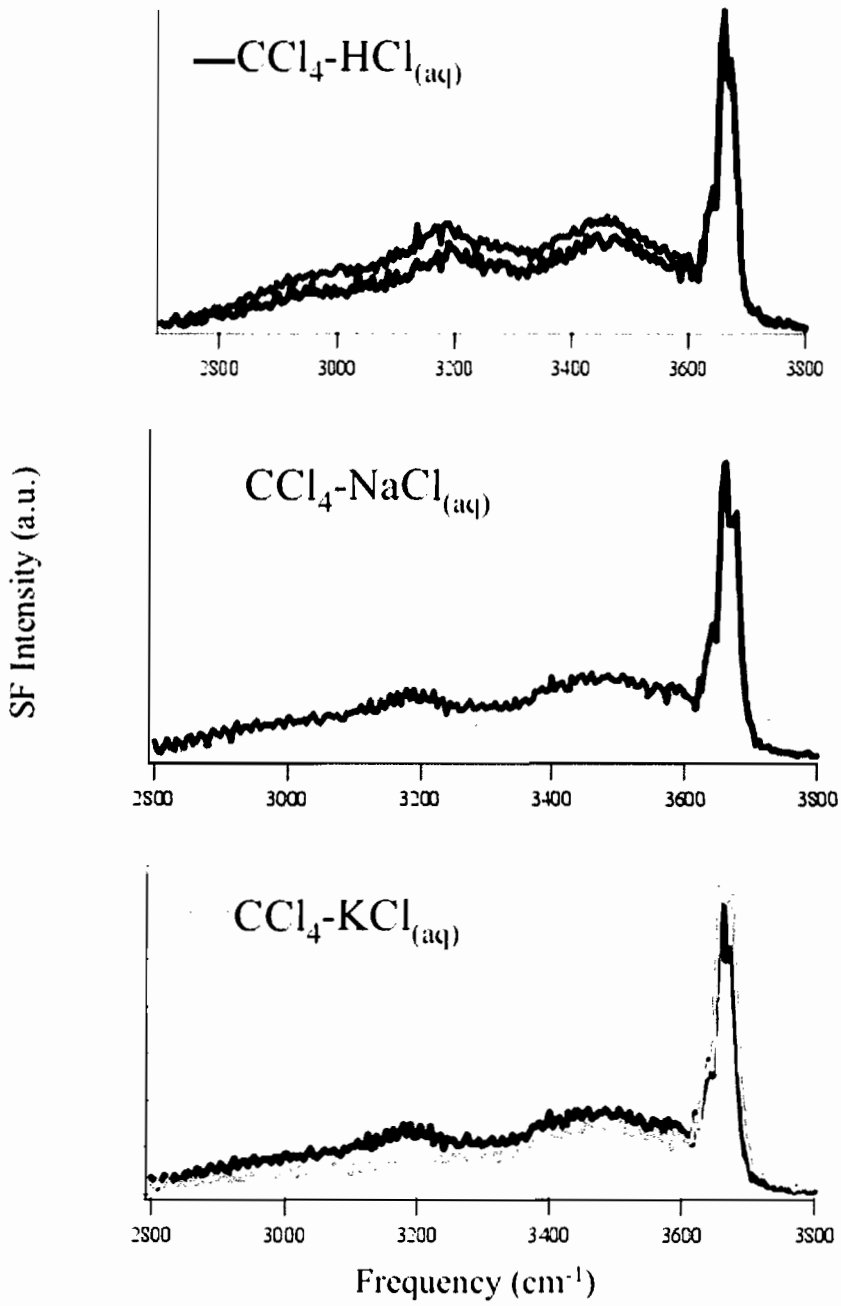

Figure 7.2 Comparison of VSF spectra taken for ~1 M solutions of NaCl, and KCl and pH 1 (HCl) to demonstrate the differences in effects from the ions H^+ and Cl^-. The traces in color are for the solutions and the black traces show the neat CCl_4-water spectrum for comparison.

Spectra of the high pH range were also acquired by adding NaOH to the aqueous phase. These spectra are shown in Figure 7.3 with the neat CCl_4-water spectrum shown in each plot in black for comparison. For these basic solutions, the trend is the opposite that of the acidic solutions. Additions of HCl shown in Figure 7.1 caused an increase in VSFS intensity for frequencies below the free OH mode. With added NaOH, bulk solutions above pH 10 show a decrease in intensity is seen across the entire spectral region below 3600 cm^{-1}. The spectrum for pH 6 is shown to demonstrate that the spectra acquired at intermediate concentrations of both HCl and NaOH do not exhibit any differences in comparison to the neat CCl_4-water interface spectrum. As more base is added to the aqueous phase, the decrease in intensity becomes more apparent both for the more highly coordinated water region (3200 cm^{-1}) and the weaker bonded region (3500 cm^{-1}). As was observed for the spectra of HCl, there are no significant changes observed for the free OH modes for these spectra.

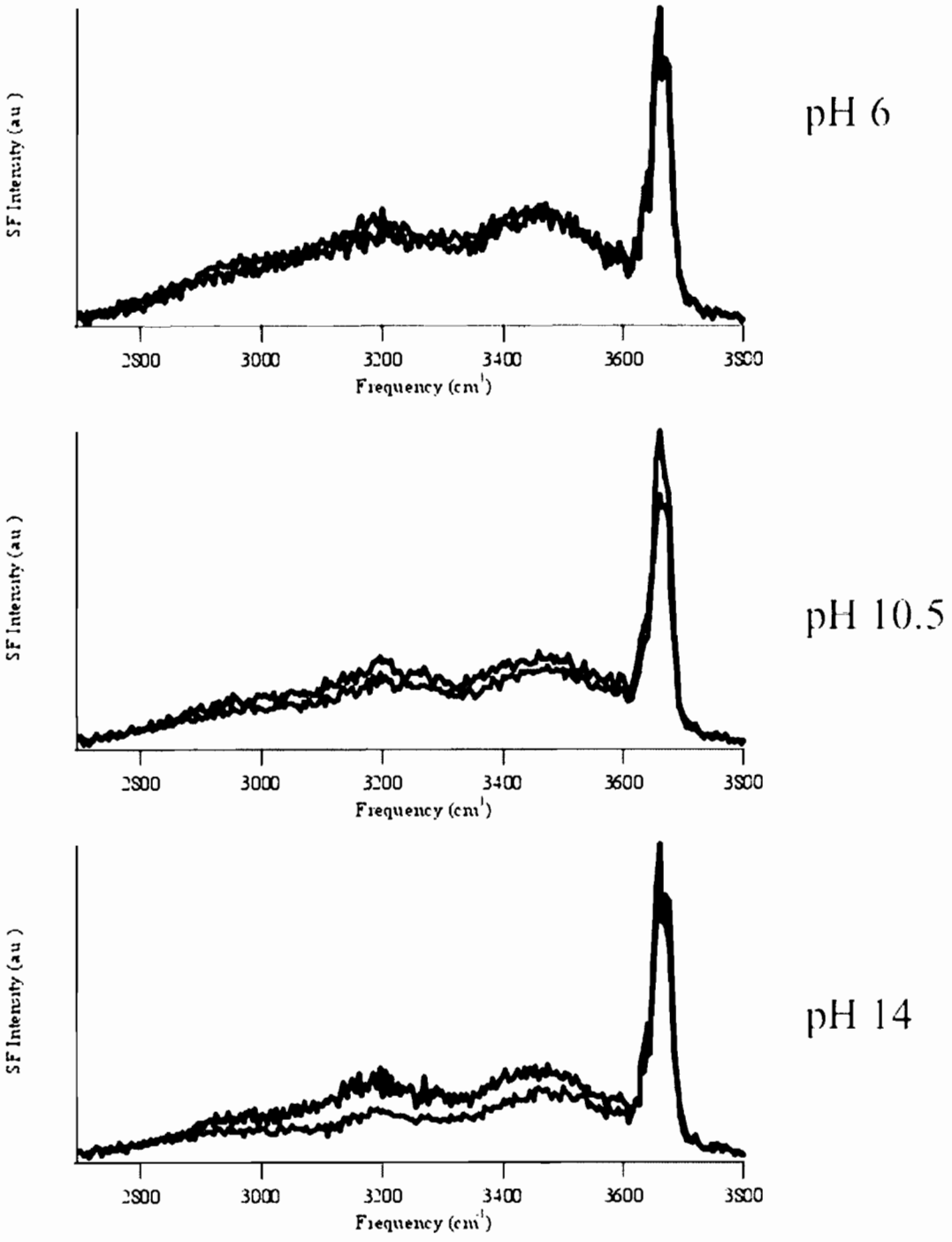

Figure 7.3 VSF spectra of high pH solutions made with additions of NaOH at the interface with CCl_4. The grey traces are the pH data and the black traces are the neat CCl_4-water interface spectra.

Discussion: pH Effects at the CCl_4-Water Interface

The addition of HCl and NaOH to the aqueous phase causes distinct changes to the VSF spectra in comparison to the neat CCl_4-water spectrum indicating there are significant changes in the molecular behavior of water molecules within the interfacial region. The comparison of spectra for both NaCl and KCl in comparison to HCl, shown in Figure 7.2 show that the salt solutions of Cl^- have very different behavior than the acid at the interface with CCl_4. From these observations, it is assumed that H^+ and OH^- are primarily responsible for the spectral changes that are observed in Figures 7.1 and 7.3. These ions will therefore be the focus of this discussion. This is consistent with previous studies that have indicated the smaller, less polarizable ions have little effect on the water structure within the interfacial region.[26-28]

Beginning with Figure 7.1, as the acidity of the aqueous phase is increased, the intensity is observed to increase throughout the OH stretching region below the free OH mode. There can be several factors that contribute to the increase in VSFS intensity, as is described in Chapter II. The possibilities are changes both to the number of contributing water bonded species in their corresponding spectral region and in orientation of various water bonded species relative to the surface normal which will contribute more or less given the chosen ssp beam geometry. These come from the relationships between number density, N, and the molecular hyperpolarizability values, β, with the non-linear susceptibility $\chi_v^{(2)}$ and the VSFS intensity. Greater values of N and water molecules in

more oriented configurations, greater average β, will both lead to increases in VSFS intensity.

While it is difficult to distinguish between the contributing factors to the observed increasing VSFS intensity, both possibilities are likely responsible for these results. With acid added to the aqueous phase of the interface, strong electrostatic interactions take place between H^+ and the surrounding water molecules. This leads to solvated proton species and can also induce further orientation of the water molecules deeper into the bulk phase. With increases in intensity across the spectral region, this indicates that the effects of H^+ reach water molecules in the topmost layer of the interface.

This same picture has been observed at the air-water interface by VSFS experiments done in our laboratory by Dr. Teresa Tarbuck and Stephanie Ota[9] that incorporate isotopic dilution and spectral fitting as well as earlier VSFS experiments of acid at the air interface.[13, 14] In addition to the experimental findings, computational VSF spectra for acid solutions at the interface with air have been done by two independent research groups.[18, 29] Their findings corroborate the conclusions that increases in intensity observed in for the VSF spectra are accounted for by enhanced orientation of water molecules in contact with the solvated protons as well as the oriented solvated protons themselves. Figure 7.4 shows the similar spectral results obtained both at aqueous interfaces in the presence of HCl. With such similar VSFS results observed, it is likely that the same fundamental interactions are taking place between the water and H^+ ions.

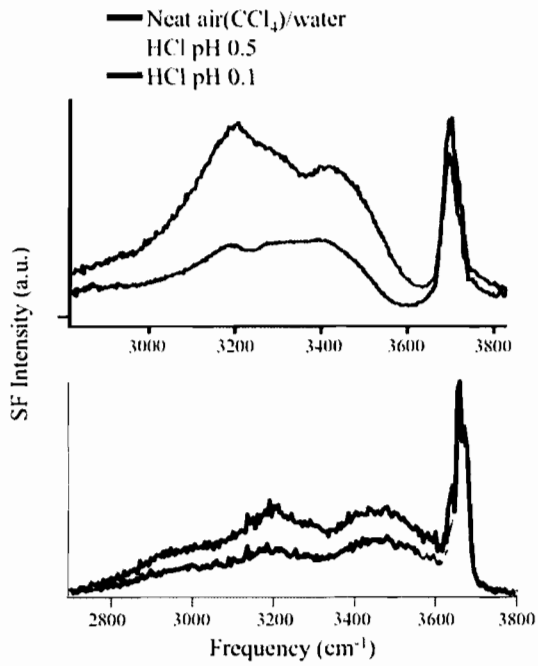

Figure 7.4 VSF spectra comparing low pH results for the air-water (top) and CCl_4-water (bottom) interfaces. The air-water data was taken from Reference 9.

The spectral features for HCl at the interface with CCl_4 are also somewhat similar to those found for Na_2SO_4 solutions. The stronger interactions between water and the divalent SO_4^{2-} ions also result in increased orientation of water molecules as evidenced by the increase in VSFS intensity. However, one difference is that the acidic spectra show greater intensity increase in the lower frequency and more strongly bonded spectral region around 3200 cm^{-1}. This could be due to contributions from the solvated protons that have been shown to have their stretching frequencies around this lower frequency OH region according to bulk IR studies.[30-32]

The spectra for the basic solutions show a distinct decrease in intensity throughout the entire spectral region below ~3600 cm^{-1}. This is the opposite behavior than was observed for the spectra of the acidic solutions indicating very different effects for OH^-

observed for the spectra of the acidic solutions indicating very different effects for OH^- on the local water environment compared to H^+. The decrease in intensity with increasing pH is attributed to a disruption of water ordering, and a displacement of water molecules in the topmost water layers, which reduce the number of contributing water molecules, N, and lower the average β thereby reducing the VSFS intensity. The spectra of NaOH solutions have similar trends as the small, inorganic ions. The spectra shown in Figure 7.3 resemble those of the ~1 M Br^- solutions, which were also concluded to reduce molecular orientation and interfacial width of the water phase. Like the solutions of HCl, the spectra of solutions at high bulk pH values are similar both at the liquid-liquid and air-water interfaces. Figure 7.5 displays the spectra for both of these systems for comparison.

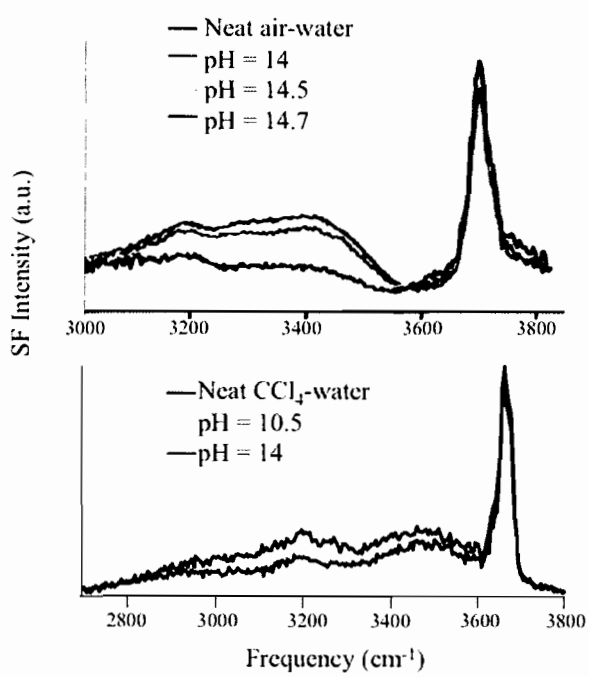

Figure 7.5 VSF spectra comparing solutions of high bulk pH at the air-water (top) and CCl_4-water (bottom) interfaces. The data for the air-water interface spectra are taken from Reference 9.

It is interesting to note that the behaviors of the acidic and basic solutions are so similar for both aqueous interfaces shown in Figures 7.4 and 7.5. Though the increase(decrease) of the different spectral regions for low(high) pH solutions is not identical for the different interfaces, the trends are the same. This was not observed for the experiments of small inorganic ions shown in Chapter VI. Clearly the ion products from water, H^+ and OH^-, incorporate themselves differently within the interfacial environment than other charged species. This is not surprising given the dynamic aqueous phase environment where they have the unique ability to undergo proton transfer processes with surrounding water molecules. The comparisons further prove the importance of considering the identity and characteristics of the adsorbates when developing theoretical models regarding charged species at interfaces.

The Debate Over OH^- Versus H^+ at Interfaces

With the increased attention being paid to pH effects at surfaces, a debate has emerged in the literature regarding the conclusions of what ionic water species are found within the interfacial region.[22, 33, 34] This is largely due to conclusions drawn from experiments analyzing potential measurements of bubbles and oil droplets.[35-39] To generally summarize one of these types of experiments most relevant to the current VSFS experiments, oil-in-water emulsions are made without the presence of surfactants at specific pH and ionic strength conditions usually with the use of HCl, NaOH, and NaCl.

The two phases are mixed either by rapid stirring using a homogenizer or heating to form the droplets, which coalesce to relatively stable emulsions around 1 μm in size. An external electric field is applied across the system and the particles are observed to move with some velocity related to the magnitude of the field, which is measured in units of velocity per electric field, i.e. electrophoretic mobility. These measurements are then related to the surface potential with respect to the bulk phase. Because the particles are measured to have increasingly negative mobilities correlating with pH, it is concluded that OH^- is preferentially adsorbing to the interface, a clear contrast to the conclusions derived from recent spectroscopic and simulation studies.

In an effort to reconcile these differences, one intriguing simulation paper recently looked not at the adsorption of the ions but at the origin for the movement and charge of oil-in-water droplets under an applied potential.[25] The authors of this study found that by simulating a potential, these heptane in water droplets actually moved without *any* ions being present in the simulation. This calls into question the conclusions of the zeta potential measurements, namely that the charge of the particle due to OH^- adsorption is what causes the mobility of the droplets. From the simulation data, they also calculate the dipolar ordering of water adjacent to heptane with respect to the interface normal. The charge from this ordering results in a potential at the interface. The applied external field then interacts with this local field set up by the oriented water molecules, which the authors attribute to the movement of the droplets.

As shown in the VSF spectra of non-polar organic liquid-water interfaces, there is a significant degree of orientation of the water molecules in response to their interactions

with the hydrophobic phase.[40, 41] The orientation and subsequent potential across the interface has also been replicated in MD simulations of the neat interfaces previously.[42, 43] However, the conclusion that the field present at the interface is solely responsible for the movement of these droplets still seems at odds with the potential measurements given the VSFS data shown in this chapter. The potential measurements show that with increased pH, the zeta potential increases (becomes more negative) within the approximate range of pH 3 – 9.[35, 39] The VSF spectra shown in Figures 7.1 and 7.3 show that only outside this pH range is the water structure significantly changed by the addition of acid or base. If water orientation were primarily responsible for the movement of the droplets, then an increase in orientation, or number of orientated molecules that occurs with the acidic solutions should cause a greater electrostatic interaction and an increase in measured potential. This is not what is observed when the results shown in Figure 7.1 are considered in light of the potential measurements.[35] Addition of HCl results in intensity enhancement throughout the water bonded regions due, at least in part, to increased orientation of the water molecules toward the surface normal. However, when the pH is decreased in the experimental droplet studies[35], the potential measurements decrease towards the isoelectric point. This suggests that the mechanism for droplet movement cannot be fully explained by the orientation of the water molecules at the organic interface. As discussed in previous chapters, the strength of VSFS as an experimental tool is its surface specificity. It has already been used to show that the air-water interface[9] is most sensitive the adsorption of solvated H^+ over OH^-, which has greatly aided the discussion between communities regarding the debate described above. The

results shown for the CCl_4-water interface also further the understanding regarding this debate.

Conclusions

Experiments in this chapter investigate the effects of altering the pH of the aqueous phase adjacent to the non-polar organic liquid CCl_4 by addition of HCl or NaOH. Through examination of the OH stretching region, the effects of the ions H^+ and OH^- on the water orientation and bonding were examined within the liquid-liquid interfacial environment. Their presence was shown to cause significant changes to the aqueous phase structure at the extremes of the pH scale.

Comparison of the spectral results for acidic and basic solutions to other interfacial systems reveals interesting information regarding the nature of the water dissociation ions. When compared to similar spectra acquired at the air-water interface, VSF spectra for H^+ and OH^- at the liquid-liquid interface showed the same trends. This is quite different than what was observed for the inorganic ions, which showed opposite trends at the CCl_4-water interface in comparison to the air-water interface spectra. The ability of the water product ions to be solvated differently than other ions and possibly their abilities to exchange protons with surround water molecules likely contribute to the different behavior than what was observed for the inorganic ions.

The VSFS studies presented here and specifically the comparisons between results at different interfaces further illustrate the emerging picture of the behavior of

different types of ions and charged species at interfaces. In particular the identity of the charged species and how it interacts with the surrounding water molecules largely determine its behavior within the interfacial region. Considering charge alone, as do some theoretical models, is not sufficient to describe interfacial phenomena. The parameters of the non-aqueous phase, the charged species, and how both of these interact with water all play a collective role in the resulting effects at the interface. This understanding has important implications when extending the interfacial models to more complex systems and will allow for more realistic results.

CHAPTER VIII

CONCLUSIONS

At first glance, the liquid-liquid interface appears to be a simple system. It is, anyway, comprised of only two immiscible liquids. In order to understand the system, there are some basic questions that can be asked. For example: Does the interface go abruptly from one liquid phase to another, or is there a degree of mixing between the two? How does the structural environment at the junction where the molecules from the two liquids interact differ with respect to the bulk environments? How far do these interactions extend into either phase? Will solutes accumulate within this environment differently than the bulk? These questions are at the crux of some of the aspects of the surface such as interfacial roughness, width, anisotropic orientation distributions, and adsorption being investigated currently using state-of-the-art experimental[1-9] and computational[10-14] approaches.

Upon closer examination there are still quite a few unknowns regarding the very thin boundary where these two liquids meet. The VSFS experiments in each of the Chapters V, VI, and VII were done to provide answers to some of these important and unanswered questions. Through examination of the aqueous phase under different

conditions, insight was gained into the molecular bonding and orientation of the water molecules, as well as their interactions with the organic liquid phase.

As the polarity of the organic liquid is increased, the interaction between it and water increases. This interaction disrupts the highly structured aqueous layer present at non-polar liquid-water interfaces. The result of increased interactions between the liquids is less orientation of the water molecules within the interface. Water molecules are also more likely to be found on the organic side of the dividing surface of the interface when the organic liquid has a greater polar nature.

The behavior of ions at the liquid-liquid interface is governed by several factors including the specific ions characteristics and the nature of the interface. The unique interaction between the organic liquid and the aqueous phase causes some ions to affect the water structure very differently in comparison to results seen at the air-water interface. The highly oriented water molecules create a potential across the liquid-liquid interfacial region that attracts the ions. The presence of the monovalent ions Cl^-, Br^-, and NO_3^- result in a decrease of water ordering and a decrease in interfacial width. The larger and more polarizable NO_3^- is most able to cause this effect due, most likely, to its greater concentration at the interface. These monovalent ion trends are opposite to that obtained by analogous air-water studies. The more highly charged SO_4^{2-} has the opposite effect as the monovalent ions and actually enhances the ordering of the interfacial water molecules. Water dissociation ions H^+ and OH^- behave somewhat differently than the monovalent and divalent inorganic ions. Solvated H^+ causes ordering of the surrounding interfacial water molecules while OH^- results in the disordering of the interface. These

trends are also observed at the air-water interface. Taken together, these studies provide a great deal of understanding regarding the emerging picture of ion behavior at interfaces revealing how complex the interfacial environment is.

Since Benjamin Franklin pondered the interactions between oil and water over two centuries ago, considerable progress has been made towards the understanding of hydrophobic-aqueous interfaces through the advances made in experimental, theoretical, and computational investigative approaches. The potential for application of liquid-liquid interfaces has been realized in the areas of synthesis[15, 16] and nanoparticle[17] formation with the promise of others ahead in the near future. This has been possible because of the growing body of knowledge regarding the fundamental aspects of the organic liquid-water interface. As Charles Tanford writes, "no good scientist wants to build on a foundation of shifting sand."[18] The research efforts presented in this dissertation contribute to laying the solid foundation for a greater understanding of the unique liquid-liquid interface.

APPENDIX

FITTING RESULTS FOR THE NEAT ORGANIC LIQUID-WATER SPECTRA

The following table summarizes the fitting results to the neat CCl_4-water and chloroform-water interfacial vibrational sum-frequency spectra discussed in chapter V.

	CCl_4			Chloroform			
	coordinated	Donor OH	Free OH	coordinated	Donor OH	Free OH	weakly bonded
Amplitude	0.252	0.349	1.43	0.269	0.364	0.925	0.23
Phase (radians)	0	3.14	0	0	3.14	0	0
Frequency (cm^{-1})	3240 (+/- 10)	3450 (+/- 15)	3669 (+/- 2)	3240 (+/- 10)	3530 (+/- 16)	3645 (+/- 2)	3594 (+/- 2)
Lorentzian Width (cm^{-1})	5	5	12	5	5	12	5
Gaussian Width (cm^{-1})	200	95	11	233	109	15	12

Table A.1 Parameters used to fit the CCl_4-water and chloroform-water VSF spectra discussed in chapter V

REFERENCES

Chapter I

1. Ball, P., Water: Water - An Enduring Mystery. *Nature* **2008,** *452* (7185), 291-292.

2. Tanford, C., *Ben Franklin Stilled the Waves : An Informal History of Pouring Oil on Water with Reflections on the Ups and Downs of Scientific Life in General.* Oxford University Press: New York, 2004; p 288.

3. Miranda, P. B.; Shen, Y. R., Liquid Interfaces: A Study by Sum-Frequency Vibrational Spectroscopy. *J. Phys. Chem. B* **1999,** *103* (17), 3292-3307.

4. Miranda, P. B.; Xu, L.; Shen, Y. R.; Salmeron, M., Icelike Water Monolayer Adsorbed on Mica at Room Temperature. *Phys. Rev. Lett.* **1998,** *81* (26), 5876-5879.

Chapter II

1. McHale, J. L., *Molecular Spectroscopy*. 1st ed.; Prentice Hall: Upper Saddle River, N.J., 1999; p 463.

2. Shen, Y. R., *The Principles of Nonlinear Optics*. J. Wiley: New York, 1984; p 563.

3. Guyotsionnest, P.; Hunt, J. H.; Shen, Y. R., Sum-Frequency Vibrational Spectroscopy of a Langmuir Film - Study of Molecular-Orientation of a Two-Dimensional System. *Phys. Rev. Lett.* **1987,** *59* (14), 1597-1600.

4. Zhu, X. D.; Suhr, H.; Shen, Y. R., Surface Vibrational Spectroscopy by Infrared-Visible Sum Frequency Generation. *Phys. Rev. B* **1987,** *35* (6), 3047-3050.

5. Shen, Y. R., Surface-Properties Probed by 2nd-Harmonic and Sum-Frequency Generation. *Nature* **1989,** *337* (6207), 519-525.

6. Bain, C. D.; Davies, P. B.; Ong, T. H.; Ward, R. N.; Brown, M. A., Quantitative-Analysis of Monolayer Composition by Sum-Frequency Vibrational Spectroscopy. *Langmuir* **1991,** *7* (8), 1563-1566.

7. Bain, C. D., Sum-Frequency Vibrational Spectroscopy of the Solid-Liquid Interface. *J. Chem. Soc., Faraday Trans.* **1995,** *91* (9), 1281-1296.

8. Lambert, A. G.; Davies, P. B.; Neivandt, D. J., Implementing the Theory of Sum Frequency Generation Vibrational Spectroscopy: A Tutorial Review. *Appl. Spectrosc. Rev.* **2005,** *40* (2), 103-145.

9. Zhuang, X.; Miranda, P. B.; Kim, D.; Shen, Y. R., Mapping Molecular Orientation and Conformation at Interfaces by Surface Nonlinear Optics. *Phys. Rev. B* **1999,** *59* (19), 12632-12640.

10. Lobau, J.; Wolfrum, K., Sum-Frequency Spectroscopy in Total Internal Reflection Geometry: Signal Enhancement and Access to Molecular Properties. *J. Opt. Soc. Am. B* **1997,** *14* (10), 2505-2512.

11. Moore, F. G.; Becraft, K. A.; Richmond, G. L., Challenges in Interpreting Vibrational Sum Frequency Spectra: Deconvoluting Spectral Features as Demonstrated in the Calcium Fluoride-Water-Sodium Dodecylsulfate System. *Appl. Spectrosc.* **2002,** *56* (12), 1575-1578.

12. Raymond, E. A.; Tarbuck, T. L.; Brown, M. G.; Richmond, G. L., Hydrogen-Bonding Interactions at the Vapor/Water Interface Investigated by Vibrational Sum-Frequency Spectroscopy of HOD/H2O/D2O Mixtures and Molecular Dynamics Simulations. *J. Phys. Chem. B* **2003,** *107* (2), 546-556.

13. Scatena, L. F.; Richmond, G. L., Orientation, Hydrogen Bonding, and Penetration of Water at the Organic/Water Interface. *J. Phys. Chem. B* **2001,** *105* (45), 11240-11250.

14. Walker, D. S.; Moore, F. G.; Richmond, G. L., Vibrational Sum Frequency Spectroscopy and Molecular Dynamics Simulation of the Carbon Tetrachloride-Water and 1,2-Dichloroethane-Water Interfaces. *J. Phys. Chem. C* **2007,** *111* (16), 6103-6112.

15. Morita, A.; Hynes, J. T., A Theoretical Analysis of the Sum Frequency Generation Spectrum of the Water Surface. *Chem. Phys.* **2000,** *258* (2-3), 371-390.

16. Morita, A.; Hynes, J. T., A Theoretical Analysis of the Sum Frequency Generation Spectrum of the Water Surface. II. Time-Dependent Approach. *J. Phys. Chem. B* **2002,** *106* (3), 673-685.

Chapter III

1. Du, Q.; Superfine, R.; Freysz, E.; Shen, Y. R., Vibrational Spectroscopy of Water at the Vapor Water Interface. *Phys. Rev. Lett.* **1993,** *70* (15), 2313-2316.

2. Shen, Y. R., Surface-Properties Probed by 2nd-Harmonic and Sum-Frequency Generation. *Nature* **1989,** *337* (6207), 519-525.

3. Hommel, E. L.; Ma, G.; Allen, H. C., Broadband Vibrational Sum Frequency Generation Spectroscopy of a Liquid Surface. *Anal. Sci.* **2001,** *17* (11), 1325-1329.

4. Hore, D. K.; King, J. L.; Moore, F. G.; Alavi, D. S.; Hamamoto, M. Y.; Richmond, G. L., Ti: Sapphire-Based Picosecond Visible-Infrared Sum-Frequency Spectroscopy from 900-3100 $cm^{(-1)}$. *Appl. Spectrosc.* **2004,** *58* (12), 1377-1384.

5. Soule, M. C. K.; Hore, D. K.; Jaramillo-Fellin, D. M.; Richmond, G. L., Differing Adsorption Behavior of Environmentally Important Cyanophenol Isomers at the Air-Water Interface. *J. Phys. Chem. B* **2006,** *110* (33), 16575-16583.

6. Stiopkin, I. V.; Jayathilake, H. D.; Bordenyuk, A. N.; Benderskii, A. V., Heterodyne-Detected Vibrational Sum Frequency Generation Spectroscopy. *J. Am. Chem. Soc.* **2008,** *130* (7), 2271-2275.

7. Hore, D. K.; Beaman, D. K.; Richmond, G. L., Surfactant Headgroup Orientation at the Air/Water Interface. *J. Am. Chem. Soc.* **2005,** *127* (26), 9356-9357.

8. Soule, M. C. K.; Blower, P. G.; Richmond, G. L., Effects of Atmospherically Important Solvated Ions on Organic Acid Adsorption at the Surface of Aqueous Solutions. *J. Phys. Chem. B* **2007,** *111* (49), 13703-13713.

9. Scatena, L. F.; Richmond, G. L., Orientation, Hydrogen Bonding, and Penetration of Water at the Organic/Water Interface. *J. Phys. Chem. B* **2001,** *105* (45), 11240-11250.

10. Lobau, J.; Wolfrum, K., Sum-Frequency Spectroscopy in Total Internal Reflection Geometry: Signal Enhancement and Access to Molecular Properties. *J. Opt. Soc. Am. B* **1997,** *14* (10), 2505-2512.

11. Zhuang, X.; Miranda, P. B.; Kim, D.; Shen, Y. R., Mapping Molecular Orientation and Conformation at Interfaces by Surface Nonlinear Optics. *Phys. Rev. B* **1999,** *59* (19), 12632-12640.

12. Lang, M. L.; Wolfe, W. L., Optical-Constants of Fused-Silica and Sapphire from 0.3 to 25-um. *Appl. Opt.* **1983,** *22* (9), 1267-1268.

13. Czarnecki, M. A.; Hawranek, J. P.; Wrzeszcz, W., Thin-Film Transmission Spectra of Liquid CDCl3 in the Infrared. *J. Mol. Struct.* **1992,** *275*, 111-121.

14. Goplen, T. G.; Cameron, D. G.; Jones, R. N., Absolute Absorption Intensity and Dispersion Measurements on Some Organic Liquids in the Infrared. *Appl. Spectrosc.* **1980,** *34* (6), 657-691.

15. Hale, G. M.; Querry, M. R., Optical Constants of Water in the 200-nm to 200-um Wavelength Region. *Appl. Opt.* **1973,** *12* (3), 555-563.

16. Raymond, E. A.; Tarbuck, T. L.; Brown, M. G.; Richmond, G. L., Hydrogen-Bonding Interactions at the Vapor/Water Interface Investigated by Vibrational Sum-Frequency Spectroscopy of HOD/H2O/D2O Mixtures and Molecular Dynamics Simulations. *J. Phys. Chem. B* **2003,** *107* (2), 546-556.

Chapter IV

1. Bain, C. D.; Davies, P. B.; Ong, T. H.; Ward, R. N.; Brown, M. A., Quantitative-Analysis of Monolayer Composition by Sum-Frequency Vibrational Spectroscopy. *Langmuir* **1991,** *7* (8), 1563-1566.

2. Scatena, L. F.; Richmond, G. L., Orientation, Hydrogen Bonding, and Penetration of Water at the Organic/Water Interface. *J. Phys. Chem. B* **2001,** *105* (45), 11240-11250.

3. Walker, D. S.; Moore, F. G.; Richmond, G. L., Vibrational Sum Frequency Spectroscopy and Molecular Dynamics Simulation of the Carbon Tetrachloride-Water and 1,2-Dichloroethane-Water Interfaces. *J. Phys. Chem. C* **2007,** *111* (16), 6103-6112.

4. Walker, D. S.; Richmond, G. L., Depth Profiling of Water Molecules at the Liquid-Liquid Interface Using a Combined Surface Vibrational Spectroscopy and Molecular Dynamics Approach. *J. Am. Chem. Soc.* **2007,** *129* (30), 9446-9451.

5. Brown, M. G.; Walker, D. S.; Raymond, E. A.; Richmond, G. L., Vibrational Sum-Frequency Spectroscopy of Akane/Water Interfaces: Experiment and Theoretical Simulation. *J. Phys. Chem. B* **2003,** *107* (1), 237-244.

6. Gragson, D. E.; Richmond, G. L., Investigations of the Structure and Hydrogen Bonding of Water Molecules at Liquid Surfaces by Vibrational Sum Frequency Spectroscopy. *J. Phys. Chem. B* **1998,** *102* (20), 3847-3861.

7. Walker, D. S.; Brown, M.; McFearin, C. L.; Richmond, G. L., Evidence for a Diffuse Interfacial Region at the Dichloroethane/Water Interface. *J. Phys. Chem. B* **2004,** *108* (7), 2111-2114.

8. Conboy, J. C.; Daschbach, J. L.; Richmond, G. L., Total Internal-Reflection 2nd-Harmonic Generation - Probing the Alkane Water Interface. *Appl. Phys. A: Mater. Sci. Process.* **1994,** *59* (6), 623-629.

9. Grubb, S. G.; Kim, M. W.; Rasing, T.; Shen, Y. R., Orientation of Molecular Monolayers at the Liquid Liquid Interface as Studied by Optical 2nd Harmonic-Generation. *Langmuir* **1988,** *4* (2), 452-454.

10. McArthur, E. A.; Eisenthal, K. B., Ultrafast Excited-State Electron Transfer at an Organic Liquid/Aqueous Interface. *J. Am. Chem. Soc.* **2006,** *128* (4), 1068-1069.

11. Steel, W. H.; Walker, R. A., Measuring Dipolar Width across Liquid-Liquid Interfaces with 'Molecular Rulers'. *Nature* **2003,** *424* (6946), 296-299.

12. Luo, G. M.; Malkova, S.; Pingali, S. V.; Schultz, D. G.; Lin, B. H.; Meron, M.; Graber, T. J.; Gebhardt, J.; Vanysek, P.; Schlossman, M. L., The Width of the Water/2-Heptanone Liquid-Liquid Interface. *Electrochem. Commun.* **2005,** *7* (6), 627-630.

13. Luo, G. M.; Malkova, S.; Yoon, J.; Schultz, D. G.; Lin, B. H.; Meron, M.; Benjamin, I.; Vanysek, P.; Schlossman, M. L., Ion Distributions near a Liquid-Liquid Interface. *Science* **2006,** *311* (5758), 216-218.

14. Mitrinovic, D. M.; Tikhonov, A. M.; Li, M.; Huang, Z. Q.; Schlossman, M. L., Noncapillary-Wave Structure at the Water-Alkane Interface. *Phys. Rev. Lett.* **2000,** *85* (3), 582-585.

15. Mitrinovic, D. M.; Zhang, Z. J.; Williams, S. M.; Huang, Z. Q.; Schlossman, M. L., X-Ray Reflectivity Study of the Water-Hexane Interface. *J. Phys. Chem. B* **1999,** *103* (11), 1779-1782.

16. Schlossman, M. L., Liquid-Liquid Interfaces: Studied by X-Ray and Neutron Scattering. *Curr. Opin. Colloid Interface Sci.* **2002,** *7* (3-4), 235-243.

17. Tikhonov, A. M.; Mitrinovic, D. M.; Li, M.; Huang, Z. Q.; Schlossman, M. L., An X-Ray Reflectivity Study of the Water-Docosane Interface. *J. Phys. Chem. B* **2000,** *104* (27), 6336-6339.

18. Bowers, J.; Zarbakhsh, A.; Webster, J. R. P.; Hutchings, L. R.; Richards, R. W., Neutron Reflectivity Studies at Liquid-Liquid Interfaces: Methodology and Analysis. *Langmuir* **2001,** *17* (1), 140-145.

19. Doshi, D. A.; Watkins, E. B.; Israelachvili, J. N.; Majewski, J., Reduced Water Density at Hydrophobic Surfaces: Effect of Dissolved Gases. *Proc. Natl. Acad. Sci. U. S. A.* **2005,** *102* (27), 9458-9462.

20. Lee, L. T.; Langevin, D.; Farnoux, B., Neutron Reflectivity of an Oil-Water Interface. *Phys. Rev. Lett.* **1991,** *67* (19), 2678-2681.

21. Benjamins, J. W.; Jonsson, B.; Thuresson, K.; Nylander, T., New Experimental Setup to Use Ellipsometry to Study Liquid-Liquid and Liquid-Solid Interfaces. *Langmuir* **2002,** *18* (16), 6437-6444.

22. Fujiyoshi, S.; Ishibashi, T.; Onishi, H., Molecular Vibrations at a Liquid-Liquid Interface Observed by Fourth-Order Raman Spectroscopy. *J. Phys. Chem. B* **2006,** *110* (19), 9571-9578.

23. Benjamin, I., Theoretical-Study of the Water 1,2-Dichloroethane Interface - Structure, Dynamics, and Conformational Equilibria at the Liquid Liquid Interface. *J. Chem. Phys.* **1992,** *97* (2), 1432-1445.

24. Benjamin, I., Hydrogen Bond Dynamics at Water/Organic Liquid Interfaces. *J. Phys. Chem. B* **2005,** *109* (28), 13711-13715.

25. Chang, T. M.; Dang, L. X., Molecular Dynamics Simulations of CCl4-H2O Liquid-Liquid Interface with Polarizable Potential Models. *J. Chem. Phys.* **1996,** *104* (17), 6772-6783.

26. Chang, T. M.; Dang, L. X., Recent Advances in Molecular Simulations of Ion Solvation at Liquid Interfaces. *Chemical Reviews* **2006,** *106* (4), 1305-1322.

27. Hore, D. K.; Walker, D. S.; MacKinnon, L.; Richmond, G. L., Molecular Structure of the Chloroform - Water and Dichloromethane - Water Interfaces. *J. Phys. Chem. C* **2007,** *111* (25), 8832-8842.

28. Hore, D. K.; Walker, D. S.; Richmond, G. L., Layered Organic Structure at the Carbon Tetrachloride-Water Interface. *J. Am. Chem. Soc.* **2007,** *129* (4), 752-753.

29. Hore, D. K.; Walker, D. S.; Richmond, G. L., Water at Hydrophobic Surfaces: When Weaker Is Better. *J. Am. Chem. Soc.* **2008,** *130* (6), 1800-1801.

30. Jedlovszky, P.; Vincze, A.; Horvai, G., Full Description of the Orientational Statistics of Molecules near to Interfaces. Water at the Interface with CCl4. *Phys. Chem. Chem. Phys.* **2004,** *6* (8), 1874-1879.

31. Morita, A.; Hynes, J. T., A Theoretical Analysis of the Sum Frequency Generation Spectrum of the Water Surface. II. Time-Dependent Approach. *J. Phys. Chem. B* **2002,** *106* (3), 673-685.

Chapter V

1. Brown, M. G.; Walker, D. S.; Raymond, E. A.; Richmond, G. L., Vibrational Sum-Frequency Spectroscopy of Akane/Water Interfaces: Experiment and Theoretical Simulation. *J. Phys. Chem. B* **2003,** *107* (1), 237-244.

2. Scatena, L. F.; Richmond, G. L., Orientation, Hydrogen Bonding, and Penetration of Water at the Organic/Water Interface. *J. Phys. Chem. B* **2001,** *105* (45), 11240-11250.

3. Walker, D. S.; Brown, M.; McFearin, C. L.; Richmond, G. L., Evidence for a Diffuse Interfacial Region at the Dichloroethane/Water Interface. *J. Phys. Chem. B* **2004,** *108* (7), 2111-2114.

4. Benjamin, I., Theoretical-Study of the Water 1,2-Dichloroethane Interface - Structure, Dynamics, and Conformational Equilibria at the Liquid Liquid Interface. *J. Chem. Phys.* **1992,** *97* (2), 1432-1445.

5. Chang, T. M.; Dang, L. X., Molecular Dynamics Simulations of CCl4-H2O Liquid-Liquid Interface with Polarizable Potential Models. *J. Chem. Phys.* **1996,** *104* (17), 6772-6783.

6. Jedlovszky, P., The Hydrogen Bonding Structure of Water in the Vicinity of Apolar Interfaces: A Computer Simulation Study. *J. Phys.: Condens. Matter* **2004,** *16* (45), S5389-S5402.

7. Sieffert, N.; Wipff, G., Adsorption at the Liquid-Liquid Interface in the Biphasic Rhodium Catalyzed Hydroformylation of Olefins Promoted by Cyclodextrins: A Molecular Dynamics Study. *J. Phys. Chem. B* **2006,** *110* (9), 4125-4134.

8. Walker, D. S.; Moore, F. G.; Richmond, G. L., Vibrational Sum Frequency Spectroscopy and Molecular Dynamics Simulation of the Carbon Tetrachloride-Water and 1,2-Dichloroethane-Water Interfaces. *J. Phys. Chem. C* **2007,** *111* (16), 6103-6112.

9. Walker, D. S.; Richmond, G. L., Depth Profiling of Water Molecules at the Liquid-Liquid Interface Using a Combined Surface Vibrational Spectroscopy and Molecular Dynamics Approach. *J. Am. Chem. Soc.* **2007,** *129* (30), 9446-9451.

10. Walker, D. S.; Richmond, G. L., Understanding the Effects of Hydrogen Bonding at the Vapor-Water Interface: Vibrational Sum Frequency Spectroscopy of H2O/HOD/D2O Mixtures Studied Using Molecular Dynamics Simulations. *J. Phys. Chem. C* **2007,** *111* (23), 8321-8330.

11. Walker, D. S.; Richmond, G. L., Interfacial Depth Profiling of the Orientation and Bonding of Water Molecules across Liquid-Liquid Interfaces. *J. Phys. Chem. C* **2008,** *112* (1), 201-209.

12. Hore, D. K.; Walker, D. S.; MacKinnon, L.; Richmond, G. L., Molecular Structure of the Chloroform - Water and Dichloromethane - Water Interfaces. *J. Phys. Chem. C* **2007,** *111* (25), 8832-8842.

13. Hore, D. K.; Walker, D. S.; Richmond, G. L., Layered Organic Structure at the Carbon Tetrachloride-Water Interface. *J. Am. Chem. Soc.* **2007,** *129* (4), 752-753.

14. Hore, D. K.; Walker, D. S.; Richmond, G. L., Water at Hydrophobic Surfaces: When Weaker Is Better. *J. Am. Chem. Soc.* **2008,** *130* (6), 1800-1801.

15. Lobau, J.; Wolfrum, K., Sum-Frequency Spectroscopy in Total Internal Reflection Geometry: Signal Enhancement and Access to Molecular Properties. *J. Opt. Soc. Am. B* **1997,** *14* (10), 2505-2512.

16. Raymond, E. A.; Tarbuck, T. L.; Brown, M. G.; Richmond, G. L., Hydrogen-Bonding Interactions at the Vapor/Water Interface Investigated by Vibrational Sum-Frequency Spectroscopy of HOD/H2O/D2O Mixtures and Molecular Dynamics Simulations. *J. Phys. Chem. B* **2003,** *107* (2), 546-556.

17. Benjamin, I., Hydrogen Bond Dynamics at Water/Organic Liquid Interfaces. *J. Phys. Chem. B* **2005,** *109* (28), 13711-13715.

18. Ji, N.; Ostroverkhov, V.; Tian, C. S.; Shen, Y. R., Characterization of Vibrational Resonances of Water-Vapor Interfaces by Phase-Sensitive Sum-Frequency Spectroscopy. *Phys. Rev. Lett.* **2008,** *1* (9), 096102-1 - 096102-4.

19. Downey, J. R.; Choppin, G. R., Peak Ssignments of D2O and HOD in Relatively Nonpolar Solvents. *Spectrochim. Acta, Part A* **1974,** *30A*, 37-42.

20. Choppin, G. R.; Jr., J. R. D., Spectroscopic Evidence for Water-Chloroform Interaction. *Spectrochim. Acta, Part A* **1974,** *30A*, 43-45.

21. Dobrowolski, J. C.; Jamroz, M. H., The IR Evidence of H2O-Aromatic Hydrocarbons Single Hydrogen-Bond. *J. Mol. Struct.* **1993,** *293*, 147-150.

22. Graener, H.; Seifert, G., Vibrational and Orientational Relaxation of Monomeric Water-Molecules in Liquids. *J. Chem. Phys.* **1993,** *98* (1), 36-45.

23. Graener, H.; Seifert, G.; Laubereau, A., Vibrational and Reorientational Dynamics of Water-Molecules in Liquid Matrices. *Chem. Phys.* **1993,** *175* (1), 193-204.

Chapter VI

1. Chang, T. M.; Dang, L. X., Recent Advances in Molecular Simulations of Ion Solvation at Liquid Interfaces. *Chemical Reviews* **2006,** *106* (4), 1305-1322.

2. Jungwirth, P.; Tobias, D. J., Specific Ion Effects at the Air/Water Interface. *Chemical Reviews* **2006,** *106* (4), 1259-1281.

3. Petersen, P. B.; Saykally, R. J., On the Nature of Ions at the Liquid Water Surface. *Annu. Rev. Phys. Chem.* **2006,** *57*, 333-364.

4. Benjamin, I., Mechanism and Dynamics of Ion Transfer across a Liquid-Liquid Interface. *Science* **1993,** *261* (5128), 1558-1560.

5. Chorny, I.; Benjamin, I., Hydration Shell Exchange Dynamics During Ion Transfer across the Liquid/Liquid Interface. *J. Phys. Chem. B* **2005,** *109* (34), 16455-16462.

6. Wick, C.; Dang, L. X., Molecular Mechanism of Transporting a Polarizable Iodide Anion across the Water-CCl4 Liquid/Liquid Interface. *J. Chem. Phys.* **2007,** *126* (13), 134702.

7. Wick, C. D.; Dang, L. X., Distribution, Structure, and Dynamics of Cesium and Iodide Ions at the H2O-CC4 and H2O-Vapor Interfaces. *J. Phys. Chem. B* **2006,** *110* (13), 6824-6831.

8. Wick, C. D.; Dang, L. X., Recent Advances in Understanding Transfer Ions across Aqueous Interfaces. *Chem. Phys. Lett.* **2008,** *458* (1-3), 1-5.

9. Luo, G. M.; Malkova, S.; Yoon, J.; Schultz, D. G.; Lin, B. H.; Meron, M.; Benjamin, I.; Vanysek, P.; Schlossman, M. L., Ion Distributions near a Liquid-Liquid Interface. *Science* **2006,** *311* (5758), 216-218.

10. Luo, G. M.; Malkova, S.; Yoon, J.; Schultz, D. G.; Lin, B. H.; Meron, M.; Benjamin, I.; Vanysek, P.; Schlossman, M. L., Ion Distributions at the Nitrobenzene-Water Interface Electrified by a Common Ion. *J. Electroanal. Chem.* **2006,** *593* (1-2), 142-158.

11. Beildeck, C. L.; Liu, M. J.; Brindza, M. R.; Walker, R. A., Solvation of P-Nitrophenol at a Water/Alkane Interface: The Role of Ionic Strength and Salt Identity. *J. Phys. Chem. B* **2005,** *109* (30), 14604-14610.

12. Tarbuck, T. L.; Richmond, G. L., Adsorption and Reaction of CO2 and SO2 at a Water Surface. *J. Am. Chem. Soc.* **2006,** *128* (10), 3256-3267.

13. Raymond, E. A.; Richmond, G. L., Probing the Molecular Structure and Bonding of the Surface of Aqueous Salt Solutions. *J. Phys. Chem. B* **2004,** *108* (16), 5051-5059.

14. Ji, N.; Ostroverkhov, V.; Tian, C. S.; Shen, Y. R., Characterization of Vibrational Resonances of Water-Vapor Interfaces by Phase-Sensitive Sum-Frequency Spectroscopy. *Phys. Rev. Lett.* **2008,** *100* (9), -.

15. Liu, D.; Ma, G.; Levering, L. M.; Allen, H. C., Vibrational Spectroscopy of Aqueous Sodium Halide Solutions and Air-Liquid Interfaces: Observation of Increased Interfacial Depth. *J. Phys. Chem. B* **2004,** *108* (7), 2252-2260.

16. Bian, H. T.; Feng, R. R.; Xu, Y. Y.; Guo, Y.; Wang, H. F., Increased Interfacial Thickness of the NaF, NaCl and NaBr Salt Aqueous Solutions Probed with Non-Resonant Surface Second Harmonic Generation (SHG). *Phys. Chem. Chem. Phys.* **2008,** *10* (32), 4920-4931.

17. Ishiyama, T.; Morita, A., Molecular Dynamics Study of Gas-Liquid Aqueous Sodium Halide Interfaces. II. Analysis of Vibrational Sum Frequency Generation Spectra. *J. Phys. Chem. C* **2007,** *111* (2), 738-748.

18. Chang, T. M.; Dang, L. X., Molecular Dynamics Simulations of CCl4-H2O Liquid-Liquid Interface with Polarizable Potential Models. *J. Chem. Phys.* **1996,** *104* (17), 6772-6783.

19. Hore, D. K.; Walker, D. S.; Richmond, G. L., Water at Hydrophobic Surfaces: When Weaker Is Better. *J. Am. Chem. Soc.* **2008,** *130* (6), 1800-1801.

20. Jedlovszky, P.; Vincze, A.; Horvai, G., Full Description of the Orientational Statistics of Molecules near to Interfaces. Water at the Interface with CCl4. *Phys. Chem. Chem. Phys.* **2004,** *6* (8), 1874-1879.

21. Walker, D. S.; Richmond, G. L., Depth Profiling of Water Molecules at the Liquid-Liquid Interface Using a Combined Surface Vibrational Spectroscopy and Molecular Dynamics Approach. *J. Am. Chem. Soc.* **2007,** *129* (30), 9446-9451.

22. Gragson, D. E.; Richmond, G. L., Investigations of the Structure and Hydrogen Bonding of Water Molecules at Liquid Surfaces by Vibrational Sum Frequency Spectroscopy. *J. Phys. Chem. B* **1998,** *102* (20), 3847-3861.

23. Otten, D. E.; Petersen, P. B.; Saykally, R. J., Observation of Nitrate Ions at the Air/Water Interface by UV-Second Harmonic Generation. *Chem. Phys. Lett.* **2007,** *449* (4-6), 261-265.

24. Gopalakrishnan, S.; Jungwirth, P.; Tobias, D. J.; Allen, H. C., Air-Liquid Interfaces of Aqueous Solutions Containing Ammonium and Sulfate: Spectroscopic and Molecular Dynamics Studies. *J. Phys. Chem. B* **2005,** *109* (18), 8861-8872.

Chapter VII

1. Kahan, T. F.; Reid, J. P.; Donaldson, D. J., Spectroscopic Probes of the Quasi-Liquid Layer on Ice. *J. Phys. Chem. A* **2007,** *111* (43), 11006-11012.

2. Markovitch, O.; Agmon, N., Structure and Energetics of the Hydronium Hydration Shells. *J. Phys. Chem. A* **2007,** *111* (12), 2253-2256.

3. Thogersen, J.; Jensen, S. K.; Petersen, C.; Keiding, S. R., Reorientation of Hydroxide Ions in Water. *Chem. Phys. Lett.* **2008,** *466* (1-3), 1-5.

4. Tuckerman, M. E.; Chandra, A.; Marx, D., Structure and Dynamics of Oh-(Aq). *Acc. Chem. Res.* **2006,** *39* (2), 151-158.

5. Voth, G. A., Computer Simulation of Proton Solvation and Transport in Aqueous and Biomolecular Systems. *Acc. Chem. Res.* **2006,** *39* (2), 143-150.

6. Wang, F.; Izvekov, S.; Voth, G. A., Unusual "Amphiphilic" Association of Hydrated Protons in Strong Acid Solution. *J. Am. Chem. Soc.* **2008,** *130* (10), 3120-3126.

7. Tian, C. S.; Ji, N.; Waychunas, G. A.; Shen, Y. R., Interfacial Structures of Acidic and Basic Aqueous Solutions. *J. Am. Chem. Soc.* **2008,** *130* (39), 13033-13039.

8. Levering, L. M.; Sierra-Hernandez, M. R.; Allen, H. C., Observation of Hydronium Ions at the Air - Aqueous Acid Interface: Vibrational Spectroscopic Studies of Aqueous Hci, Hbr, and Hi. *J. Phys. Chem. C* **2007,** *111* (25), 8814-8826.

9. Tarbuck, T. L.; Ota, S. T.; Richmond, G. L., Spectroscopic Studies of Solvated Hydrogen and Hydroxide Ions at Aqueous Surfaces. *J. Am. Chem. Soc.* **2006,** *128* (45), 14519-14527.

10. Gopalakrishnan, S.; Liu, D. F.; Allen, H. C.; Kuo, M.; Shultz, M. J., Vibrational Spectroscopic Studies of Aqueous Interfaces: Salts, Acids, Bases, and Nanodrops. *Chem. Rev.* **2006,** *106* (4), 1155-1175.

11. Mucha, M.; Frigato, T.; Levering, L. M.; Allen, H. C.; Tobias, D. J.; Dang, L. X.; Jungwirth, P., Unified Molecular Picture of the Surfaces of Aqueous Acid, Base, and Salt Solutions. *J. Phys. Chem. B* **2005,** *109* (16), 7617-7623.

12. Schnitzer, C.; Baldelli, S.; Shultz, M. J., Sum Frequency Generation of Water on NaCl, NaNO3, KHSO4, HCl, HNO3, and H2SO4 Aqueous Solutions. *J. Phys. Chem. B* **2000,** *104* (3), 585-590.

13. Baldelli, S.; Schnitzer, C.; Shultz, M. J., The Structure of Water on HCl Solutions Studied with Sum Frequency Generation. *Chem. Phys. Lett.* **1999,** *302* (1-2), 157-163.

14. Baldelli, S.; Schnitzer, C.; Shultz, M. J., First Spectroscopic Evidence for Molecular HCl on a Liquid Surface with Sum Frequency Generation. *J. Chem. Phys.* **1998,** *108* (23), 9817-9820.

15. Petersen, P. B.; Saykally, R. J., Is the Liquid Water Surface Basic or Acidic? Macroscopic Vs. Molecular-Scale Investigations. *Chem. Phys. Lett.* **2008,** *458* (4-6), 255-261.

16. Buch, V.; Milet, A.; Vacha, R.; Jungwirth, P.; Devlin, J. P., Water Surface Is Acidic. *Proc. Natl. Acad. Sci. U. S. A.* **2007,** *104* (18), 7342-7347.

17. Dang, L. X., Solvation of the Hydronium Ion at the Water Liquid/Vapor Interface. *J. Chem. Phys.* **2003,** *119* (12), 6351-6353.

18. Ishiyama, T.; Morita, A., Molecular Dynamics Analysis of Interfacial Structures and Sum Frequency Generation Spectra of Aqueous Hydrogen Halide Solutions. *J. Phys. Chem. A* **2007,** *111* (38), 9277-9285.

19. Kudin, K. N.; Car, R., Why Are Water-Hydrophobic Interfaces Charged? *J. Am. Chem. Soc.* **2008,** *130* (12), 3915-3919.

20. Pegram, L. M.; Record, M. T., Quantifying Accumulation or Exclusion of H+, HO-, and Hofmeister Salt Ions near Interfaces. *Chem. Phys. Lett.* **2008,** *467* (1-3), 1-8.

21. Petersen, M. K.; Iyengar, S. S.; Day, T. J. F.; Voth, G. A., The Hydrated Proton at the Water Liquid/Vapor Interface. *J. Phys. Chem. B* **2004,** *108* (39), 14804-14806.

22. Vacha, R.; Buch, V.; Milet, A.; Devlin, P.; Jungwirth, P., Autoionization at the Surface of Neat Water: Is the Top Layer PH Neutral, Basic, or Acidic? *Phys. Chem. Chem. Phys.* **2007,** *9* (34), 4736-4747.

23. Vacha, R.; Horinek, D.; Berkowitz, M. L.; Jungwirth, P., Hydronium and Hydroxide at the Interface between Water and Hydrophobic Media. *Phys. Chem. Chem. Phys.* **2008,** *10* (32), 4975-4980.

24. Zangi, R.; Engberts, J. B. F. N., Physisorption of Hydroxide Ions from Aqueous Solution to a Hydrophobic Surface. *J. Am. Chem. Soc.* **2005,** *127* (7), 2272-2276.

25. Knecht, V.; Risselada, H. J.; Mark, A. E.; Marrink, S. J., Electrophoretic Mobility Does Not Always Reflect the Charge on an Oil Droplet. *J. Colloid Interface Sci.* **2008,** *318* (2), 477-486.

26. Chang, T. M.; Dang, L. X., Recent Advances in Molecular Simulations of Ion Solvation at Liquid Interfaces. *Chem. Rev.* **2006,** *106* (4), 1305-1322.

27. Jungwirth, P.; Tobias, D. J., Specific Ion Effects at the Air/Water Interface. *Chem. Rev.* **2006,** *106* (4), 1259-1281.

28. Petersen, P. B.; Saykally, R. J., On the Nature of Ions at the Liquid Water Surface. *Annu. Rev. Phys. Chem.* **2006,** *57*, 333-364.

29. Buch, V.; Tarbuck, T.; Richmond, G. L.; Groenzin, H.; Li, I.; Shultz, M. J., Sum Frequency Generation Surface Spectra of Ice, Water, and Acid Solution Investigated by an Exciton Model. *J. Chem. Phys.* **2007,** *127* (20), 204710-1-15.

30. Diken, E. G.; Headrick, J. M.; Roscioli, J. R.; Bopp, J. C.; Johnson, M. A.; McCoy, A. B., Fundamental Excitations of the Shared Proton in the H3O2- and H5O2+ Complexes. *J. Phys. Chem. A* **2005,** *109* (8), 1487-1490.

31. Headrick, J. M.; Diken, E. G.; Walters, R. S.; Hammer, N. I.; Christie, R. A.; Cui, J.; Myshakin, E. M.; Duncan, M. A.; Johnson, M. A.; Jordan, K. D., Spectral Signatures of Hydrated Proton Vibrations in Water Clusters. *Science* **2005,** *308* (5729), 1765-1769.

32. Stoyanov, E. S.; Hoffman, S. P.; Kim, K. C.; Tham, F. S.; Reed, C. A., The Structure of the H3O+ Hydronium Ion in Benzene. *J. Am. Chem. Soc.* **2005,** *127* (21), 7664-7665.

33. Beattie, J. K., Comment on Autoionization at the Surface of Neat Water: Is the Top Layer PH Neutral, Basic, or Acidic? By R. Vacha, V. Buch, A. Milet, J. P. Devlin and P. Jungwirth, Phys. Chem. Chem. Phys., 2007, 9, 4736. *Phys. Chem. Chem. Phys.* **2008,** *10* (2), 330-331.

34. Vacha, R.; Buch, V.; Milet, A.; Devlin, J. P.; Jungwirth, P., Response to Comment on Autoionization at the Surface of Neat Water: Is the Top Layer PH Neutral, Basic, or Acidic? By J. K. Beattie, Phys. Chem. Chem. Phys., 2007, 9, Doi : 10.1039/B713702h. *Phys. Chem. Chem. Phys.* **2008,** *10* (2), 332-333.

35. Beattie, J. K.; Djerdjev, A. M., The Pristine Oil/Water Interface: Surfactant-Free Hydroxide-Charged Emulsions. *Angew. Chem., Int. Ed.* **2004,** *43* (27), 3568-3571.

36. Beattie, J. K.; Djerdjev, A. M.; Franks, G. V.; Warr, G. G., Dipolar Anions Are Not Preferentially Attracted to the Oil/Water Interface. *J. Phys. Chem. B* **2005,** *109* (33), 15675-15676.

37. Beattie, J. K.; Djerdjev, A. M.; Warr, G. G., The Surface of Neat Water Is Basic. *Faraday Discuss.* **2009,** *141*, 31-39.

38. Creux, P.; Lachaise, J.; Graciaa, A.; Beattie, J. K., Specific Cation Effects at the Hydroxide-Charged Air/Water Interface. *J. Phys. Chem. C* **2007,** *111* (9), 3753-3755.

39. Marinova, K. G.; Alargova, R. G.; Denkov, N. D.; Velev, O. D.; Petsev, D. N.; Ivanov, I. B.; Borwankar, R. P., Charging of Oil-Water Interfaces Due to Spontaneous Adsorption of Hydroxyl Ions. *Langmuir* **1996,** *12* (8), 2045-2051.

40. Brown, M. G.; Walker, D. S.; Raymond, E. A.; Richmond, G. L., Vibrational Sum-Frequency Spectroscopy of Akane/Water Interfaces: Experiment and Theoretical Simulation. *J. Phys. Chem. B* **2003,** *107* (1), 237-244.

41. Scatena, L. F.; Richmond, G. L., Orientation, Hydrogen Bonding, and Penetration of Water at the Organic/Water Interface. *J. Phys. Chem. B* **2001,** *105* (45), 11240-11250.

42. Chang, T. M.; Dang, L. X., Molecular Dynamics Simulations of CCl4-H2O Liquid-Liquid Interface with Polarizable Potential Models. *J. Chem. Phys.* **1996,** *104* (17), 6772-6783.

43. Hore, D. K.; Walker, D. S.; Richmond, G. L., Water at Hydrophobic Surfaces: When Weaker Is Better. *J. Am. Chem. Soc.* **2008,** *130* (6), 1800-1801.

Chapter VIII

1. Walker, D. S.; Richmond, G. L., Interfacial Depth Profiling of the Orientation and Bonding of Water Molecules across Liquid-Liquid Interfaces. *J. Phys. Chem. C* **2008,** *112* (1), 201-209.

2. Girault, H.; Kornyshev, A. A.; Monroe, C. W.; Urbakh, M., Functionalized Liquid-Liquid Interfaces. *J. Phys. Cond. Matt.* **2007,** *19* (37), 370301.

3. Chen, X.; Yang, T.; Kataoka, S.; Cremer, P. S., Specific Ion Effects on Interfacial Water Structure near Macromolecules. *J. Am. Chem. Soc.* **2007,** *129* (40), 12272-12279.

4. Petersen, P. B.; Saykally, R. J., On the Nature of Ions at the Liquid Water Surface. *Annu. Rev. Phys. Chem.* **2006,** *57*, 333-364.

5. Luo, G. M.; Malkova, S.; Yoon, J.; Schultz, D. G.; Lin, B. H.; Meron, M.; Benjamin, I.; Vanysek, P.; Schlossman, M. L., Ion Distributions near a Liquid-Liquid Interface. *Science* **2006,** *311* (5758), 216-218.

6. Fujiyoshi, S.; Ishibashi, T.; Onishi, H., Molecular Vibrations at a Liquid-Liquid Interface Observed by Fourth-Order Raman Spectroscopy. *J. Phys. Chem. B* **2006,** *110* (19), 9571-9578.

7. Scatena, L. F.; Richmond, G. L., Aqueous Solvation of Charge at Hydrophobic Liquid Surfaces. *Chem. Phys. Lett.* **2004,** *383* (5-6), 491-495.

8. Scatena, L. F.; Richmond, G. L., Isolated Molecular Ion Solvation at an Oil/Water Interface Investigated by Vibrational Sum-Frequency Spectroscopy. *J. Phys. Chem. B* **2004,** *108* (33), 12518-12528.

9. Schlossman, M. L., Liquid-Liquid Interfaces: Studied by X-Ray and Neutron Scattering. *Curr. Opin. Colloid Interface Sci.* **2002,** *7* (3-4), 235-243.

10. Wick, C. D.; Dang, L. X., Recent Advances in Understanding Transfer Ions across Aqueous Interfaces. *Chem. Phys. Lett.* **2008,** *458* (1-3), 1-5.

11. Jungwirth, P.; Winter, B., Ions at Aqueous Interfaces: From Water Surface to Hydrated Proteins. *Annu. Rev. Phys. Chem.* **2008,** *59*, 343-366.

12. Walker, D. S.; Moore, F. G.; Richmond, G. L., Vibrational Sum Frequency Spectroscopy and Molecular Dynamics Simulation of the Carbon Tetrachloride-Water and 1,2-Dichloroethane-Water Interfaces. *J. Phys. Chem. C* **2007,** *111* (16), 6103-6112.

13. Benjamin, I., Hydrogen Bond Dynamics at Water/Organic Liquid Interfaces. *J. Phys. Chem. B* **2005,** *109* (28), 13711-13715.

14. Chandler, D., Hydrophobicity: Two Faces of Water. *Nature* **2002,** *417* (6888), 491-491.

15. Narayan, S.; Muldoon, J.; Finn, M. G.; Fokin, V. V.; Kolb, H. C.; Sharpless, K. B., "On Water": Unique Reactivity of Organic Compounds in Aqueous Suspension. *Angew. Chem. Int. Ed.* **2005,** *44* (21), 3275-3279.

16. Jung, Y. S.; Marcus, R. A., On the Theory of Organic Catalysis on Water. *J. Am. Chem. Soc.* **2007,** *129* (17), 5492-5502.

17. Rao, C. N. R.; Kalyanikutty, K. P., The Liquid-Liquid Interface as a Medium to Generate Nanocrystalline Films of Inorganic Materials. *Acc. Chem. Res.* **2008,** *41* (4), 489-499.

18. Tanford, C., *Ben Franklin Stilled the Waves : An Informal History of Pouring Oil on Water with Reflections on the Ups and Downs of Scientific Life in General.* Oxford University Press: New York, 2004; p 288.